

Regulation of dystrophin Dp71 during Müller glial cells edema in mouse retina

Lourdes Montserrat Siqueiros Márquez

▶ **To cite this version:**

Lourdes Montserrat Siqueiros Márquez. Regulation of dystrophin Dp71 during Müller glial cells edema in mouse retina. Sensory Organs. Université Pierre et Marie Curie - Paris VI; Centro de Investigación y de Estudios Avanzados del Instituto Politécnico Nacional (Mexico), 2017. English. NNT : 2017PA066361 . tel-01739690

HAL Id: tel-01739690

https://theses.hal.science/tel-01739690

Submitted on 21 Mar 2018

HAL is a multi-disciplinary open access archive for the deposit and dissemination of scientific research documents, whether they are published or not. The documents may come from teaching and research institutions in France or abroad, or from public or private research centers.

L'archive ouverte pluridisciplinaire **HAL**, est destinée au dépôt et à la diffusion de documents scientifiques de niveau recherche, publiés ou non, émanant des établissements d'enseignement et de recherche français ou étrangers, des laboratoires publics ou privés.

Université Pierre et Marie Curie

Centro de Investigación y de Estudios Avanzados del Instituto Politécnico Nacional

ED394: Ecole Doctorale Physiologie, Physiopathologie et thérapeutique

"Regulation of dystrophin Dp71 during Müller glial cells edema in mouse retina"

Par :

Lourdes Montserrat Siqueiros Márquez

Thèse de doctorant de :

Vision-Physiopathologie

Dirigée par :

Dr. Florian Sennlaub et Dr. Silvia Cecilia Irene Montañez Ojeda

Présentée et soutenue publiquement le 30 novembre 2017 à 16h

Devant un jury composé de :

Dr. Vaillend Cyrille	Rapporteur
Dr. Estrada Mena Francisco Javier	Rapporteur
Dr. Romo Yañez José	Rapporteur
Pr. Hardin Pouzet Hélène	Examinateur
Dr. Bermúdez Cruz Rosa María	Examinateur
Dr. Rendon Alvaro	Présidente du jury

Je dédie cette thèse à ma famille qui a toujours été avec moi et sans qui je ne serais pas arrivé en ce moment

Pour votre amour, soutien et compagnie tous les jours de ma vie ; parce que peu importe où nous sommes, vous êtes toujours avec moi

Los AMO

Acknowledgments

Je souhaite remercier en premier lieu tous les membres du jury qui me font l'honneur d'évaluer ce travail. Je remercie très sincèrement M. Cyrille Vaillend, M. Javier Estrada et M. Jose Romo pour avoir accepté d'être rapporteurs de ce travail et pour y consacrer un temps précieux. J'adresse également mes sincères remerciements à Mme Hélène Hardin-Pouzet pour me faire l'honneur d'être présidente de ce jury.

Gracias a mis asesores y revisores en México, Dra. Rosa Ma. Bermúdez y Dr. Luis Álvarez por su apoyo y consejos a lo largo de este trabajo, por sus valiosas contribuciones desde el desarrollo de mi trabajo hasta la realización del manuscrito final.

Je souhaite remercier particulièrement M. Florian Sennlaub qui a accepté d'être mon directeur de thèse et m'a soutenu tout au long de mon séjour à l'IDV.

Un agradecimiento especial a la Dra. Cecilia Montañez primero por aceptarme en su laboratorio, pero especialmente por su guía, apoyo y consejos durante tantos años en su laboratorio. Gracias por confiar en mí y por su apoyo incondicional para realizar mi meta de estudiar en el extranjero.

Je tiens à remercier M. Xavier Guillonneau et Mme. Deniz Dalkara pour votre soutien et votre collaboration dans ce travail, pour avoir consacré leur temps à ce projet et partagé votre connaissance avec moi.

M. Alvaro Rendon, un remerciement ne suffit pas à exprimer la gratitude que j'ai, vous a cru en moi et a participé à ma formation professionnelle en consacrant du temps et des efforts. Cependant, non parce que sa contribution à mon travail a été moindre, mais en raison de l'énorme gratitude que j'ai pour vous en plus d'avoir été au moment le plus difficile de mon séjour à Paris, pour ses conseils et son soutien à

tout moment je ne peux pas plus remercier l'énorme fortune de vous avoir rencontré. Cher Alvaro, muchas gracias.

Je tiens à remercier M. José-Alain Sahel pour m'avoir accueillie dans un très agréable environnement de travail à l'IDV

Merci à tous mes collègues et amis a l'IDV : Marcela, William, Fanny, Kevin, Paul-Henri, Corentin, Elric, Laure, Anna.... Sans vous mon séjour à l'IDV n'aurait pas été pareil, merci pour les repas, les jeudis, les pique-niques, pour m'avoir parlé en français !! et déchiffrant mes réponses. Vous es le meilleur bureau où je pourrais être. Merci William pour tous les détails que vous avez eu avec moi vous êtes un grand ami, j'espère vous voir bientôt.

Hugo mon partenaire à l'IDV et à Paris, merci pour toute votre aide dans l'IDV, pour les milliers d'heures que nous avons partagées en faisant de la science. Merci de m'avoir appris à survivre à Paris. Hugo, tu a beaucoup compté pour moi ces dernières années et puisque je sais que tu parles mieux l'espagnol que moi ... Gracias por los secretos, las salidas, los consejos, las risas, los abrazos, las largas noches y las mañanas en el IDV, por dejarme conocer a tu familia y compartir conmigo el Paris y la vida real de un parisino, gracias por tanto. Te quiero ! Se que encontré a un gran amigo.

Mary et Ophelie, mille grâces pour tout, vous m'ont toujours accompagné, vous m'avez donné votre temps pour m'apprendre et me soutenir tout le temps, merci pour les câlins et les bons moments que nous partageons. Muchas gracias ! Las quiero !.

Gracias a mis amigos y colegas en el CINVESTAV: Ale, Jorge, Victor, Clemen han hecho que mi estancia en el laboratorio sea recordada como mi segunda casa, además de su apoyo y consejos para este trabajo han sido más que colegas para mí, Gracias !!.

Coztli, Irais, Mayram, Sandy, Pablo, Chano, Karina, Cesar quiero agradecerles porque la vida es más que ciencia y sin ustedes no habría podido hacer esto que tanto me gusta, gracias por mantenerme enfocada en

el trabajo y por invitarme a distraerme cuando era necesario. Hoy son más que mis colegas de laboratorio, son mis amigos y los quiero mucho !

A mi familia que esta y estuvo y estará siempre conmigo sin importar nada, gracias por su apoyo, mensajes, compañía por hacerme saber que siempre están ahí.... Sin ustedes nada habría sido posible, los AMO. Abuelitos gracias por todo lo que han hecho por quererme tanto que no importa nada más. Papis, gracias por TODO porque sin ustedes no estaría aquí, gracias por tantas muestras de apoyo y cariño yo se lo afortunada que soy de contar con dos personas que me aman tanto, que siempre confían en mí y que siempre están dispuestas a hacerme saber que puedo lograrlo Los AMO

Gracias Gaby Mora, sin tu ayuda y paciencia todo habría sido muy difícil.

Enfin, je tiens à remercier ECOS-Nord pour son soutien favorisant notre collaboration entre des laboratoires au Mexique et France sur un projet commun. Quiero igualmente agradecer al CINVESTAV y a CONACyT por el brindarme el apoyo económico necesario para la realización de este trabajo tanto en México como en Paris.

Index

Index _____ - 1 -

Preface _____ - 4 -

Abbreviations _____ - 6 -

Introduction _____ - 9 -

Retina _____ - 9 -

Overview _____ *- 9 -*

Structure _____ *- 11 -*

Müller Glial Cells (MGC) _____ *- 13 -*

Astrocytes _____ *- 14 -*

Homeostasis _____ *- 17 -*

Angiogenesis _____ *- 17 -*

Inflammation _____ *- 18 -*

Ocular diseases _____ *- 20 -*

Treatments _____ *- 21 -*

Dystrophin _____ - 22 -

Overview _____ *- 22 -*

Dystrophin Dp71 _____ - 26 -

Dystrophin Dp71 isoforms _____ *- 27 -*

Dp71 functions _____ *- 30 -*

Dp71 in Retina _____ *- 31 -*

Dp71 in the Brain _____ *- 34 -*

Cell junctions _____ *- 35 -*

General objective _____ - 37 -

First part objectives: _____ *- 37 -*

Second part objectives: _____ *- 37 -*

Methods _____ - 38 -
Animals _____ - 38 -
Experimental Models _____ - 38 -
1. Lens surgery _____ - 38 -
2. Retinal Explants _____ - 39 -
3. Cells culture _____ - 40 -
DNA extraction and PCR _____ - 41 -
Protein extraction and Western blot assay _____ - 41 -
Immunofluorescence assay _____ - 43 -
PC12 cells _____ - 43 -
Müller Glial cells stain _____ - 43 -
Flat mounted retinas _____ - 44 -
Quantitative RT-PCR analysis of retinal RNA _____ - 45 -
Quantification and measurement of cells groups _____ - 46 -
Statistical Analysis _____ - 46 -
FIRST PART _____ - 47 -
"Molecular alterations in mouse Müller glial cells during cellular edema and treatment action mechanism analysis" _____ - 47 -
Background _____ - 47 -
Results _____ - 53 -
1. Astrocytes morphology after Lens surgery _____ - 53 -
2. Effect of dexamethasone injections post-surgery on Dp71, AQP4, and Kir4.1 _____ - 56 -
3. Dp71, Kir4.1 and AQP4 expression in retinal explant model and Dex effect _____ - 61 -
4. Dexamethasone, Triamcinolone and Fluocinolone effect in hypotonic plus Barium retinal explant model _____ - 65 -
5. Effect of prostaglandins and leukotriene pathway inhibitors on Dp71 and HSF1 expression _____ - 68 -
Discussion and perspectives _____ - 70 -

Conclusions _____ - 76 -
SECOND PART _____ - 77 -
"Role of Dp71 and ε-SG in the intercellular junctions of PC12 cells." - 77 -
Background _____ - 77 -
PC12 cells model _____ - 82 -
Results _____ - 84 -
1. Colocalization of Dp71d isoforms with ε-SG _____ - 84 -
2. Colocalization of Dp71d isoforms with adhesion molecules- 86 -
3. Effect of the overexpression of $Dp71_{\Delta 71}$ and $Dp71_{\Delta 71\text{-}74}$ on cell to cell adhesion in PC12 cells _____ - 89 -
Discussion and perspectives _____ - 90 -
Conclusions _____ - 93 -
References _____ - 94 -
Annexes _____ - 107 -
List of figures _____ - 108 -
Résumé _____ - 110 -
Abstract _____ - 111 -
Resumen _____ - 113 -

Preface

Dystrophin Dp71, the main DMD product expressed in central nervous system has been highly studied due to its functional implication in different cell processes such as: neuronal plasticity, cell adhesion, retinal homeostasis, cell differentiation, cell proliferation, actin-cytoskeleton remodeling and nuclear envelope-associated function. Remarkably, mutations in Dp71 have been associated with alterations in the functioning of the central nervous system, specifically in the mental impairment observed in patients with DMD. In retina, Dp71 is associated with the correct expression and localization of AQP4 and Kir4.1 channels in Müller Glial Cells (MGC), additionally, in retinal astrocytes Dp71 participates regulating the astrocyte morphology and density and is associated with the subsequent normal blood vessel development.

The blood-retinal barrier (BRB) plays an important role in the regulation of the homeostatic and the microenvironment in the retina. The internal BRB is formed by tight junctions between the endothelial cells of the retinal capillaries. MGC, astrocytes and pericytes contribute to the functioning of the internal BHR. Breakdown of the inner blood–retinal barrier (iBRB) occurs in many retinal disorders and may cause retinal edema often responsible for vision loss. As dystrophin Dp71 is involved in the correct functioning of both, astrocytes and MGC, and on the other hand the importance of the formation and maintenance of BRB, it is of great interest to study the role of Dp71 as well as the changes in its expression during a pathological process present in different retinal diseases such as edema.

In this work, we studied the role of dystrophin Dp71 during the edema formation and resolution, the molecular changes associated with this edema, the pathway leading to the edema formation and where are the dexamethasone (Dex) targets and the use of lower doses of different

glucocorticoids (GCs) to prevent the molecular changes associated with MGC edema.

Due to the relevance of tight junctions in the correct functioning of BRB and the previous knowledge regarding the presence of specific isoforms of Dp71 and ε-SG in the contact sites between PC12 cells, we also investigated the possible interactions between Dp71 isoforms and ε-SG in the intercellular region.

The work was performed in two institutions in which the retina and PC12 cells are being studied: Institute de la Vision in Paris and Centro de Investigación y de Estudios Avanzados del IPN in Mexico. The two groups involved in this work are experts in the study of Dp71 function in the nervous system. Due to the questions answered in this thesis, the manuscript has been structured in two parts: the first one involves the role of Dp71 in the formation and resolution of retinal edema as well as the study of Dex mechanism of action and the use of other GCs as therapeutic alternatives and the second part refers to the participation of Dp71 and ε-SG in the intercellular interactions in PC12 cells.

Abbreviations

AA: Arachidonic acid

ATP: Adenosine triphosphate

Ba^{2+}: Barium

BRB: Blood-Retinal Barrier

Bromo: 4-Bromofenacil bromide

Ca^{2+}: Calcium

CNS: Central Nervous system

COX: Cyclooxygenase

C-terminal: Carboxy-terminal

Cx43: Connexin 43

DAPC: Dystrophin Associated Protein Complex

DAPs: Dystrophin Associated Proteins

Dex: Dexamethasone

DMD: Duchenne Muscular Dystrophy

Dox: Doxycycline

EIU: Endotoxin-induced uveitis

FGF: Fibroblast Growth Factors

Fluo: Fluocinolone acetonide

GC: Glucocorticoids

GCL: ganglion cell layer

GFAP: Glial fibrillary acidic protein

GS: Glutamine synthetase

HBE: Human Bronchial Epithelium

HE: Hematoxylin-Eosine

HETE: Hydroxyeicosatetraenoic acids

HPETEs: Hydroperoxyeicosatetraenoic acids

BRB: Blood-Retinal Barrier

iBRB: inner Blood-Retinal Barrier

ILM: inner limiting membrane

Indo: Indomethacin

INL: inner nuclear layer

IPL: inner plexiform layer

K^+: Potassium

LOX: Lipoxygenase

LTs: Leukotrienes

LXs: Lipoxins

MGC: Müller Glial Cells

mRNA: messenger Ribonucleic Acid

NGF: Neuronal Growth Factor

nNOS: neuronal Nitric Oxide Synthases

N-terminal: Amino-terminal

OLM: outer limiting layer

ONL: outer nuclear layer

PGs: Prostaglandins

PLA2: Phospholipase A2

RT-qPCR: Quantitative reverse transcription PCR

TGF: Transforming Growth Factor

TJ: Tight junction

TNF: Tumor Necrosis Factor

Triam: Triamcinolone

VEGF: Vascular Growth Factor

Introduction

Retina

Overview

The vision comprises the acquisition of luminous stimulus in the anterior segment of the eye, then the transduction and transmission of the information by the retina to the visual areas of the brain through the optical nerve. The retina is the innermost layer of the eye that allows the reception and transmission of visual information to specialized cerebral structures. In the retina, the complex neural circuitry converts the photoreceptors electrical activity into action potentials that travel to the brain. Then, the retina is considered an extension of the central nervous system (Purves, Dale et al., 2001).

Retinal function consists of early detection and analysis of visual information; it is an integrated part of the visual analysis apparatus present in the thalamus, cortex and other areas of the central nervous system. The retina, located in the posterior part of the eye, between the vitreous and the choroid consists of vascular cells (endothelial cells and pericytes), macroglia (Müller cells and astrocytes), microglia, neurons (photoreceptors, bipolar cells, amacrine cells, horizontal cells and ganglion cells), pigmented epithelium and microglia (resident macrophages).

Into the retina, the cell bodies and processes from these cells are organized into eight layers: the nerve fiber, the cellular ganglion layer, the inner plexiform layer, the inner nuclear layer, the outer plexiform layer, the outer nuclear layer, the photoreceptor layer (cones and rods) and retinal pigment epithelium (Fig. 1) (Dyer and Cepko, 2001; Runkle and Antonetti, 2011). The processes and synaptic contacts are located in the inner plexiform and outer plexiform layers; the major route of information flow goes thru photoreceptor cells to bipolar cells to ganglion cells to optic nerve.

The cell bodies and processes of these neurons are stacked in alternating layers, with the cell bodies located in the inner nuclear, outer nuclear, and ganglion cell layers, and the processes and synaptic contacts are located in the inner plexiform and outer plexiform layers (Fig. 1). A direct three neuron chain—photoreceptor cell to bipolar cell to ganglion cell—is the major route of information flow from photoreceptors to the optic nerve.

It has been proved that the isolated retina has multiple advantages to study interactions in intact nervous system. The retina can be dissected intact, can be conserved, activated and monitored in culture conditions (Newman, 2004).

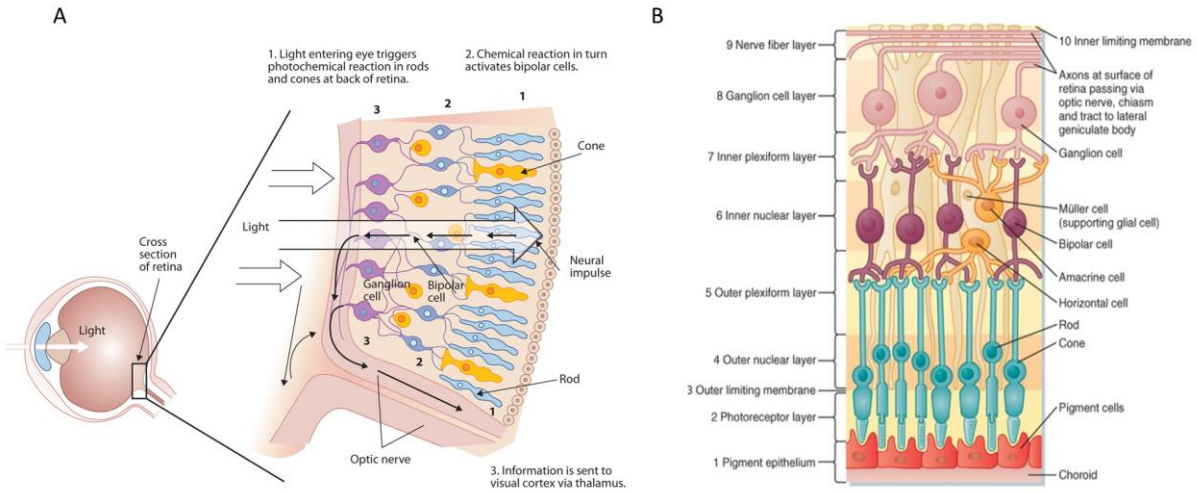


Figure 1.-Cellular organization in the retina.

A. The incident light enters the eye through the cornea, cross the pupil and the lens; on the back of the eye, the light reaches the retina, here is absorbed by the cone and rod photoreceptors after traversing several retinal layers **B.** cellular organization in the retina. Observed retinal pigment epithelium (1) followed by photoreceptor layer (2) rods and cones, the external limiting membrane (3) photoreceptor cell bodies are found in the outer nuclear layer (4), the axons of the photo-receptors end up in the outer plexiform layer (5), the synapse with the horizontal

and bipolar cells happen in the inner nuclear layer (6), the Müller glial cells and amacrine cells are also found. Bipolar cells transmit signals through synapses to the amacrine and ganglion cells in the inner plexiform layer (7). The ganglion cell layer (8). The axons of ganglion cells extend through the optic nerve and carry the signal to the brain. The endfeet of the Müller glial cells of forms part of the external and internal limiting membranes. http://open.lib.umn.edu/intropsyc/ and (Koeppen Bruce M and Stanton Bruce A, 2008).

Structure

The human retina is a thin structure, being thicker near the optical disc (0.56 mm) and decreasing to 0.1 mm in front of the equatorial line, continuing in this thickness up to the ora serrata. The optic part of the retina extends from the optic disc to the ora serrata, is soft, translucent and purple due to the presence of rhodopsin (visual purple), but becomes opaque and whitish as soon as it is exposed to light. Near the center of the retina a region of 5-6 mm diameter contain the macula lutea, an elliptical area of yellowish color; its color is due to the presence of xanthophyll derivatives. The macula lutea harbors a central depression, the central fovea or foveola, where the visual resolution is higher (Standring, Susan et al., 2008; Trattler William et al., 2012).

All the specialized cells that conform the layered structure of the retina, are interconnected through synapses. The light that enters the eye is captured by the photo-receptor cells (rods and cones) that are in the outermost layer of the retina, this initiates a cascade of neuronal signals that reaches the ganglion cells whose axons form the optic nerve; this specialized tissue is responsible for converting visible light into a neurochemical stimulus that is interpreted by the brain as vision (Standring, Susan et al., 2008).

The vascular structure that supports the retina provides the necessary nutrients for correct functioning, must exert minimal interference on the

light signal making necessary the presence of a barrier that maintains the neural environment (Runkle and Antonetti 2011, London, Benhar et al., 2013). Oxygen and nutrients are provided by two distinct vascular systems which are the choroidal and retinal network. The choroidal vascular network forms a set of capillaries under the retinal pigment epithelium called choriocapillaris. This choroidal network feeds the external retina, which includes the photoreceptors and is characterized by fenestrated blood vessels that allows transit of proteins with diverse molecular mass. The retinal vascular network is subdivided into two upper and lower branches, that support the supply of metabolic needs to the internal layers of the retina. The retinal capillaries are not fenestrated (Standring, Susan et al., 2008).

The BRB should be regarded as consisting of 2 major components, the endothelium of the retinal blood vessels (inner BRB) and the retinal pigment epithelium (RPE) (outer BRB) (Cunha-Vaz, 2017). The spaces between the endothelial cells are sealed by tight junctions (Fig. 2), resulting in a restricted paracellular permeability. Because the neuro retina is highly vulnerable, changes that lead to reduce BRB properties can affect visual function (Klaassen et al., 2013).

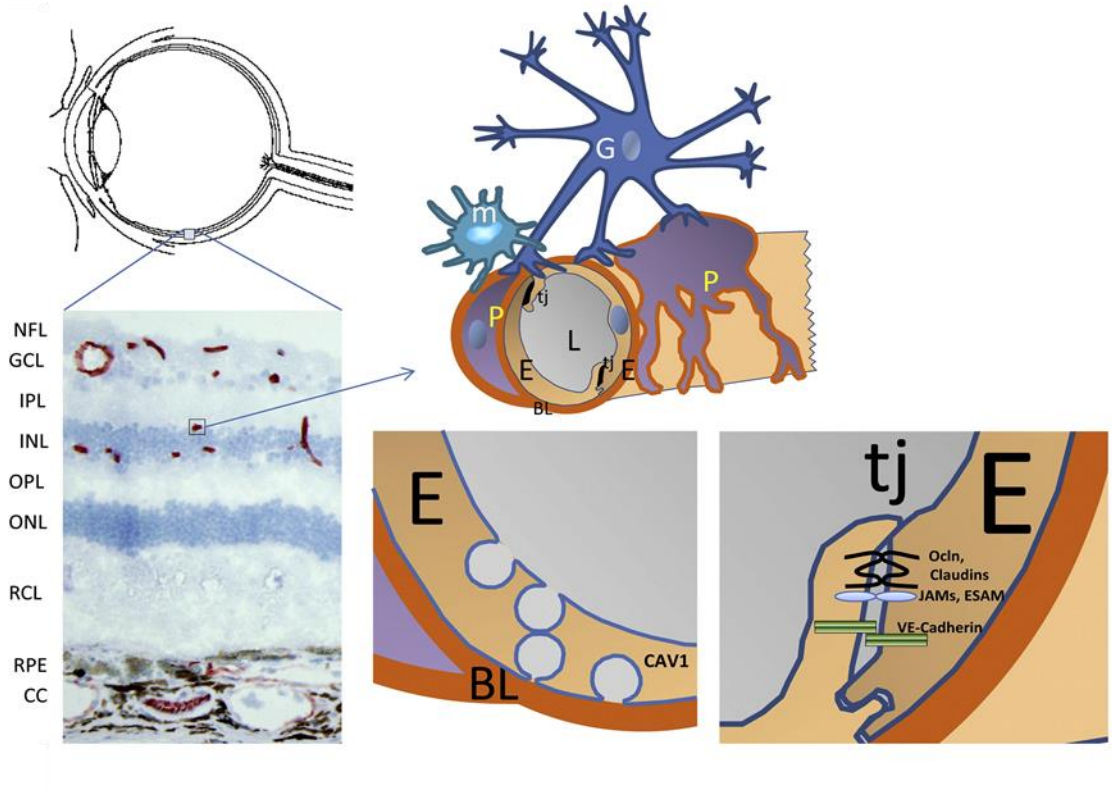


Figure 2.- Blood Retina Barrier

Schematic representation of the blood retinal barrier (BRB). Left panel, cryosection of human retina stained for claudi-5 (red). Upper panel, endothelial cells forms the inner BRB; the pigment epithelial cells form the outer BRB surrounded by pericytes and glial cell food processes (Klaassen et al., 2013).

Müller Glial Cells (MGC)

Müller glial cells (MGC) are the mayor macroglial cells in vertebrate's retina. Müller cells are specialized glial cells that span the entire thickness of the neuronal retina from the vitreous surface to the subretinal space. MGC form an anatomical link between the neurons and the spaces where the exchange of molecules to maintain the retinal homeostasis and environment takes place (Bringmann et al., 2006; Reichenbach and Bringmann, 2013). MGC feeds forms the inner border of the retina and

they extend their apical processes into the photoreceptor layer (Newman, 2004).

MGC are extremely important for retinal function as most of the nutrients, ions, water, waste molecules among other molecules are transported through MGC located between retinal vessels and retinal neurons. To achieve their functions MGC are supplied with different ions channels (Kir family channels, Ca^{2+}-dependent K^{+} channels, tandem-pore (TASK) channels, ligand receptors (insulin-like growth factor 1), transmembrane transporters and enzymes (glutamine synthetase). In healthy retina MGC are involved in glucose metabolism, regulation of retinal blood flow, formation and maintenance of retinal blood barrier, maintaining the ion and water homeostasis, neuronal signaling processes by uptake and recycling of neurotransmitters as well as release and recycling of other factors (Bringmann et al., 2006; Goldman, 2014; Reichenbach and Bringmann, 2013).

Astrocytes

The astrocytes have a stellate shape cells almost exclusively confined to the innermost retinal layers; astrocytes make extensive contacts. Like MGC, astrocytic processes cover the blood vessels forming the retinal blood barrier and they have a significant role in the ion homeostasis. Among the functions in which the astrocytes participate in the brain is the vascular development based on the principle of angiogenesis. In the central nervous system, it has been shown that a pre-established astrocyte network is crucial for vascular development. A potentially direct role of astrocytes in the promotion of cerebral angiogenesis by interaction with vessel expansions blood and endothelial cells has been suggested (Ma et al., 2012; Vecino et al., 2016).

Indeed, the conditional genetic inhibition of astrogliogenesis during the perinatal period, by inhibition of a glial *orc3* progenitor (a gene necessary for DNA replication) reduced dramatically the number of glial progenitor cells in the sub-ventricular zone, and the number of astrocytes in the early

postnatal cerebral cortex delaying the astrogliogenesis. This results in a decrease of the density and branching of cortical blood vessels. These elements correspond to a delayed growth of the vessels without regression of the vascular density. Concomitantly, endothelial cell proliferation, enlargement of vessel lumen, and increased expression of pericyte cytoskeletal genes were observed, suggesting compensatory mechanisms. These results show the importance of cerebral astrocytes in promoting cerebral vascular growth during development (Ma et al., 2012).

In our laboratory, we have shown that in retina Dp71 play a role in the regulation of astrocyte density and morphology (Giocanti-Auregan et al., 2016). In this study where the postnatal retinal vessel development was compared between WT and Dp71-null mice; the results showed that WT mice development of the inner vasculature represented 3% of the total retinal surface, with progressive growth of the first vessel layer covering 23% at P3 and 65% at P6. In Dp71-null mice, the vasculature represented 2% of the entire retina and 16% of the wild-type retinal surface was covered, corresponding to a subtle, but significant, delay in angiogenesis.

Moreover, at P6 this difference increased, showing a dramatic reduction in vascular network spreading by 37% in Dp71-null mice and 65% in WT mice. The deep plexus developed later with a highly significant difference at P12. However, despite the difference in vasculature development, the retinal surface appeared totally covered by vessels in adult Dp71-null mice (Fig. 3) (Giocanti-Auregan et al., 2016).

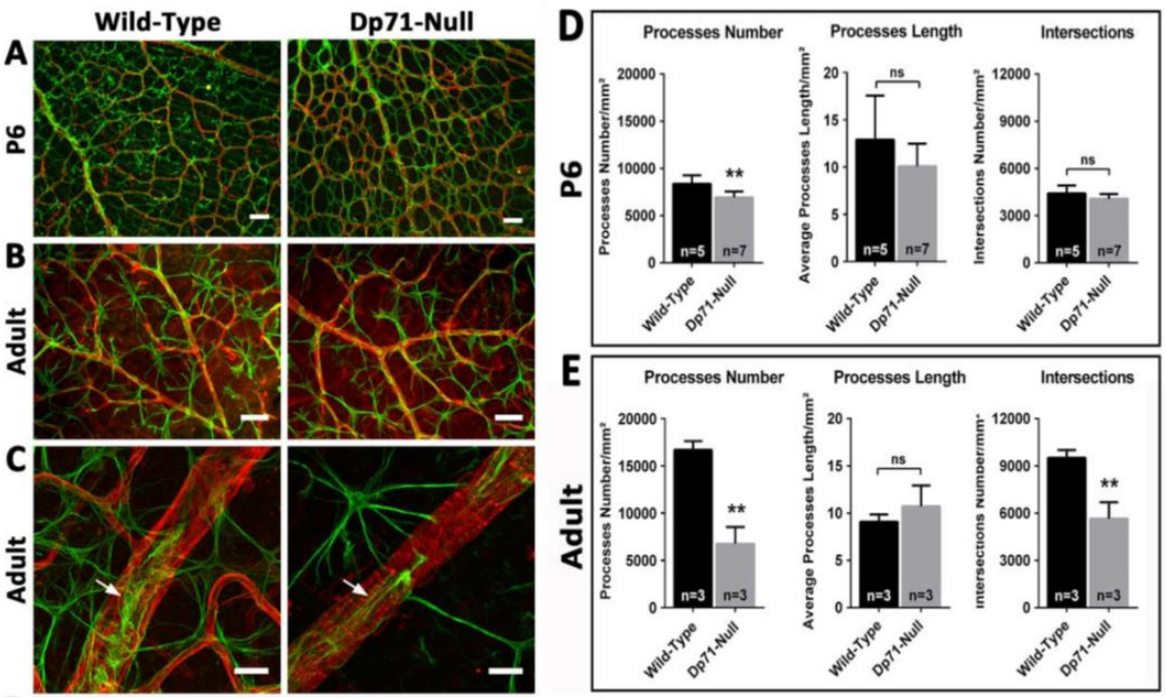


Figure 3.- Astrocytes morphology of WT and Dp71-null mice retina.

Visualization of the astrocyte network labeled with anti-GFAP antibody (green) and of the vascular network labeled with lectin GS (red) at post-natal day 6 **A.** and at the adult age **B.** (scale bars525 µm). **C.** Higher magnification of astrocyte network around major vessels in adult WT and Dp71-null mouse retinas. Flat-mount retinas labeled with lectin GS (red) and anti-GFAP antibody (green). Note the changes in morphology of retinal astrocytes in A and B in Dp71-null mice compared with control. In **C**, the white arrows point the different morphology of the astrocyte endfeet. **D**, **E**. Quantification of the astrocytes processes number, of their length and of their intersection number on images such as A for P6 (n=5–7) and B for adults (n=3) was obtained, using Analyze Skeleton plugin of Fiji (Giocanti-Auregan et al., 2016)

Homeostasis

Astrocytes and MGC seem to play a key role in retinal ion homeostasis needed for communication within and between neurons. Glial cells are responsible for potassium (K^+) homeostasis, neutralizing the potassium variations resulted from neuronal activity in this process, the glial cells dissipate local K^+ gradients by transferring the K^+ ions from areas of high concentration to those with low concentration. In MGC, K^+ conductance was determined to be asymmetrically distributed to their endfeet and perivascular processes. (Kofuji and Connors, 2003; Newman et al., 1984). Newman concluded that "in vascularized retinas, excess of K^+ is transferred into retinal capillaries as well as into the vitreous" (Newman, 1987).

In normal conditions, water is accumulated in the retina due to: an endogenous and continuous production associated with the synthesis of ATP, the inflow of water from blood vessels

Angiogenesis

Angiogenesis is the physiological process of formation of new vessels from a preexisting vascular network; which is essential for embryonic development and healing. A deregulation of angiogenesis is involved in pathological processes such as cancer, ischemia and certain retinal pathologies.

Angiogenesis under physiological conditions is controlled by pro-angiogenic molecules such as fibroblast growth factors (FGF) (Folkman and Shing, 1992), vascular growth factor (VEGF) (Ferrara et al., 1992) angiogenin (Fett et al., 1985), transforming growth factor (TGF) (Derynck, 1990), interferon (Brem et al., 1993), tumor necrosis factor (TNF) (Beutler and Cerami, 1986) platelet-derived growth factor (Ishikawa et al., 1989).

Inflammation

Inflammation is a host response to injury or infection in which is necessary to restore the homeostasis with the successful elimination of the injurious agent. The innate and the adaptive immune system work together during inflammatory response. It is initiated by the resident cells which release pro-inflammatory mediators which increase the capillary permeability and cellular migration into injured tissue. Successful inflammation process is a highly regulated process. If the injury stimulus persist, the inflammation become chronical, involving a deregulation of the healing response leading to an excessive response and destructive inflammation (Coutinho and Chapman, 2011).

The retinal inflammation characteristically presents an increase expression of inflammatory factors, an increased vascular permeability and a leucocytes recruitment associates with a retinal capillaries degeneration. Glucocorticoids inhibit vasodilation, some pro-inflammatory chemokines, enzymes, cytokines, and adhesion molecules are inhibited, it also induces expression of some genes like annexin 1, β2-adrenergic receptor and several cytokine receptors, decrease leukocyte migration into inflamed sites, alter cellular differentiation due to the transcriptional effect of GR, both up and down (Ashwell et al., 2000; Perretti and Ahluwalia, 2000).

Cell membranes are composed of fatty acids arranged in phospholipid bilayers; the arachidonic acid (AA) is particularly important as precursor of many bioactive lipids that regulated different processes like inflammation. AA is released from membrane by phospholipase A2 (PLA2) activity. One group of these bioactive lipids is the named class I which includes eicosanoids derived from AA: prostaglandins (PGs), leukotrienes (LTs) and lipoxins (LXs). Eicosanoids have roles in physiological processes like: regulation of smooth muscle tone, vascular permeability and platelet aggregation; they also participates in inflammation, autoimmunity, allergic diseases and cancer (Harizi et al., 2008; Wymann and Schneiter, 2008).

The synthesis of these inflammatory mediators are generated through either cyclooxygenase (COX) or lipoxygenase (LOX) activities; COX pathway catalyze the formation of PGG2 and PGH2 which are subsequently transformed in PGs and tromboxanes; meanwhile, LOX pathway leads the formation of diverse hydroperoxyeicosatetraenoic acids (HPETEs) and hydroxyeicosatetraenoic acids (HETEs) LTs; 5-HETE is converted into the leukotriene LTA4, which is the precursor of LTB4, cysteinyl-LTs (CysLTs) and LXs (Fig. 4) (Burgermeister et al., 2003; Harizi et al., 2008; Wymann and Schneiter, 2008).

Eicosanoids bind to membrane receptors; this can trigger an increase or decrease in the rate of cytosolic second messenger generation (cAMP or Ca2+), activation of a specific protein kinase or a change in membrane potential. Eicosanoids seem to have an important role in immunopathology, they have been implicated in pathobiology of cancer and inflammatory related disorders; the immunology function continuous to be investigated as well as the possibility to use PLA2 inhibitors as preventive or therapeutic agents (Harizi et al., 2008; Yarla et al., 2016).

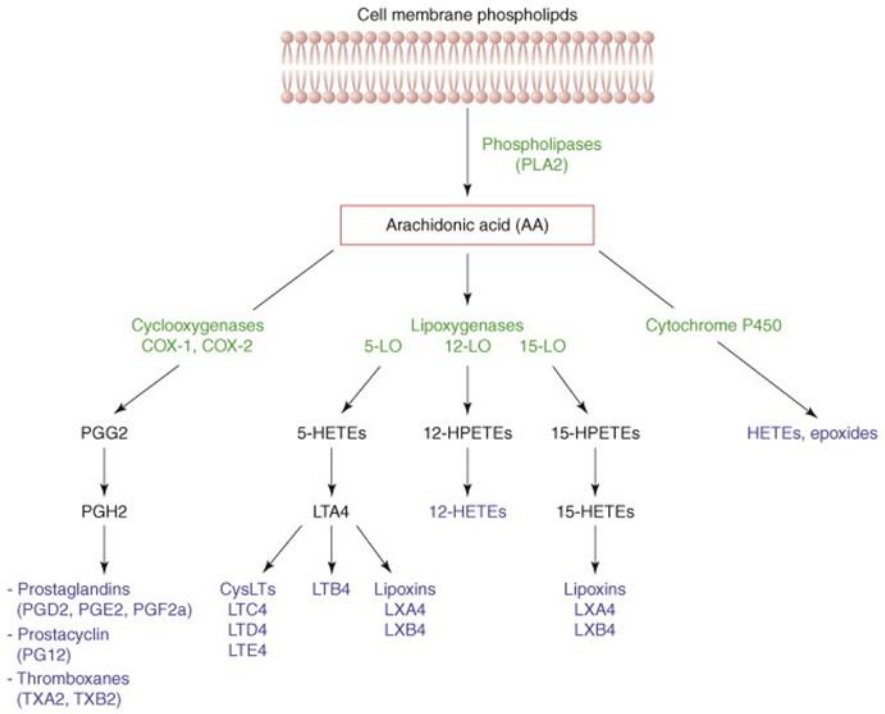


Figure 4.- Eicosanoid biosynthesis from arachidonic acid

Arachidonic acid derived eicosanoid pathway through the cell membrane phospholipids transformed in AA by phospholipase A2 and it subsequences transformation according with the different enzyme activities. The final products, prostaglandins, leukotrienes and lipoxins are shown (Harizi et al., 2008).

Ocular diseases

Many eye diseases present characteristic of neurodegenerative disorders, this can be explained by the similarities between the eye and the brain including structure, cell interactions and immune system. These similarities make the eye a convenient model for central nervous system studies due to its relatively accessible manipulation and administrations (intra vitreous or subretinal injection) as well as the retinal layer organization, which allow the identification of neurons and their interactions (London et al., 2012). Glaucoma, age-related macular edema, retinal vein occlusion, uveitis and diabetic retinopathy are diseases in

which an increase in vascular permeability is involved; the small solutes can diffuse through the vascular wall increasing the protein concentration in the interstitial and contribute to increase the tissue osmotic pressure leading to edema formation (Klaassen et al., 2013).

After intraocular surgery, a macular edema may occur; surgical damage to the iris/ciliary body or lens induces the synthesis of prostaglandins, which results in accumulation of other inflammatory mediators by this point, the BRB is disrupted. Vascular leakage is the mayor cause of vision loss.

Treatments

Glucocorticoids (GCs) are adrenal cortex-derived steroids that drives different physiologic functions; they have been widely used as effective treatments to control inflammatory and autoimmune diseases. Importantly for this work, the GCs have a robust effect on BRB by altering many pathophysiological pathways. They have a powerful anti-inflammatory role and also improve the barrier properties by increasing the integrity of tight junctions between endothelial cells (Barnes, 2006, 2011; Cronstein et al., 1992; Keil et al., 2013). Occludin and Claudin are transmembrane components of the tight junctions contributing to barrier properties. These two proteins also play a key role in the brain. Indeed, deletion of claudin gene leads to an increase in permeability of the blood brain barrier (BBB) and death shortly after birth (Runkle and Antonetti, 2011). Corticosteroids have been used for decades in the treatment of edema cerebral tumors (Keil et al., 2013) acting by reducing the VEGF-dependent signal and by increasing the properties of barrier. At the retinal level, corticosteroids have been shown to be effective in clinical practice on the resorption of macular edema, linked to venous occlusions, uveitis and diabetes (Lam et al., 2015). The role of occludin in tight junctions is complex, since phosphorylation and ubiquitination of occludin are necessary for the permeability of BRB induced by VEGF (Murakami et al., 2012). The glucocorticoid treatment leads to increased transcription of occludin and claudin-5 (Antonetti et al., 2002; Felinski et al., 2008). A decrease in

occludin phosphorylation, leads to an increase in the sealing of the tight junctions and a reduction of paracellular leaks (Antonetti et al., 2002). The corticosteroid action window is 24 to 48 hours. Therapy with GCs also have unwanted effects like diabetes-like syndrome and hypertension, especially after chronic use.

There is at present no formal proof in the literature of a direct effect of Dexamethasone (a synthetic GC) on the expression of the Dp71 protein. There are, however, elements in favor of this hypothesis, since the expression of the HSF1 protein, which was recently discovered as one of the transcription factors regulating the expression of Dp71 (Tan et al., 2015). In a murine model of Huntington's disease, associated with a decrease in expression of HSF1 in mice brain, daily subcutaneous administration of Dexamethasone helps restore HSF1 levels similar to healthy control (Maheshwari et al., 2014).

Dystrophin

Overview

The dystrophin protein is encoded by the DMD gene, discovered in 1987. This gene is located at the Xp21 locus (Koenig et al., 1987), and it is the largest gene described in humans with approximately 2.5 Mb. DMD gene is composed of 79 exons whose transcription generates a 14 Kb mRNA that translates into a protein of approximately 427 kD. This protein correspond to the full-length dystrophin also called Dp427 (Blake et al., 2002; Roberts et al., 1993).

The expression of dystrophin Dp427 is regulated by three independent tissue-specific promoters: brain, muscle and Purkinje promoters (Blake et al., 2002). DMD gene possesses at least four internal promoters that leads the expression of dystrophins: Dp260 (D'Souza et al., 1995), Dp140

(Lidov and Kunkel, 1997), Dp116 (Byers et al., 1993), Dp71 (Lederfein et al., 1992) and Dp40 (Tinsley et al., 1993) (Fig. 5).

The Duchenne muscular dystrophy (DMD) is a disease linked to the X chromosome that affects one in every 3,500 males. This disease is characterized mainly by the progressive degeneration of muscle cells (Blake et al., 2002; Spence et al., 2002). In addition to muscle disorders, about 30% of patients with DMD have mental retardation and retinal abnormalities.

DMD is caused by mutations that generate the absence of dystrophin Dp427 protein, whereas Becker's muscular dystrophy (DMB), a less severe analogue, is caused by mutations that generate reduced expression or a partial loss of dystrophin function (Blake et al., 2002; Monaco et al., 1986). Cells that lack dystrophin Dp427 show membrane instability with progressive and fatal degeneration of muscle cells, calcium homeostasis alterations, increased membrane permeability and increased susceptibility to oxidative toxins (Blake et al., 2002).

Patients with DMD at birth only show increased levels of the muscle isoform creatine kinase enzyme, it is up to the age of 3 to 5 years when they present the first symptoms that are: delay, instability and difficulty walking as well as difficulty to climb stairs. Subsequently, the appearance of pseudo-hypertrophy of the calf muscles, muscle weakness of the limbs, and the Gowers sign (the child uses his arms to sit up when he moves from a lying position to stand) suggest DMD. Finally, there is a decrease in the strength of the lower muscles and contractures in the joints which causes patients to be confined to a wheelchair, usually at age 12, weakness in the upper extremities occurs later. Most patients die in the second or third decade of life because of respiratory complications or as a result of cardiac dysfunction with cardiomyopathy. In patients with DMB the onset of the disease is late and the course of the disease is slower (Blake et al., 2002).

In skeletal muscle, dystrophin Dp427 interacts with different proteins, called DAPs (dystrophin-associated proteins). The N-terminal domain of

dystrophin interacts with actin while the cysteine rich region and the C-terminal domain interacts with a set of glycosylated transmembrane proteins and cytoplasmic components to form the dystrophin-associated protein complex (DAPC). This complex consists of three sub-complexes: the dystroglycan complex, the sarcoglycan sarcospan complex and the cytoplasmic protein complex. Among the proteins that form the DAPC are: dystrophin or utrophin, α- and β-dystroglycan, α-, β-, δ-, γ-, ε- and ζ-sarcoglycans, sarcospan, α- and β-dystrobrevin, α- and β-syntrophin, caveolin-3, neuronal nitric oxide synthase (nNOS), calmodulin, etc. (Fig.5) (Blake et al., 2002; Suzuki et al., 1992, 1994). This complex is critical to maintain the integrity of muscle fibers, since it mediates the interaction between the actin cytoskeleton and the extracellular matrix; also, it has been assigned as a scaffold for other proteins including signaling proteins.

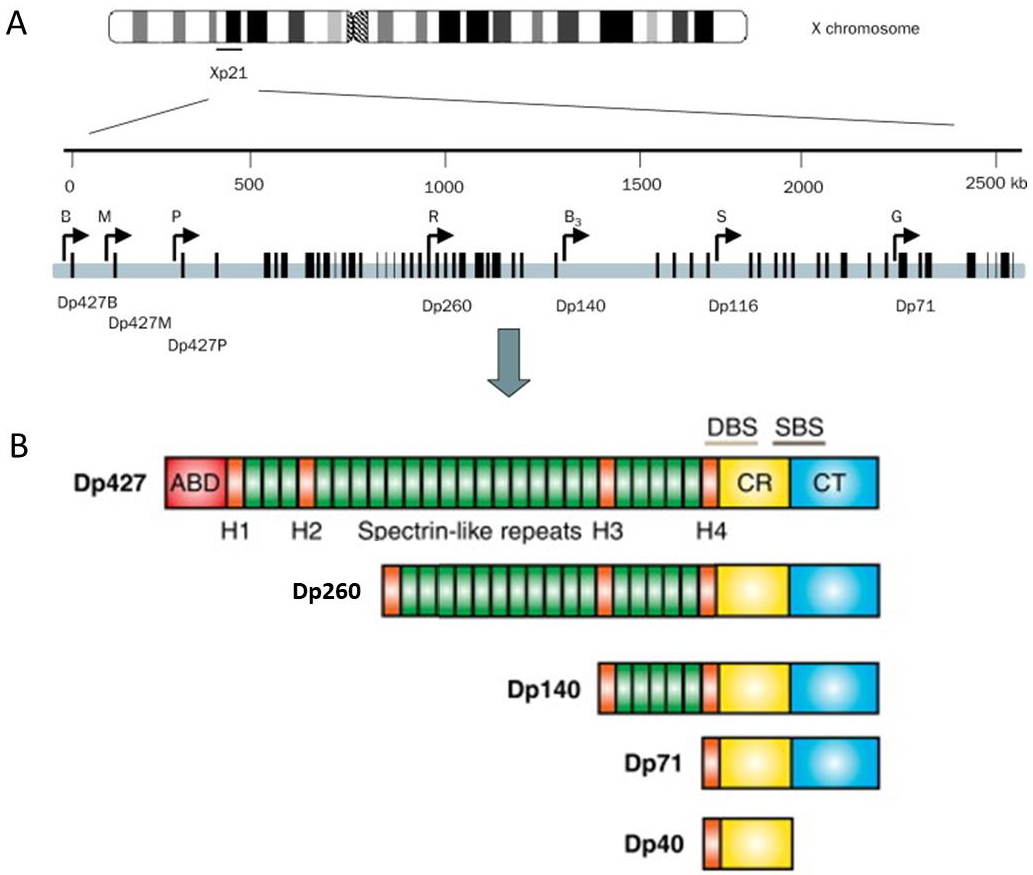


Figure 5.- Schematic representation of DMD gene and dystrophin protein.

A. The dystrophin (DMD) gene located at Xp21 and has three promoters that expressed the full-length dystrophin, called Dp427. Each promoter expresses Dp427 in tissue dependent manner: brain (B), muscle (M) or purkinje (P) cells. This gene also contains internal promoters that expresses smaller DMD products named according to their molecular weight as dystrophin: Dp260, Dp140, Dp116, Dp71 and Dp40 respectively. **B.** Dp427 protein representation. The amino-terminal domain (red) with the actin binding domain, the central rod domain with the spectrin-like repeats (green) and proline-rich hinge regions (H1-H4 orange), the cysteine-rich domain (CR yellow) including the β-dystroglycan binding site (DBS) and finally the carboxy-

terminal domain (CT blue) which contains the syntrophin and dystrobrevin binding sites. Modified from: (Muntoni et al., 2003; Waite et al., 2012).

The DAPC is present in numerous non-muscular tissues, notably in the central and peripheral nervous system, tissues with secretory functions, in barriers between physiological compartments such as the blood-brain barrier, choroid plexus or kidney. Although the role of the DAPC in these tissues is unclear, there is evidence that it is involved in brain development, synapse, neuronal plasticity as well as water and ion homeostasis. In non-muscle tissues the DAPC is generally concentrated in the cell membrane facing the basal lamina and the components that form it have binding sites for membrane channels or transporters. Reports indicate that dystrophin and DAPs promote the clustering and subcellular distribution of Kir4.1 channels in MGC (Blake et al., 2002; Haenggi and Fritschy, 2006; Kofuji and Connors, 2003).

Dystrophin Dp71

Dystrophin Dp71 was identified by studying a 6.5 kb mRNA that is transcribed from the promoter located within the intron 62 of DMD gene, which translates into one of the smaller products of this gene with a molecular weight of 70.8 KDa (Hugnot et al., 1992). The Dp71 promoter (classic promoter) is under complex regulation, which is tissue dependent, cell type and embryonic development stage specific (Sarig et al., 1999).

Dp71 has a ubiquitous expression except for skeletal muscle, it has been identified in several non-muscular tissues and identified as the main product of the DMD gene in the brain. Dp71 amino terminal domain contains actin binding sites, this dystrophin lacks the spectrin-like repeats

present in the full-length dystrophin (Dp427), contains the cysteine-rich domain and the carboxy-terminal domain (C-terminal domain) characteristic of all dystrophins (Lederfein et al., 1992).

Dystrophin Dp71 is expressed in: retina, cerebellum, cerebral cortex, epidermis and choroid; in addition, it is abundantly expressed in the dentate gyrus of the hippocampus and in lower levels in the olfactory bulb, CA3 region of the hippocampus and the cerebral cortex. It has been reported that Dp71 plays an important role in brain development, synapse formation and brain plasticity (Benabdesselam et al., 2010; Lumeng et al., 1999; Tadayoni et al., 2012).

An increase in Dp71 expression during differentiation of the central nervous system has been reported, suggesting that the complex formed between Dp71 and DAP's in brain functions as scaffold for proteins involved in cell membrane stability and in transmembrane signaling (Tadayoni et al., 2012). Approximately 30% of patients with DMD have reported cognitive deficits, which have been associated with mutations that prevent the correct expression of small dystrophins, specifically Dp140 and Dp71 (Daoud et al., 2009a; Perronnet and Vaillend, 2010; Sarig et al., 1999).

Dystrophin Dp71 isoforms

In 1980, the existence of alternative RNA processing at the 3' end of Dp71 transcript was described, giving rise to a large variety of dystrophin isoforms which differ from each other at the C-terminal domain (Feener et al., 1989). Alternative C-terminal domain let us to classified Dp71 isoforms into three groups: Dp71d, Dp71f and Dp71e; the isoforms present in each group are represented in figure 6 (Aragón et al., 2017).

Isoforms that lack exon 78 produces a protein in which the last 13 amino acids of the Dp71 are replaced by 31 new residues, which form a hydrophobic C-terminal domain so-called the "founder" sequence. The isoforms with founder sequence belong to the Dp71f group (Bar et al.,

1990). The loss of exon 71 ($Dp71d_{\Delta 71}$, $Dp71f_{\Delta 71}$ and $Dp71e_{\Delta 71}$) or exons 71-74 ($Dp71d_{\Delta 71\text{-}74}$, $Dp71f_{\Delta 110}$ and $Dp71e_{\Delta 71\text{-}74}$) do not generate changes in the open reading frame. However the loss of exons 71-74 causes that the protein lack the syntrophin binding site (Ceccarini et al., 1997). The identification of $Dp71f_{\Delta 110}$ in human adult brain was made by Austin et al., who sequenced a smaller than expected PCR product finding the absence of exons: 71-74; subsequently, they reported the presence and absence of exon 78. Finally, a protein of approximately 58 kDa was demonstrated using antibodies against Exon 77, this same protein is not detected by antibodies against exons 73-74 (Austin et al., 2000).

The dystrophin $Dp71e_{\Delta 71}$ (Fig. 6) has a new alternative RNA processing site which adds 34 bp from intron 77 between exons 77 and 78. This generates a stop codon that impedes exons 78 and 79 translation, and provides the protein a different C-terminal domain with 10 hydrophilic amino acids, some of them with potential for phosphorylation; There is also an isoform that possesses this intronic sequence and lacks exons 71-74 called $Dp71e_{\Delta 71}$ (Saint Martín et al., 2012).

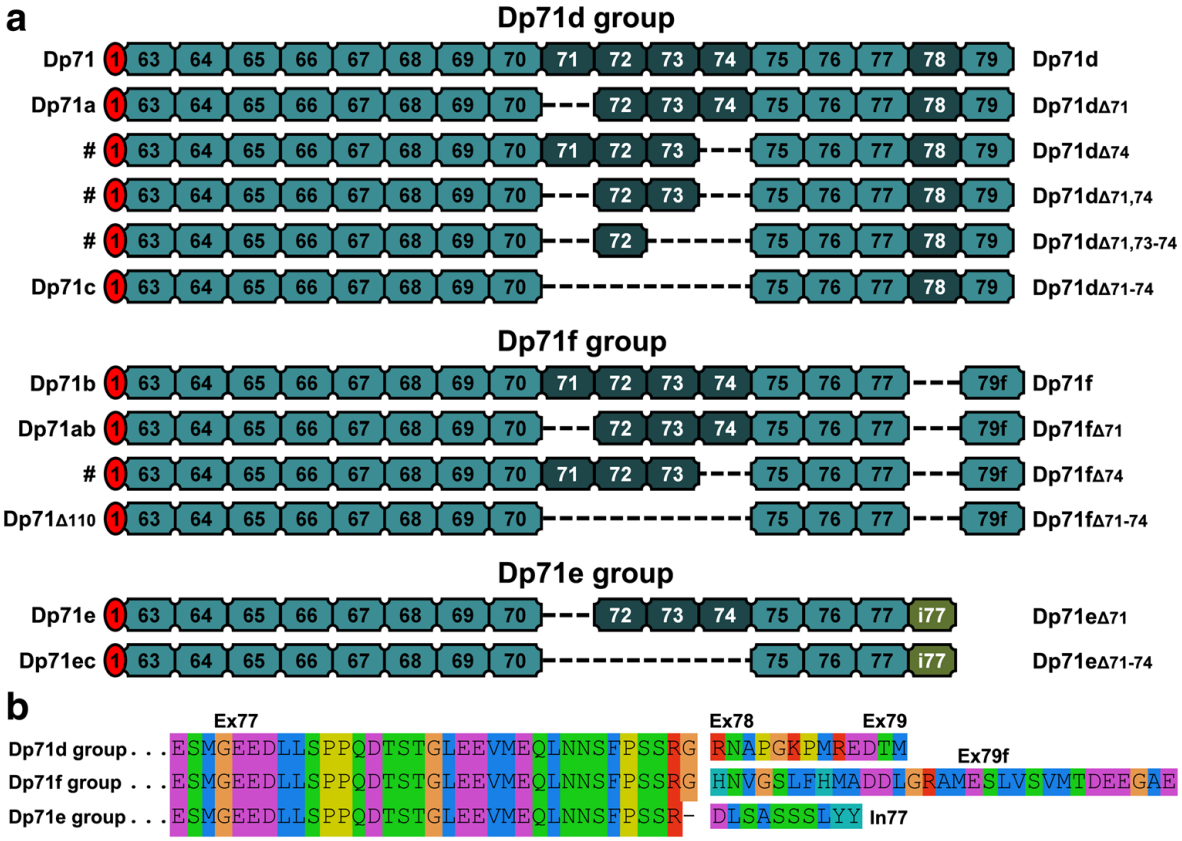


Figure 6.- Schematic representation of Dp71 isoforms.

A. Groups of Dp71 isoforms (Dp71d, Dp71f, and Dp71e). Dp71d group carries exons 78 and 79; Dp71f group lacks exon 78 and has the "founder" sequence and Dp71e group contains the intron 77 (i77) and lacks exons 78 and 79 at the protein level. Dotted lines show the exon lost by alternative splicing. Names of Dp71 isoforms suggested by Aragon et al. are indicated at right. **B.** Alignment of Dp71 amino acid sequences covering the exons 77, 78, and 79. The exons (Ex), alternative exon 79 (Ex79f) or intron 77 (In77) are indicated (Aragón et al., 2017).

Dp71 functions

As Dp71 is able to restore the DAPC components, expression and localization, but it fails to ameliorate muscular dystrophy (Cox et al., 1994); it is reasonable to think that Dp71 has a particular role with different functions than muscular dystrophin. The main non-muscular DMD phenotypes that are: non-progressive mental retardation and retinal dysfunction are associated to Dp71. Different studies involved Dp71 in specific cell processes like: neuronal plasticity (Górecki et al., 1998), cell adhesion (Cerna et al., 2006), retinal homeostasis (Fort et al., 2008; Sene et al., 2009), cell differentiation (Romo-Yáñez et al., 2007), cell division (Villarreal-Silva et al., 2011), actin-cytoskeleton remodeling (Cerecedo et al., 2006) and nuclear envelope-associated function (Villarreal-Silva et al., 2010).

Dp71 is the main DMD product expressed in the brain mainly in astrocytes and neurons. Dp71 is expressed in the cell membrane of cultured astrocytes, forebrain astrocytes (Dp71d) and retinal astrocytes. Dp71d immunolabeling is also detected in hippocampal neurons, while nuclear immunostaining of Dp71f has been observed exclusively in neurons. Interestingly, one study showed that activation of glutamate receptors by kainate alters mRNA expression of dystrophin and Dp71 in rat hippocampus, suggesting the involvement of the DMD gene in neuronal plasticity (González-Ramírez et al., 2008; Górecki et al., 1998; Tadayoni et al., 2012).

Another non-muscular characteristic present in DMD patients, corresponds to an altered electroretinogram (ERG), present in 80% of the patients who also exhibit a reduction of the wave B amplitude. The small dystrophins Dp260, Dp140 and Dp71 are expressed in retina; importantly, Dp71 has been located around blood vessels and in the limiting membrane. Studies in retina show that the DAPs and specifically Dp71 are involved in the expression and localization of water channels (aquaporin AQP4) and potassium channel (Kir4.1) in MGC, regulating essential functions such as

retinal homeostasis and maintenance of blood retinal barrier (Fort et al., 2008; Tadayoni et al., 2012).

Dp71 also plays an important role in cell adhesion either between cells or interacting with the extracellular matrix. Marquez et al. (2003) described how Dp71d accumulates in cell-cell junctions (Marquez et al., 2003) while Cerna et al. (2006) proposed the formation of a cell adhesion model to the extracellular matrix through the interaction of Dp71f and the beta1-integrin adhesion system (Cerna et al., 2006).

A role in cell division has been attributed to Dp71 since Villarreal-Silva et al. (2011) postulated that Dp71 is a component of the mitotic spindle and of multiprotein cytokinesis devices that can modulate the cell division cycle by lamin B1 and β-dystroglycan thus conferring a correct localization and stability (Villarreal-Silva, Centeno-Cruz et al., 2011). The importance of the Dp71 isoforms for NGF-mediated cell differentiation in PC12 cells has also been identified. An increase in $Dp71_{\Delta 71}$ (Dp71ab) expression was observed during the differentiation of these cells (Marquez, Cisneros et al., 2003). On the other hand, the components of the $Dp71f_{\Delta 71}$-associated protein complex in non-differentiated PC12 cells: β-dystroglycan, α1-syntrophin, β-dystrobrevin and α-, β- and γ-sarcoglycan changed upon differentiation induction to: β-dystroglican, α1-syntrophin, β-dystrobrevin and γ-sarcoglycan (Romo-Yanez, Ceja et al., 2007).

Dp71 in Retina

The abnormal ERG observed in patients with DMD has been attributed to the altered expression of the short products of the DMD gene since patients with deletions in the central region of the gene have an abnormal ERG whereas most patients with mutations within the gene 5'-end have a normal ERG. Dystrophins Dp260, Dp140 and Dp71 are expressed in the mouse retina (D'Souza et al., 1995), and although the retina of Dp71 null mice appears physiologically normal, it is more vulnerable to ischemic lesions than the retina of wild-type mice.

Sarig and collaborators were the first to identify the activity of the Dp71 promoter in the retina, in this tissue, Dp71 is located around the blood vessels of the ganglion cell layer and within the internal limiting membrane (Howard et al., 1998; Sarig et al., 1999). In MGC, clusters are observed for Dp71f with a particularly strong staining at the end of the feet of these cells, whereas dystrophin-associated proteins have a predominantly membranal location. DAPs (β-Distroglycan, δ- and γ-sarcoglycans and α1-syntrophin) are also localized in other retinal cell types whereas Dp71f expression is restricted to MGC and Astrocytes, suggesting a specific function within these cells (Claudepierre et al., 2000; Giocanti-Auregan et al., 2016).

Retinal studies demonstrate that DAPs and Dp71 control the expression and localization of water channels (aquaporin AQP4) and potassium (Kir4.1) in MGC. Correct expression and localization of AQP4 and Kir4.1 channels are essential for the adequate function of these cells; their functions include retinal homeostasis and maintenance of the blood-retinal barrier. The Dp71 associated DAPC described in retina (Fig. 7) includes: ε-sarcoglycan (ε-SG), β-dystroglycan (β-DG), water channel: aquaporin 4 (AQP4), Inward rectifying potassium channel Kir4.1, α-syntrophin (α-Syn) and α-dystrobrevin (α-DB); it is localized in MGC endfeet in the cholesterol rich plasmatic membrane domain (Dalloz et al., 2003; Fort et al., 2008; Tadayoni et al., 2012).

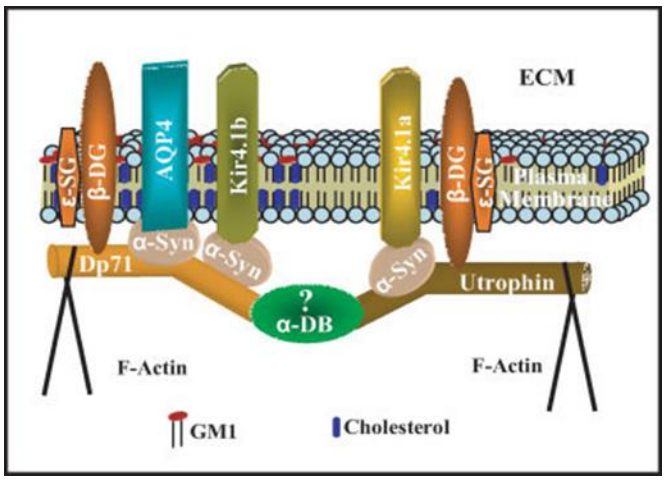


Figure 7.- Model of Dp71 complex binding Kir4.1 and AQP4 in retina

Dp71-DAP complex at the endfeet of MGC, localized in GM1 cholesterol enriched plasma membrane domain. The DAP includes: ε-sarcoglycan (ε-SG), β-dystroglycan (β-DG), water channel: aquaporin 4 (AQP4), Inward rectifying potassium channel Kir4.1, α-syntrophin (α-Syn), α-dystrobrevin (α-DB) (Fort et al., 2008).

On the other hand, experimental retinal detachment triggers a decrease in Dp71 expression, delocalization of Kir4.1 channels and decrease of AQP4 in MGC. In addition, in the absence of Dp71, vascular permeability of the retina increases. With the above data, it can be stated that the lack of Dp71 leads to physiological alterations of the MGC similar to those observed in lesions or diseases of the retina (Sene et al., 2009). Therefore, by controlling the expression and subcellular distribution of potassium and water channels, Dp71 and DAP are essential for the functioning of MGC helping to maintain the BRB.

Dystrophin Dp71 spliced isoforms that lack exon 78, Dp71f group, are also localized in MGC; with a clustered intracellular localization and surrounding the cell nucleus. In MGC, the Dp71f levels are higher than those observed for utrophin (Claudepierre et al., 1999, 2000).

It has been reported that Dystrophin Dp71 is expressed in retinal astrocytes around blood vessels and at the inner limiting membrane. In astrocytes Dp71 had been related with the development of the complex astrocytes network and astrocyte morphology as well as angiogenesis delay in processes of the retina. However, it seems like dystrophin Dp71 is not involved in the postnatal astrocytes migration during retinal development (Giocanti-Auregan et al., 2016). The Dp71 null-mice presents an overexpression of VEGF, ICAM-1 and AQP4, as well as an increase in the number of adherent leukocytes, meaning an implication of Dp71 in inflammation (El Mathari et al., 2015).

Dp71 in the Brain

The presence of non-progressive mental retardation is now widely accepted and recognized as a common feature for a substantial proportion of patients with DMD (1 standard deviation below average). The analysis of intellectual functioning and DMD revealed that both verbal and nonverbal intelligence is affected in children with DMD(Cotton et al., 2001). Some mutations located in Dp71 transcript and deletion in Dp140 transcript were correlated with patients with severe mental retardation; molecular analyses in 81 DMD or BMD patients showed that mutations affecting Dp71 expression or mutations in exons 75 and 76 are associated with mental retardation. Moreover, DMD patients with mutations upstream of exon 62 (not affecting Dp71 expression), are associated with normal or borderline cognitive IQ values. The lack of Dp71 expression constitutes a factor that contributes to the severity of mental retardation (Daoud et al., 2009a; Moizard et al., 1998).

Dp71 is expressed in different CNS structures and cells, including neurons in the hippocampus, olfactory bulb (Górecki and Barnard, 1995), post-synaptic densities (Blake et al., 1999), perivascular astrocytes (Szabó et al., 2004) and MGC in the retina(Claudepierre et al., 2000).

Recently, several isoforms expressed in CNS were reported including; Dp71, Dp71d$_{\Delta 71}$ (Dp71a), Dp71d$_{\Delta 71\text{-}74}$ (Dp71c), Dp71f (Dp71b), Dp71f$_{\Delta 71}$ (Dp71ab), and Dp71$_{\Delta 110}$ and the newest isoforms: Dp71d$_{\Delta 71,74}$. The isoforms Dp71d$_{\Delta 71}$, and Dp71d$_{\Delta 71\text{-}74}$ are the most highly expressed in the brain compared with the retina. The Dp71d group is more expressed in brain while in retina the Dp71f group was more abundant (Aragón et al., 2017).

One study of Dp71-null mice provided the first strong evidence to understand how the loss of Dp71 can alter neuronal and cognitive functions; assigning a regulatory role of Dp71 in glutamatergic synapse organization and function (Daoud et al., 2009b). The data suggested that Dp71-DAPC associate with the multiproteic complex that cluster the glutamate receptor and organize signaling proteins required for synaptic transmission and plasticity.

Cell junctions

The formation of epithelia, the anchoring of cells with the basement membrane, cell migration, cell polarization as well as the formation of neuronal projections are examples of processes and cellular behaviors for which the selective adhesion of the cells is indispensable either to other cells or to the extracellular matrix. The specificity of cell adhesion is due to the expression and interaction of various receptor molecules as well as ligand molecules present in another cell or in the extracellular matrix (Hynes, 1999).

An important feature that allows these adhesion molecules to regulate the functions of proliferation, survival and differentiation is that in their intracellular domains they possess binding sites with the actin filaments. They may also interact with other molecules capable of transmitting signals in response to stimuli received from outside the cell (Burridge and Chrzanowska-Wodnicka, 1996). Among the most important cell adhesion receptor families are integrins, cadherins, selectins as well as the immunoglobulin superfamily (Hynes, 1999).

In 2002 the presence of a cadherin homolog domain within the ε-SG sequence was found (Dickens et al., 2002), this domain is characteristic of molecules involved in cell adhesion interactions. This suggests the possibility that there is interaction between ε-SG and the molecules that make up the complexes of cellular interaction.

General objective

TO STUDY THE ROLE OF DYSTROPHIN Dp71 IN BOTH, PATHOLOGICAL AND PHYSIOLOGICAL CELLULAR PROCESSES.

First part objectives:

- Characterize the impact of a surgically induced iBRB breakdown on retinal homeostatic changes due to dystrophin Dp71, AQP4, and Kir4.1 alterations in MGC in a mouse model.
- Elucidate the mechanism of action of dexamethasone during the prevention of retinal edema.
- Compare the effect of different glucocorticoids on Dp71, AQP4, and Kir4.1 expression.

Second part objectives:

- Analyzes the interaction between Dp71d ($Dp71d_{\Delta 71}$ and $Dp71d_{\Delta 71\text{-}74}$) and ε-SG in PC12 cells.
- Identify proteins that form part of the complex formed by Dp71d and ε-SG in PC12 cells.
- Measure the cell to cell interaction ability of PC12 cells that over-express $Dp71d_{\Delta 71}$ and $Dp71d_{\Delta 71\text{-}74}$.
- Propose a specific role of $Dp71d_{\Delta 71}$ and $Dp71d_{\Delta 71\text{-}74}$ isoforms at the intercellular junction sites.

Methods

Animals

All experiments were done in compliance with the European Communities Council Directives (86/609/EEC) for animal care and experimentation (HMG). Mice were handled in accordance with the ARVO statement for the use of animals in ophthalmic and vision research (IOVS).

Experimental Models

Three different experimental models were used:

1. Lens surgery

For this study, 8-week-old C57BL/6J mice (Janvier, St Bethervin, France) were used in accordance with the ARVO Statement for the Use of Animals in Ophthalmic and Vision Research.

Surgical procedure was performed using isoflurane; pupils were dilated with topical phenylephrine (2.5%) and tropicamide (1%). Under surgical microscope, a 30-gauge needle was inserted into the posterior part of the lens to remove it, allowing a direct contact between remaining lens fragments and the vitreous to induce vitreous inflammation and inner BRB breakdown in the context of an Irvine Gass syndrome model (Fig. 6).

Under isoflurane, a single dose (1 µL) of 10 mg/mL dexamethasone (Sigma-Aldrich, Saint-Quentin, France) diluted in balanced saline solution (BSS) (Alcon Laboratories, Inc., Rueil- Malmaison, France) was injected intravitreally with a 33-gauge microinjector (Hamilton, Bonaduz, Switzerland). A control group received an equal volume of vehicle (BSS). Lens surgery was performed at day 0. Twenty-four hours post-surgery, mice received a dexamethasone or vehicle injection (n=22). Inner BRB permeability was measured 24 hours (n=5 per group) and 48 hours (n=5 per

group) after injection, and at 48 hours, total proteins extracts were prepared (n=12 per group).

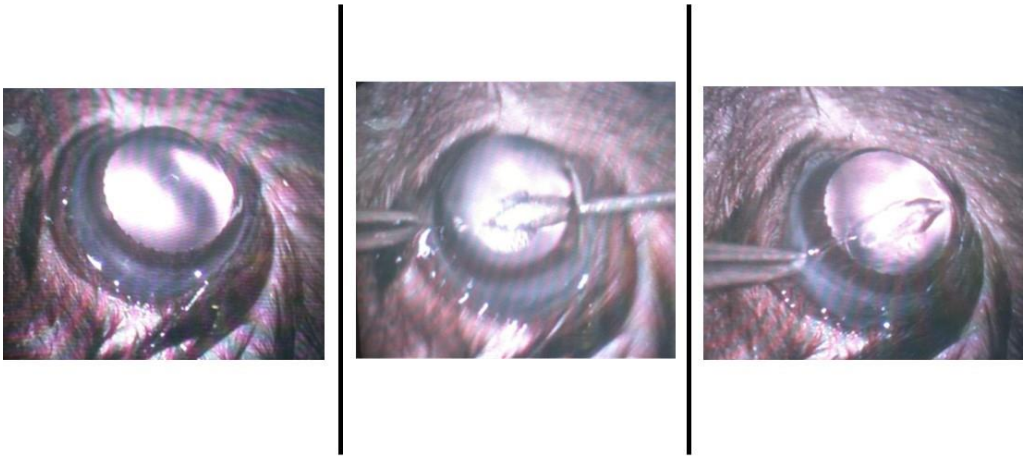


Figure 8.- Lens surgery.

Wild-type mice lens observed through microscope. The normal lens (left photo), the eye during the surgery (central photo) where the gauge is in the posterior part of the lens and the eye post-surgery that presents the lens scar (right photo) are shown. Photos obtained from the surgical microscope.

2. Retinal Explants

Three Millicell insert membranes were placed in a sterile six-well plate containing 500 µL/well of isotonic solution (136 mM NaCl, 3 mM KCl, 2 mM $CaCl_2$, 1 mM $MgCl_2$, 10 mM HEPES, and 11 mM glucose, adjusted to pH 7.4 with Tris) or hypoosmotic solution (60% of isotonic solution) containing 1 mM of Ba^{2+} ions (potassium channel blockers). The membranes were placed into each well with the hydrophilic side facing the well bottom in contact with the respective solution.

After enucleation, eyes were maintained in CO_2-independent medium (Gibco, Waltham, MA, USA) and quickly processed to perform the retina dissection (Sawamiphak et al., 2010).

Retinas were placed with the photoreceptors facing the membrane, and 1 mL solution was added to each well. Dexamethasone (10 mg/mL) was added on the retina top. The plates were incubated at 358C in a humidified incubator with 5% CO_2 for 8 hours. After incubation, the retinas were processed to obtain RNA or treated with papain (0.3 mg/mL) and immune-stained using an anti-GS antibody and DAPI (Sigma-Aldrich) to identify MGC. Images were captured using an Olympus FV1000 laser-scanning confocal microscope. The size quantification of the soma was performed selecting the soma area of individual cells and using the area measure tool of ImageJ software ($n \geq 30$ cells); the values are expressed in percentages.

3. Cells culture

PC12 and PC12/Tet-On cells were cultured in DMEM medium (Dulbecco's Modified Eagle Medium, Gibco) supplemented with 10% horse serum (Gibco) and 5% fetal bovine serum (Gibco); added with penicillin (100 Uml), streptomycin (1 mg/ml) and mycostatin (0.25 µg/ml) then incubated at 37°C in a humidified atmosphere with 5% CO_2. For maintenance, cells lines: PC12/TetOn-Dp71a, PC12/TetOn-Dp71ab, PC12/TetOn-Dp71c, PC12/TetOn-Dp71e and PC12/TetOn-Dp71ec; the medium were supplemented with Puromycin (200 µg/ml).

Cells were cultured in P100 (100 mm), P60 (60 mm) dishes or in 4, 6 and 12 well plates previously treated with collagen or on top of poly-L-lysine treated coverslips (100 µg/ml) as required.

For differentiation induction, 20,000 cells were seeded in 4 well plates or 30,000 in 6-well plates and incubated in supplemented medium (1:10) for 5 hours. Doxycycline (100 µg/ml, Dox) was added to induce Dp71 isoform expression and the cells incubated for 18-20 hours. The medium was replaced with fresh medium supplemented with neuronal growth factor (NGF) 50 ng/ml, every 3 days. Cells were harvested after 9 days of differentiation induction for analysis.

DNA extraction and PCR

Cell cultures were processed immediately after removal from the incubator. Grown cells in suspension where resuspended and centrifuged at 8000g for 5 min at RT (15-25 ºC) and supernatant discarded; the cell pellet was washed with PBS. Trizol (1 ml reagent per 1 × 10^7 cells) was added to cell pellets, the lysate was resuspended with a sterile disposable 1 ml pipette tip. Then the tissue or cell lysate was transferred to a 1.5 ml new tube.

The homogenate was incubated at RT (15-25 ºC) for 5 min for complete dissociation of nucleoprotein complexes. Then 200 µl of chloroform were added and the samples were vortexed vigorously for 15 seconds. The homogenate was incubated at RT for 3 min.

Samples were centrifuged at 12,000 x g for 15 min at 4°C. The upper aqueous phase (600 µl) was transferred to a new 1.5 ml RNase-free tube. Finally, the DNA was precipitated with alcohol.

Protein extraction and Western blot assay

Cells were collected and washed with PBS buffer. Extraction buffer 2 (1% Triton X-100, 150 mM NaCl, Tris HCl 50 mM pH = 7.4; complemented with protease inhibitor cocktail before being used) was added according with the cell pellet size. After 20 minutes incubated at room temperature, sample buffer volume (100 mM Tris, 20% glycerol, 0.05% bromophenol blue, pH 6.5) was added and then the samples were boiled (10 minutes) before freezing at -20 °C until use.

For protein extraction starting from tissue, 100 µl of RIPA buffer (NaCl 150 mM, Triton 1%, SDS 0,1 %, Desoxycholate 0.01%, Tris HCL 50 mM pH = 7.2; complemented with protease inhibitor cocktail before being used) were added to each retina. Tissue was disintegrated using Polytron then centrifugated and supernatant transferred to a new tube. Finally, one volume of sample buffer (100 mM Tris, 20% glycerol, 0.05% bromophenol blue, pH 6.5) was added and the samples were boiled by 10 minutes before

storage at -20 °C until use. Total protein was quantified by the Bradford method using 96-well plates, using a bovine serum albumin as standard (0.5-5 µg).

For immunoassays, denaturing SDS-10% polyacrylamide gels were loaded with 20 µg of total protein and run at 100 volts. Proteins were blotted to nitrocellulose membranes at 300 mAmp for 2 h at 4 °C. Membranes were blocked in TBS-T buffer (Trizma Base 100 mM, NaCl 1.5M, Tween-20 0.5%) containing 5% dry milk (1 hour at room temperature) and incubated with the primary antibody at 4 °C overnight in the same blocking buffer. The dilution and specific conditions for each antibody used are presented in Table No1. Membranes were washed and incubated with the respective secondary antibody, anti-mouse or anti-rabbit IgG, conjugated to horseradish peroxidase. A chemiluminescent peroxidase substrate (Western Lightning Plus-ECL from PerkinElmer) was added and chemiluminescence was detected using X-ray films.

Table 1.- Antibodies. Sense and antisense oligonucleotides using for quantitative RT-PCR

Name	Protein	Reference	Immunostaining	Wester Blot
GFAP	Glial Fibrillary Acidic Protein	Sigma Aldrich	1:500	-
H4	Dystrophins	Mornet *	1:500	1:5000
Cx43	Connexin 43	Abcam	1:50	1:6,000
β-Act	β-actin		-	1:500
AQP4	Water channel Aquaporin 4	Alomone Labs	1:500	1:100
Kir4.1	Inward rectifying potassium channel Kir4.1	Alomone Labs	1:500	1:100
GS	Glutamine synthetase		1:500	-
LG7	ε-sarcoglycan	Mornet*	1:25	1:5000
Myc	α-Myc	Abcam	1:300	1:500
HSF1	Heat shock factor 1	Cell Signaling Technology	-	1:1000

* H4 a rabbit polyclonal antibody that recognizes all dystrophin isoforms (Rivier et al., 1999).

Immunofluorescence assay

PC12 cells

For cell differentiation studies, 20,000 to 30,000 cells were seeded on coverslips covered with poly L-lysine (100 µg/ml). For non-differentiated cells immunofluorescence, cells were cultivated to 80% confluence on treated coverslips. For indirect immunofluorescence (IFI), cells adhered to the coverslip were washed with cytoskeletal buffer (CB) (10 mM MES, 150 mM NaCl, 5 mM EGTA, 5 mM MgCl 2, 5 mM Glucose) and fixed with 4% paraformaldehyde. Permeabilization was performed with paraformaldehyde-triton (4% and 0.4% respectively) in CB. Blocking was performed using 0.5% gelatin in PBS (0.5%) for 40-50 minutes.

Primary antibodies are (Table No1) were incubated at 4 °C/18-20 hours. Secondary antibody was incubated 1 hour at room temperature. Cells were stained with 1:1000 DAPI (4',6-diamidino-2-phenylindole). Vecta Shield (Vector laboratories, Inc) was used to mount the coverslips and sealed with nail varnish.

The images were obtained by confocal microscopy using the Leica TCS SPE microscopes and the Leica multiphotonic SP8.

Müller Glial cells stain

The retinas were incubated at 37°C for 30 minutes in 500 µl of 0.3 mg/mL of papain (Papain from Carica papaya, 10108014001, Roche) in PBS in a 1.5 ml micro tube. They were washed in 1ml of PBS and briefly fixed in 4% paraformaldehyde (PFA) for 10 minutes, followed by 3 washes in PBS added with DNase (160 U/ml Invitrogen).

The retinas were homogenized using a 1 ml pipette (up and down) until dissociation (5-10 times max). 100-200 µl of the fresh homogenate was layered on glass slides and left to dry on a hot plate until white residue

appear (5 minutes max). The attached cells were rehydrated with 200 µl of PBS, briefly fixed in 2% PFA for 30 minutes and washed with PBS. The permeabilization was done using PBS added with 0.1% Triton for 5 min at room temperature. The samples were block 1 hour with a 0.1% Tween20 + 3% NGS + 1% BSA PBS solution.

Cells were incubated with primary antibodies (Table No1) overnight at 4°C, washed 3 times with PBS added with 0.1% Tween for 2 minutes. Then, the Alexa-coupled secondary antibodies and DAPI (1:500) diluted in PBS, were added and the cells were incubated for 1 hour at room temperature. Finally, the slices were washed 2 times with PBS / 0.1%Tween (2 min) and 1 time with water (2 min). The cells were mounted between slides with mounting medium.

Flat mounted retinas

Immediately after sacrificing the animals, the eyes were enucleated, and a perforation was made in the cornea with a scalpel. The entire eye was put in 4% PFA for 15-30 minutes after that the retina was dissected as previously reported (Sawamiphak et al., 2010). Fixation of the retina during 10 min in PFA was followed by 5 minutes washes in PBS.

The retinas were put in blocking buffer (PBS with 1% BSA, 2% normal goat serum, 0.5% Triton X-100) and incubate 4 hours at room temperature or 4°C overnight. The primary antibody was diluted in blocking buffer and the retinas were incubated in primary antibody either 4 hours at room temperature or 4ºC overnight. After 3 washes (5 minutes in PBS), the secondary antibody and DAPI were added and incubated 2 hours at room temperature. The samples were washed 3 times with PBS.

Relieving cuts to the retina were done to flat-mount the retina onto a glass slide with either the photoreceptor or RGC side facing upwards. A drop of Vecta shield was added before the coverslip was placed.

Quantitative RT-PCR analysis of retinal RNA

Total RNA was extracted from hole retina using Trizol reagent (Invitrogen, Waltham, MA, USA) at 24, 48, and 72 hours after lens surgery (n=4). Reverse transcription was performed with 5 µg of total RNA using SuperScript III (Thermo Fisher Scientific) and random hexamers (Invitrogen). Complementary DNA was amplified using SYBR Green (Applied Biosystems, Waltham, MA, USA) on a LightCycler instrument (Applied Biosystems) following the manufacturer's instructions. PCR primers were designed using Primer3 software24 and are listed in Table No2. The Ct values of RT-qPCR products were compared using the ΔCt method. The amount of Dp71 cDNA was normalized to mouse β-actin.

Table 2.- Oligonucleotides. Sense and antisense oligonucleotides used for RT-qPCR.

Primer name		Sequence	Target
β-Act	Sense	5'-GCTCTTTTCCAGCCTTCCTT- 3'	β-Actin
	Antisense	5'-CTTCTGCATCCTGTCAGCAA- 3'	
Dp71	Sense	5'-ACAACCATGAGGGAACACCT- 3'	Dystrophin Dp71
	Antisense	5' -TCTGGAGCCTTCTGAGCTTC- 3'	
AQP4	Sense	5' -CTTTCTGGAAGGCAGTCTCAG- 3'	Aquaporin 4
	Antisense	5' -CCACACCGAGCAAAACAAAGAT- 3'	
Kir4.1	Sense	5' -CCGCGATTTATCAGAGC- 3'	Inwardly rectifying K channel Kir4.1
	Antisense	5' -AGATCCTTGAGGTAGAGGAA- 3'	
HSF1	Sense	5' -AACGTCCCGGCCTTCCTAA- 3'	Heat shock factor protein 1
	Antisense	5' -AGATGAGCGCGTCTGTGTC- 3'	
5'UTR-Dp71	Sense	5'-AGTGCTTTCGGCTGCGAGC-3'	5'UTR-Dp71
rDp71dR-Not	Antisense	5'-GATCTAGCGGCCGCTACATTGTGTCCTCTCTCATTGGC-3'	Dp71 group d isoforms

Quantification and measurement of cells groups

Cells expressing the different Dp71 isoforms (PC12/TetOn-Dp71d$_{\Delta 71}$ PC12/TetOn-Dp71d$_{\Delta 71\text{-}74}$) were seeded on 6 wells plates (100,000 cells/dish) and incubated with Dox (500 µg/µl) to induces the respective Dp71 isoform expression. After 24h of Dox induction, cells were resuspended using 1 ml pipet (20 times each well) in order to seed 50,000 cells on 12-well plates.

Cells were incubated during 2h to lead cell group formation. Photos were taken with a SLR Canon camera with a microscope adapter; the image analysis was done with AxioVision (cell group size) and ImageJ software (cell counter tool).

Statistical Analysis

All the data was analyzed using the nonparametric Mann-Whitney test and expressed as means 6 SEM. GraphPad Prism 6 software (La Jolla, CA, USA) was used for all analyses, and statistical significance was set at $P < 0.05$.

FIRST PART

"Molecular alterations in mouse Müller glial cells during cellular edema and treatment action mechanism analysis"

Background

The cystoid macular edema (CME) can occur in different retinal disease such as intraocular inflammation, central or branch retinal vein occlusion, diabetic retinopathy and most commonly following cataract extraction. When CME occurs after cataract surgery and the cause seems to be directly related to the surgery, it is referred as Irvine-Gass syndrome; this is the most common cause of visual impairment after cataract surgery. However, the exact pathogenesis of Irvine-Gass syndrome remains uncertain (Rotsos and Moschos, 2008).

With the purpose to better understand the impact of blood-retinal barrier (BRB) breakdown on retinal homeostasis changes due to dystrophin Dp71 alterations in Müller Glial cells we used a surgically induced iBRB breakdown mice model. After partial lens surgery, the posterior capsular lens discontinuation was confirmed on post-surgery cryosections stained with Hematoxylin-Eosine (HE) (Fig. 9A). The permeability of the iBRB increase 24 and 48 hours after surgery was compared with the control retinas without surgery. The iBRB permeability returns to normal (no significant difference compared with control retinas) 72 hours post-surgery (Fig. 9B) (Siqueiros-Marquez et al., 2017).

Expression of Dp71 also showed changes after partial lens surgery. Dp71 mRNA decreased significantly (30%) 24 hours after surgery and this continues for at least 72 hours (15%) when it starts to return to normal

levels as compared with control retinas (Fig. 10A). Moreover, Western blot analysis showed downregulation of Dp71 72 hours post-surgery (Fig. 10B). Immunostaining with H4 (pan-specific dystrophin antibody) showed a dramatic decrease (50%) in H4 staining 72 hours post-surgery as assessed by measuring pixel intensity both at the inner limiting membrane (ILM) and around the blood vessels (Fig. 10C and D).

In control retinas, as previously described, Kir4.1 was localized at MGC endfeet at the ILM and around the blood vessels (Fig. 10Eb). Kir4.1 was distributed all along MGC membranes 72 hours post-surgery (Fig. 10Ec), mainly at the inner plexiform layer (IPL) (Fig. 10F) without change in overall protein expression as shown by Western blot (Fig. 11A).

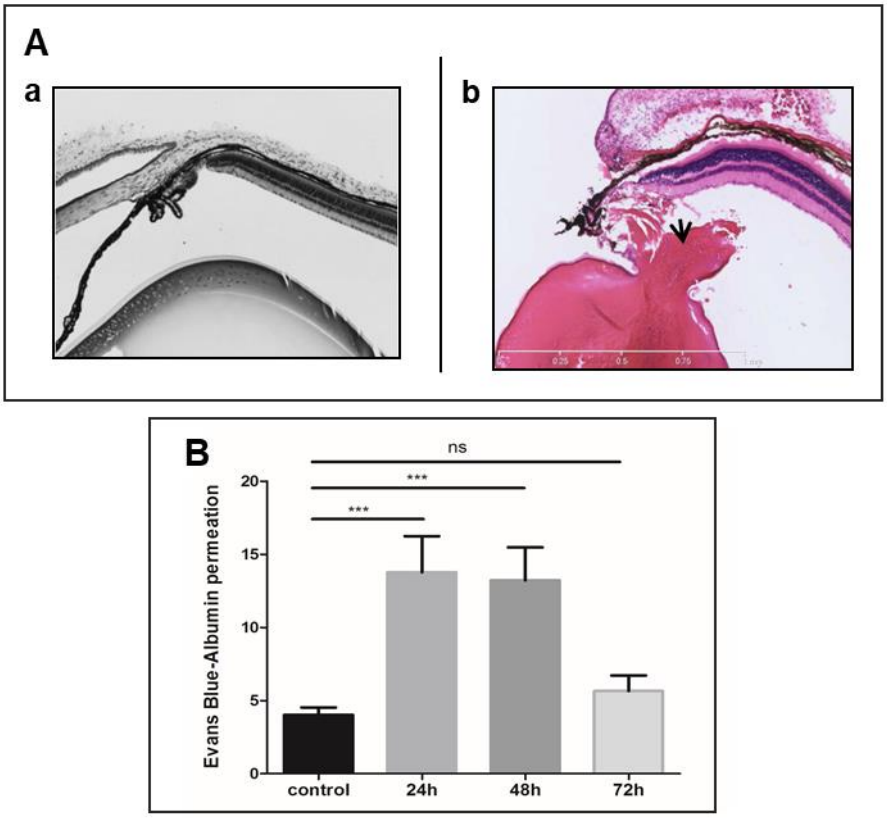


Figure 9.- Partial lens surgery induces iBRB breakdown for 48 hours.

A. Hematoxylin– eosin staining of a control eye without surgery (a) and an eye after surgery (b): posterior capsular lens discontinuation (arrow). **B.** Quantification of iBRB permeability post-surgery at different time points (expressed in microliters of EB per gram of dry retina per hour). Vascular permeability increased significantly 24 and 48 hours after surgery compared to control retinas and returned to normal after 72 hours. Scale bar: 1 mm. Data are expressed as means 6 SEM, n=8. ***P < 0.001 was considered significant versus controls (Siqueiros-Marquez et al., 2017).

In control retinas, AQP4 was localized at MGC endfeet (Fig. 10Ee). However, an overall downregulation of AQP4 was observed 72 hours post-surgery (Fig. 10Ef) 30% at the ILM and 15% around the vessels (Fig. 10G). Nevertheless, AQP4 was still mainly localized around the vessels and at the ILM (Fig. 10Ef). Downregulation of AQP4 was confirmed by Western blot analyses (Fig. 11B).

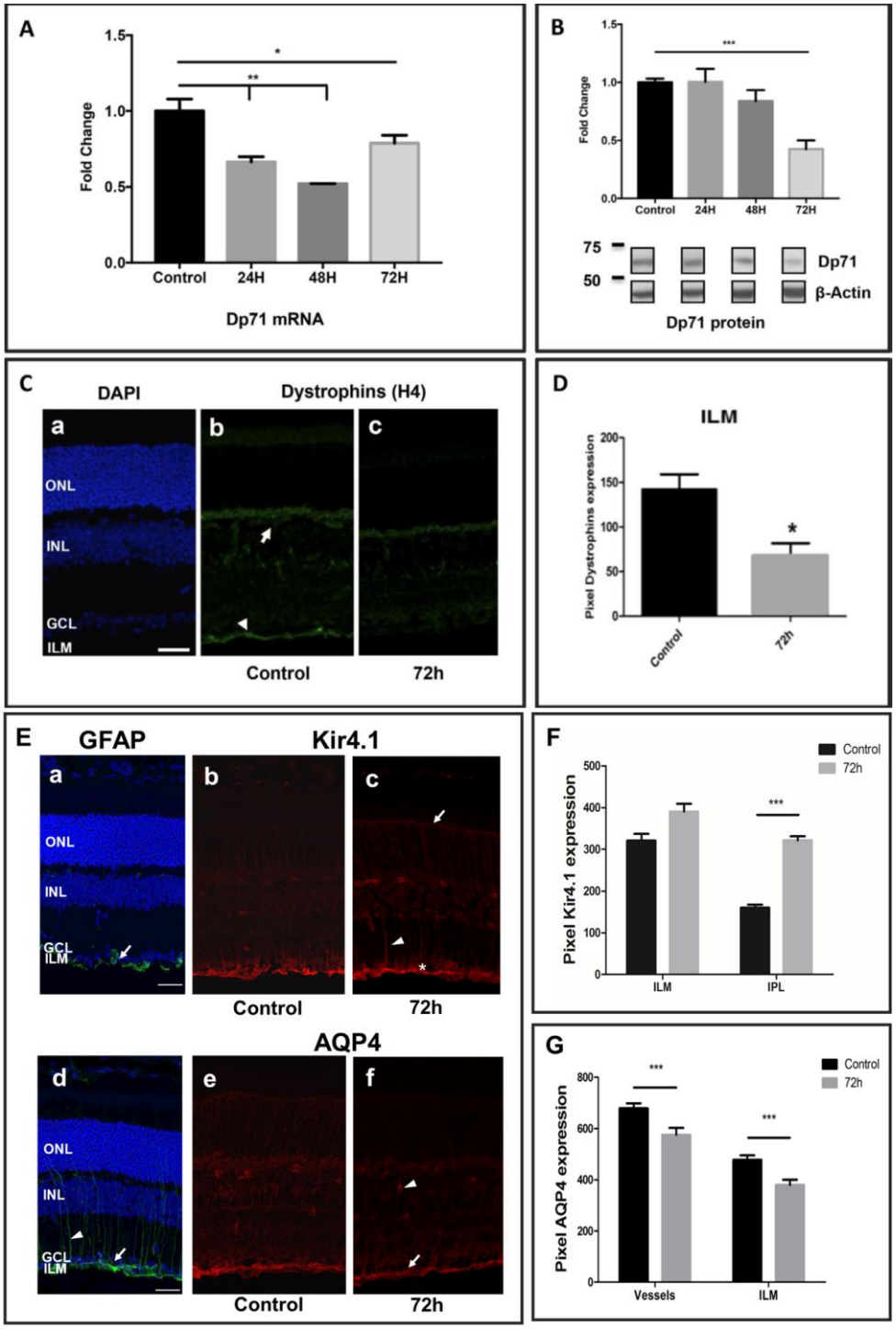


Figure 10.- Downregulation of dystrophin Dp71, Kir4.1 and AQP4 after partial lens surgery.

A. The mRNA level of Dp71 was quantified by real-time PCR and by **B.** Western blot in control retinas (prior to surgery) and

in retinas 24, 48, and 72 hours after lens surgery (normalized to β-actin). Dp71 mRNA level decreased significantly until 48 hours post-surgery and Dp71 protein level is significantly lower at 72 hours post-surgery. Approximate molecular weights given in kD (at the left side of the boxes) are shown. **C.** Immunostaining on retinal sections (a) DAPI of control retinas (b) and retinas 72 hours post-surgery (c) with H4, (green). Dystrophin Dp71 staining is localized at the ILM (arrowhead) and around the blood vessels (arrow). **D.** Pixel quantification of dystrophins at the ILM of retinal sections with ImageJ software. Dystrophin expression decreased at the ILM 72 hours after lens surgery. **E.** Immunostaining on retinal section of GFAP (green), DAPI (blue) (a) in control retinas, and in retinas (d) after surgery. Lens surgery induced an upregulation of GFAP along Müller cell membranes (arrowhead) and in astrocytes from inner retinas (arrow). iBRB breakdown induced Kir4.1 misplacement along Müller cell membranes (arrowhead) and at the ONL (arrow) while the staining at the ILM (star) remained unchanged (b, c). AQP4 staining at the ILM (arrow) and around the blood vessels (arrowhead) decreased post-surgery (e, f). **F.** Pixel quantification confirm a significant increase of Ki4,1 staining in ILM and IPL 72 hours after surgery. **G.** AQP4 pixel quantification confirmed a significant decrease of AQP4 staining at the ILM and IPL 72 hours after surgery. Scale bars: 30 µm. Data were expressed as means SEM, n=6. *P < 0.05; ***P < 0.001 considered significant versus control retinas. ILM, inner limiting membrane; GCL, ganglion cell layer; INL, inner nuclear layer; ONL, outer nuclear layer; IPL, inner plexiform layer; OLM, outer limiting layer.

The strong downregulation of Dp71 mRNA and protein levels post-surgery, possibly leads to Kir4.1 mislocalization and AQP4 downregulation. Moreover, MGC gliosis may occur in cases of retinal injury (Sene et al.,

2009). Here, in control retinas, GFAP was expressed only in astrocytes (Fig. 10Ea, arrow), but 72 hours post-surgery, GFAP was unequivocally upregulated in MGC (Fig. 10Ed, arrowhead).

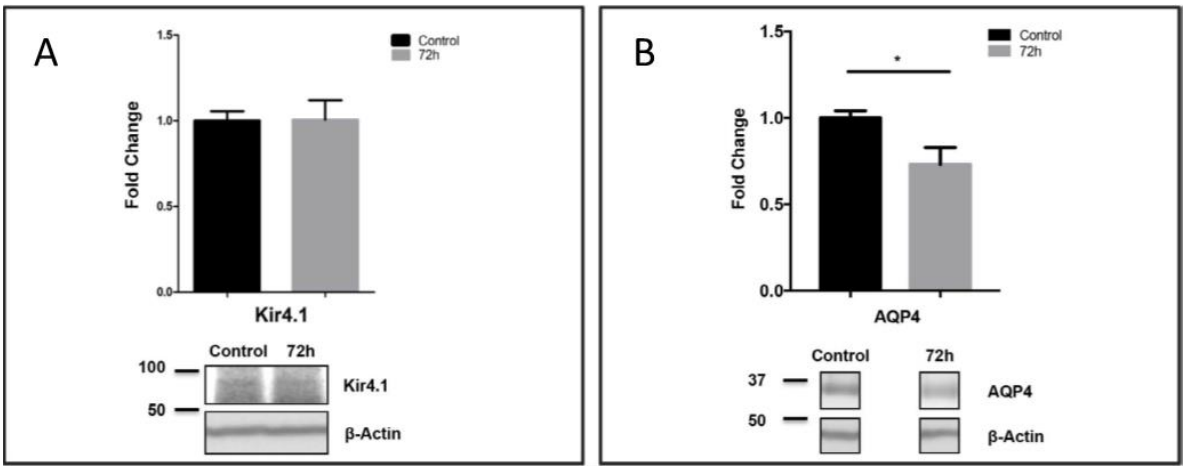


Figure 11.- Downregulation of Kir4.1 and AQP4 protein expression after partial lens surgery.

Western blots of Kir4.1 and AQP4 normalized using β-actin of control retinas and in retinas 72 hours post-surgery. **A.** Kir4.1 showed no significant difference respect to control retinas and **B.** only AQP4 was downregulated 72 hours post-surgery. Molecular weights given in kD are indicated to the left. Data expressed as means + SEM, n=4. *P < 0.05 considered significant versus control retinas.

Results

1. Astrocytes morphology after Lens surgery

The constitutive lack of Dp71 induces changes in astrocyte morphology and density (Giocanti-Auregan et al., 2016). We decided to explore whether a similar phenomenon is observed after Dp71 downregulation induced by partial lens surgery and associated with a transient iBRB breakdown. However, no changes in astrocyte morphology nor in processes number, processes length or intersections number (Fig. 12) were observed 24 and 48 hours post-surgery.

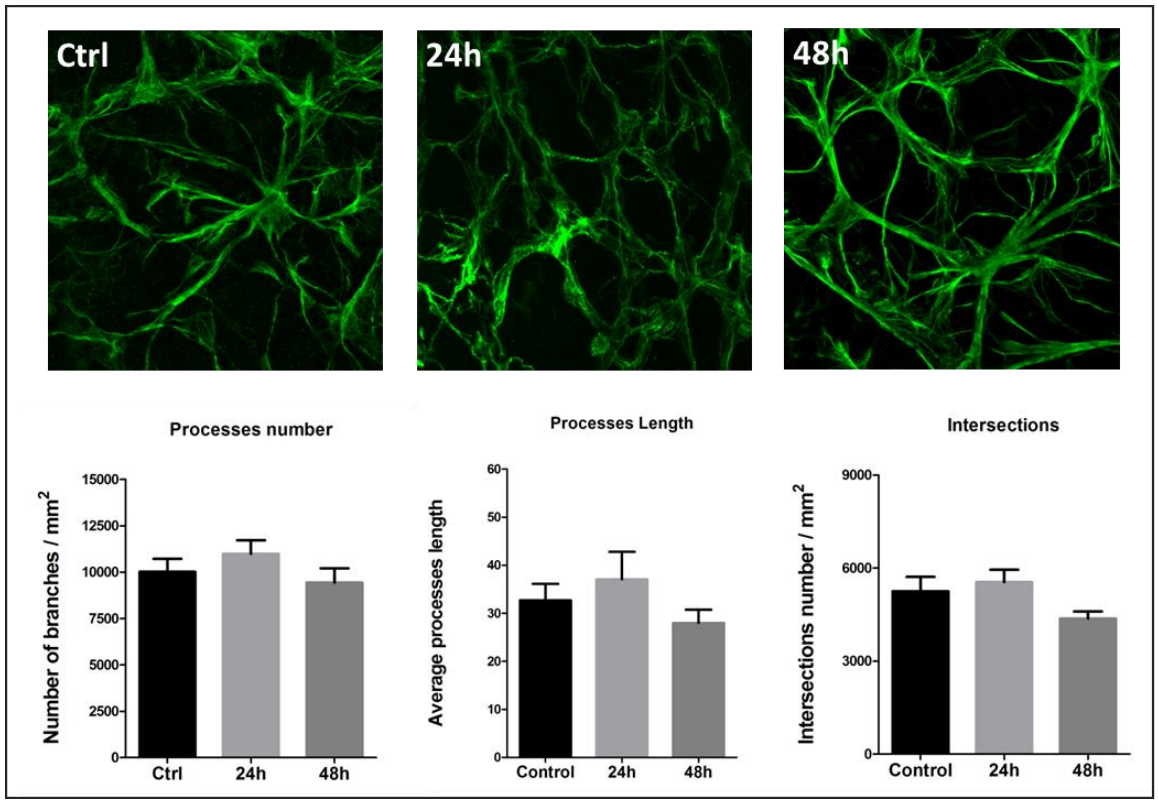


Figure 12.- Astrocytes morphology in control and 24 and 48 hours post-surgery retinas.

Immunostaining of flat mounted retinas with an anti GFAP antibody. Visualization of the astrocyte network (green) in control, 24 and 48 hours after surgery retinas. No changes in

morphology of retinal astrocytes were observed after surgery. The pixel quantification of the astrocytes processes number, of their length and of their intersection number on images using Analyze Skeleton plugin of Fiji, showed no significant difference after lens surgery compared with control retinas.

The absence of Dp71 is a cause of retinal inflammation with overexpression of VEGF, ICAM-1 and AQP4, as well as an increase in the number of adherent leukocytes associated with the degeneration of capillaries and rupture of the blood-brain barrier in Dp71 null mice (El Mathari et al., 2015).

To establish the involvement of inflammatory factors in our retinal model, the mRNA expression of inflammatory factors was determined by quantitative PCR in control (without surgery) and post-surgery retinal tissue. No elevation of inflammatory markers in the retina of post-surgery mice versus control retina was demonstrated (Fig. 13). However, proteins levels remain to be investigated.

Inflammation biomarker	24 h		48 h	
	Mean	SEM	Mean	SEM
VEGF	0.718	0.1350	1.059	0,3051
VEGFA	0.878	0.4390	0.998	0,7767
VEGFB	0.706	0.1620	0.977	0,8103
iNOS	1.442	0.3680	1.809	0,2540
IL1b	0.725	0.3570	0.203	0,9131
TNFa	0.531	0.2310	0.056	0,0440 *
ICAM1	1.763	0.3910	1.024	0,2136
PGF	1.808	0.5590	1.396	0,4252
nNOS	0.475	0.1980	0.525	0,3953
COX2	0.662	0.4190	0.326	0,7159

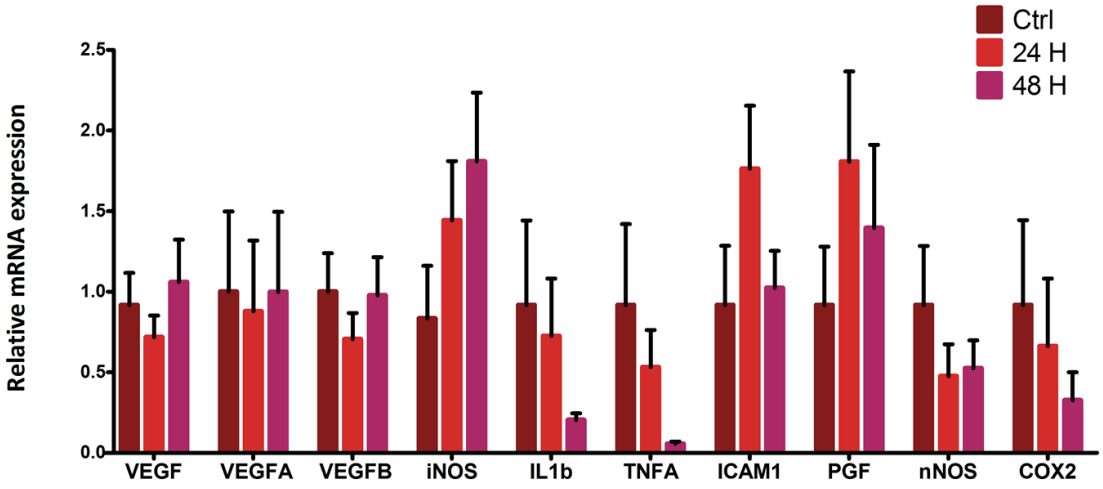


Figure 13.- Inflammation in WT retinas 24 and 48 hours post-surgery.

Retinal expression of different biomarkers of interest assessed by quantitative PCR 24h and 48h after partial lens surgery compared to control retinas (without surgery). No significant upregulation in any biomarker was observed in the retina except for the TNFα mRNA expression 48 h after surgery. Graphic representation of mRNA inflammation biomarkers quantification.

Using the retinal explant model, we reproduced an inflammation environment using interleukin 1β (IL1β) (7.5 ng/ml) in the culture medium; however, after 6 and 12 hours, the Dp71 mRNA expression

remains unchanged, compared with retinal explants incubated in DMEM medium without IL1β (Fig. 14).

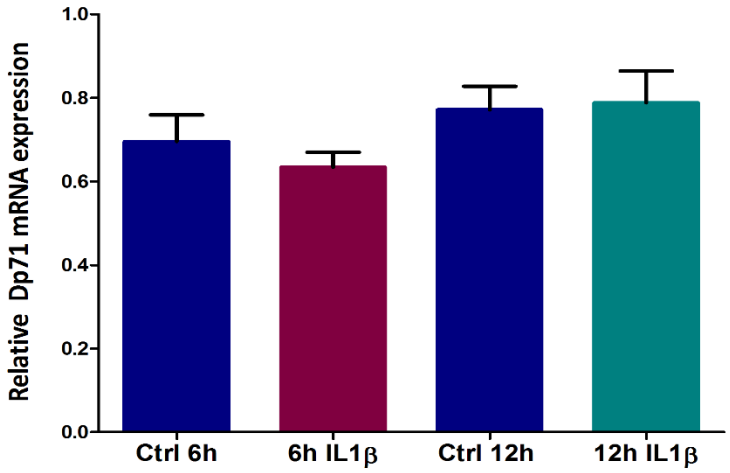


Figure 14.- Dp71 expression after 6 and 12 hours in an inflammation environment.

Dp71 mRNA quantification by real time PCR showed no significant difference between the control retinas (incubated in DMEM medium) and the retinas in inflammation conditions, during 6 or 12 hours. n=6

2. Effect of dexamethasone injections post-surgery on Dp71, AQP4, and Kir4.1

Dex has already proven efficiency in the treatment of retinal edema in humans, and its anti-inflammatory effect was higher than other corticosteroids. The injection of Dex in this model was very useful to partially understand the molecular mechanisms that occurs after BRB breakdown.

A low dose of Dex (23 nM) was injected intravitreally 24 hours post-surgery. iBRB permeability as well as Dp71, AQP4 and Kir4.1 expression

was quantified 48 and 72 hours post-surgery. Permeability of iBRB increased 5 and 6-fold higher than in control retinas (48 and 72 hours respectively) (Fig. 15A). The permeability after Dex treatment was not reduced compared to vehicle injection or control retinas. This showed that, at this concentration, dexamethasone was unable to restore the increased iBRB permeability observed post-surgery in the partial lens surgery model (Fig. 15A).

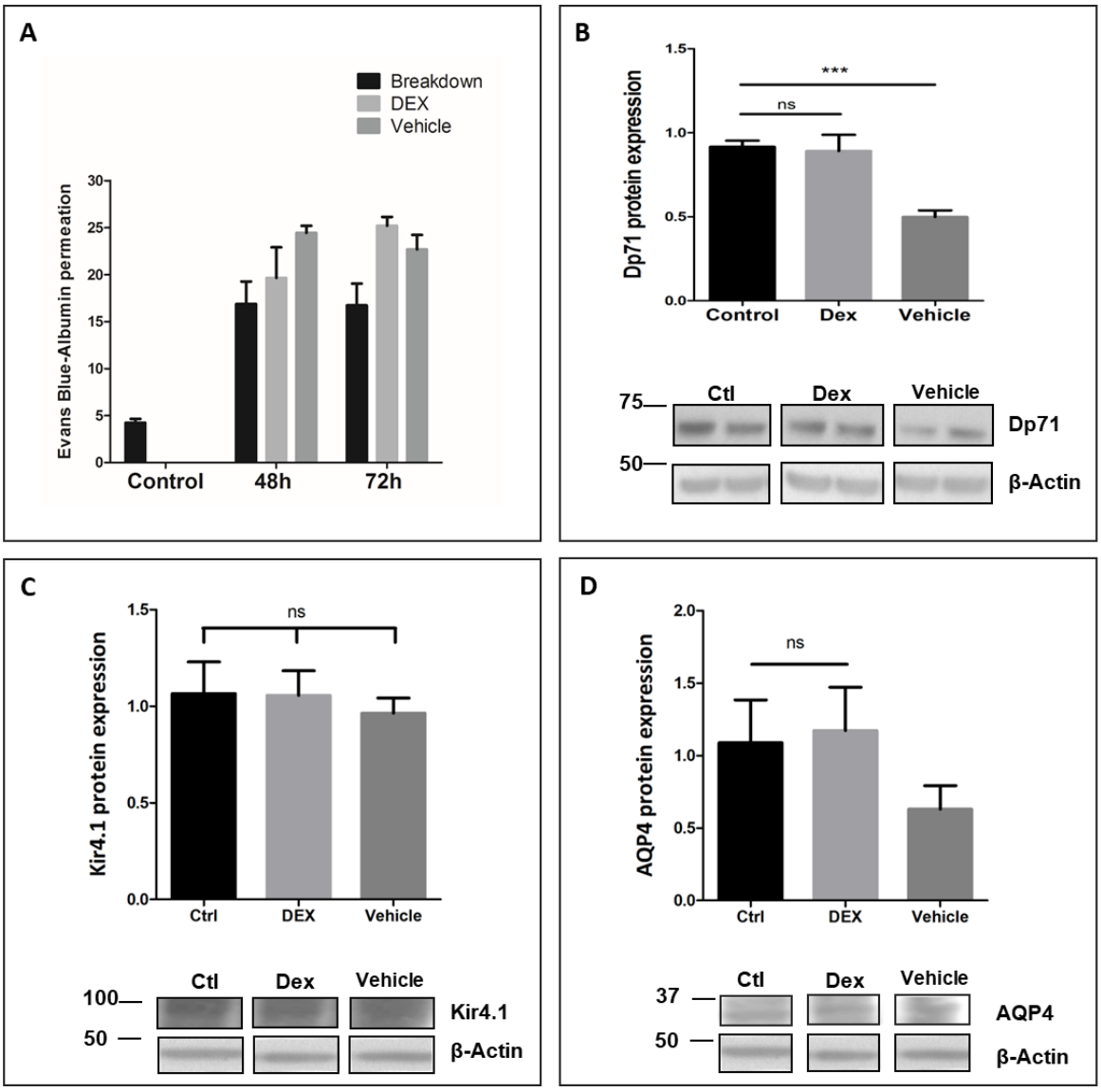


Figure 15.- Dexamethasone prevented Dp71 downregulation, but did not restore permeability after partial lens surgery.

A. Post-surgery iBRB permeability followed by Dex or vehicle injection. At 48 or 72 hours post-surgery, dexamethasone did not restore iBRB permeability compared to control retinas. **B.** Western blot of Dp71 and β-actin in control retinas; 72 hours after lens surgery comparing control retinas and retinas injected with dexamethasone or vehicle injection. Dexamethasone prevented Dp71 downregulation, but not the vehicle. **C.** Western blot of Kir4.1 72 hours post-surgery. The injection of

dexamethasone or the vehicle did not change the overall expression of Kir4.1 after surgery. **D.** Analysis of AQP4 Western blot showed a trend toward a downregulation of AQP4 after intravitreal injection of the vehicle, while dexamethasone prevented this downregulation. Data are expressed as means SEM, n=10. **P < 0.01; ***P < 0.001 were considered significant versus control retinas. (B, C, D) Values were normalized to controls.

However, in the same experimental conditions, Western blot analysis showed that Dex significantly prevented the downregulation of Dp71 and AQP4 observed 72 hours post-surgery (Fig. 15B and D respectively) with no effect on Kir4.1 expression (Fig. 15C). Moreover, immunofluorescence of dystrophins and AQP4 showed that the intravitreal injection of Dex not only prevented their downregulation but also unequivocally preserved Dp71 immunoreactivity (Fig. 16A and C) and Kir4.1 localization, mainly around blood vessels and at the ILM was also preserved (Fig. 16B).

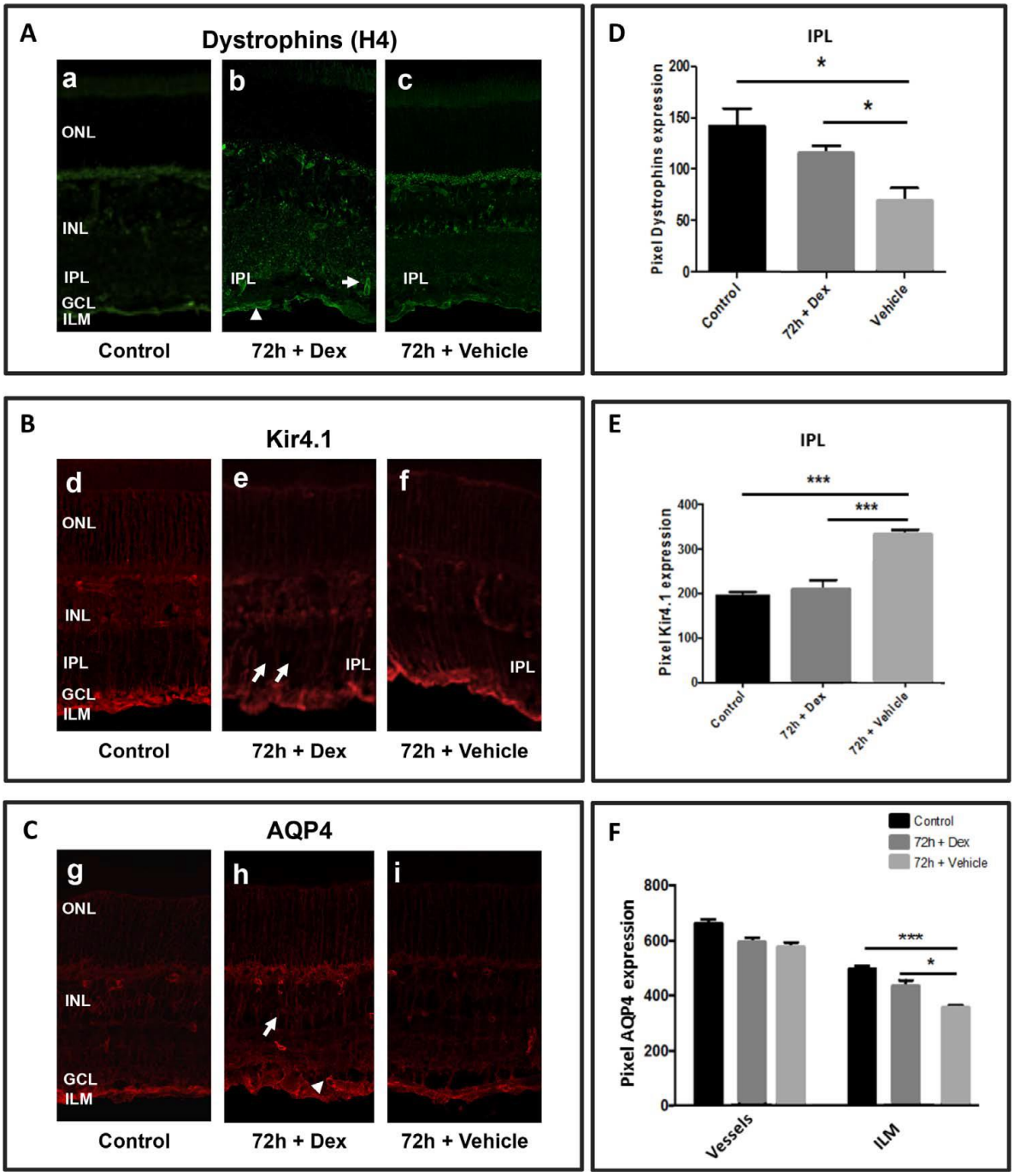


Figure 16.- Dexamethasone prevented Dp71, Kir4.1, and AQPA alterations.

A. Dystrophin immunofluorescence with H4 antibody in (a) control retina; there was no downregulation of dystrophin Dp71 at the ILM and around the vessels (arrow and arrowhead) after (b) dexamethasone injection compared to eyes injected with the

vehicle after surgery (c). **B.** Kir4.1 immunofluorescence in a (d) normal retina; (e) Dex prevented delocalization of Kir4.1 at the IPL (star) and around the vessels (arrow) after surgery while the (f) vehicle did not. **C.** AQP4 immunofluorescence in (g) normal retina; (h) dexamethasone prevented downregulation of AQP4 at the ILM (arrowhead) and around the blood vessels (arrow) after surgery compared to (i) vehicle injection. **D.** Decreased expression of Dp71 prevented by dexamethasone at the ILM (pixel quantification of retinal sections). **E.** Increased expression of Kir4.1 at the IPL (delocalization) prevented by dexamethasone. **F.** Decreased expression of AQP4 at the ILM partially prevented by dexamethasone. Data are expressed as means SEM, n=3. *P < 0.05; ***P < 0.001 considered significant versus control retinas.

3. Dp71, Kir4.1 and AQP4 expression in retinal explant model and Dex effect

In order to better understand the downregulation of Dp71, Kir4.1 and AQP4 after lens surgery induce BRB breakdown and the role of Dex restoring their expression levels and localization; we decided to continue with the retinal explant model. It has been reported a MGC swelling comparable with that observed in diabetic retinas using a hypotonic solution added with barium (Ba^{2+}) (Pannicke et al., 2006). This MGC swelling was also comparable with the swelling present in MGC from Dp71 null mice (Sene et al., 2009).

First, we determined the optimal conditions to measure Dp71, Kir4.1 and AQP4 mRNA expression levels. After 8 hours in hypotonic solution plus Ba^{2+}, we observed that mRNA expression of Dp71, Kir4.1 and AQP4 was significantly lower than in control retinas (incubated in isotonic solution without Ba^{2+}) importantly, we associated the decrease on Dp71 mRNA

expression with a significant increase in MGC soma (Fig. 17). Moreover, Dex was able to prevent the downregulation observed in hypotonic plus Ba^{2+} incubation and to prevent MGC swelling (Fig. 17).

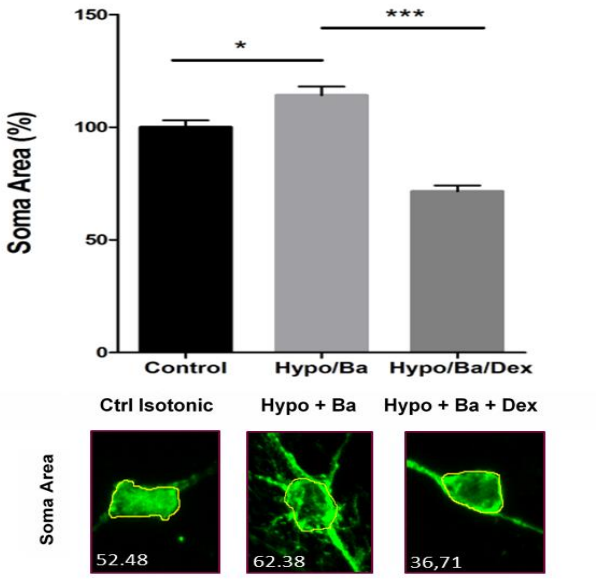


Figure 17.- MGC swelling after hypotonic solution plus Ba^{2+} and hypotonic solution plus Ba^{2+} and Dex incubation.

Quantification of the soma area of retinal MGC using ImageJ software; the retinas were incubated 8 hours in isotonic solution (control retinas), hypotonic solution plus Ba and hypotonic solution plus Ba^{2+} (barium) and Dex (dexamethasone). In the bottom of the graph a representative MGC soma is presented. *P < 0.05; ***P < 0.001 considered significant versus control retinas n≥30 cells.

As Dp71 in retina interact with the DAPs (Fort et al., 2008) we evaluated the mRNA expression of β-distroglycan (β-DG), β-sarcoglycan (β-SG), ε-sarcoglycan (ε-SG) and nNOS in order to identify the proteins whose expression is altered during MGC swelling in the retinal explant model. When the retinas were incubated in hypotonic solution with Ba^{2+} we observed that β-DG was downregulated while β-SG, ε-SG and nNOS

showed no significant changes compared with control retinas (Fig. 18). When the retinas were incubated in hypotonic solution but also in presence of Dex, the mRNA expression of Dp71, Kir4.1, AQP4, β-SG, ε-SG and nNOS were not significantly different from their expression in control retinas (Fig. 18) β-DG mRNA expression showed a slight increase after Dex treatment (Fig. 18).

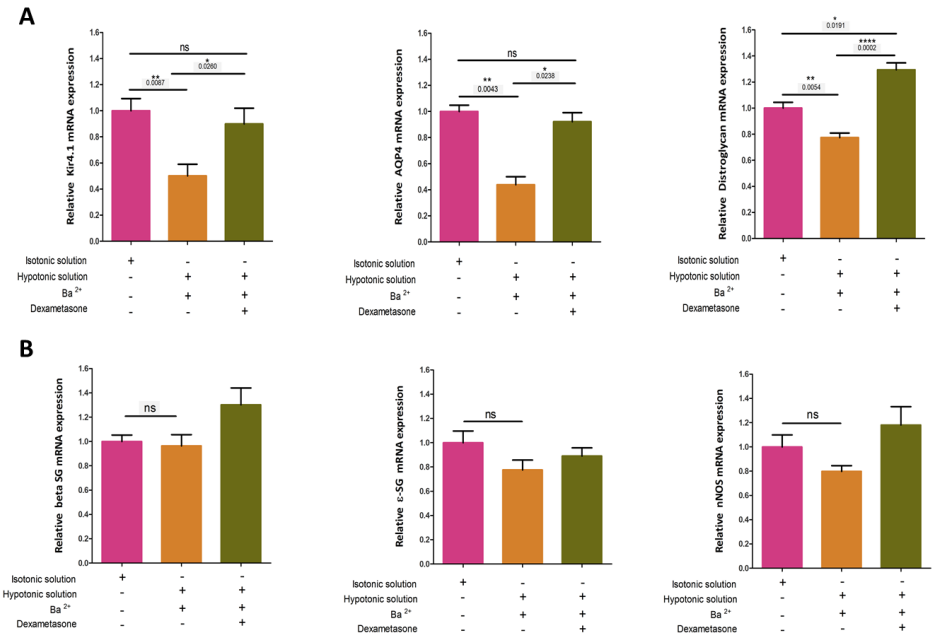


Figure 18.- DAPs mRNA expression in complete retinas incubated in hypotonic solution plus Ba^{2+} or in hypotonic solution plus Ba^{2+} and Dex.

A. mRNA quantification by real time PCR of Kir4.1, AQP4 and dystroglycan. The expression of these DAPs was significantly lower when the retinas were incubated in hypotonic solution plus Ba^{2+} (MGC swelling). However, incubation in the same solution added with Dex showed no significant difference compare with control retinas (isotonic solution) meaning that Dex is able to prevent Kir4.1, AQP4 and dystroglycan mRNA expression during MGC swelling. **B.** mRNA quantification of β-sarcoglycan, ε-sarcoglycan and nNOS expression. The

expression of these DAPs showed no significant difference during MGC swelling compare with control retinas. n=6 *P < 0.05; ***P < 0.001 considered significant versus control retinas.

It has been reported that Utrophin is able to compensate the lack of dystrophin (Deconinck et al., 1997; Grady et al., 1997) and that HSF1 (heat shock protein 1) is a transcriptional factor for Dp71 expression (Tan et al., 2015); for that reasons, we quantified the mRNA expression of Utrophin and HSF1 in our retinal explant model. After 8 hours, the retinas incubated in hypotonic solution added with Ba^{2+} and in presence of Dex, showed a significant increase in utrophin and HSF1 mRNA expression. Utrophin and HSF1 expression in retinas incubated without Dex showed no significant difference compared with control retinas (Fig 19).

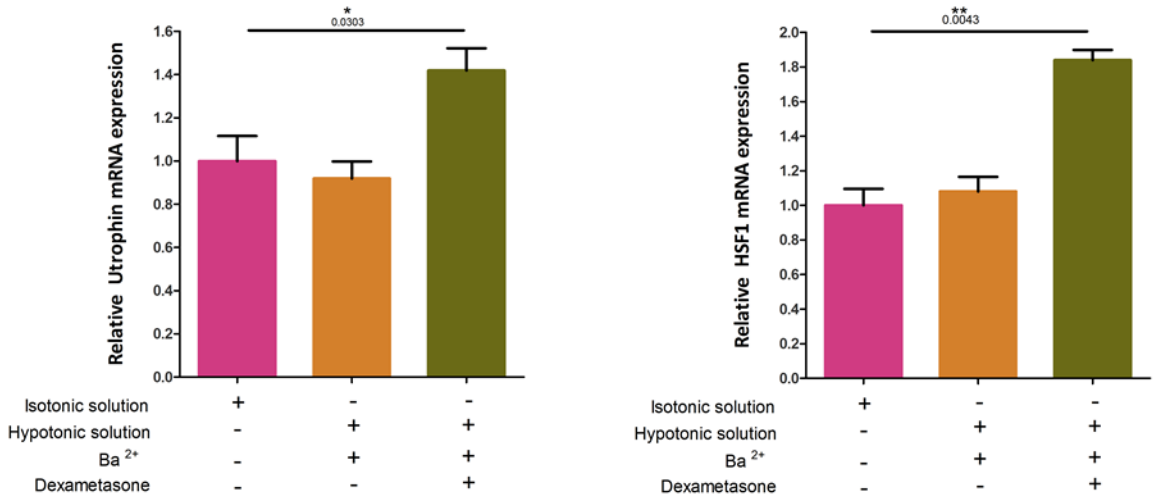


Figure 19.- Utrophin and HSF1 mRNA expression in complete retinas incubated in hypotonic solution plus Ba^{2+} or in hypotonic solution plus Ba^{2+} and Dex.

mRNA quantification by real time PCR of utrophin and HSF1. The expression of utrophin and HSF1 showed no difference when the retinas were incubated in hypotonic solution plus Ba^{2+} (MGC swelling) compare with control retinas (isotonic solution). However, incubation in hypotonic solution plus Ba^{2+} added with

Dex showed a significant increase in utrophin and HSF1 mRNA expression. *P < 0.05; ***P < 0.001 considered significant versus control retinas n=6.

4. Dexamethasone, Triamcinolone and Fluocinolone effect in hypotonic plus Barium retinal explant model

Corticosteroids (GCs) have been used to treat different retinal diseases due to their ability to act on several pathways reducing the inflammation, leukostasis, improve the integrity of tight junctions, among others. The use of corticosteroids is an increasing therapy for diseases like: diabetic macular edema (DME), ocular inflammatory conditions, macular edema following retinal vein occlusion (branch or central vein) and uveitis (Yang et al., 2015).

With the aim to compare the efficacy of three corticosteroids preventing the downregulation of Dp71, Kir4.1 and AQP4 expression in our retinal explant model we quantified the Dp71, Kir4.1 and AQP4 expression in hypotonic plus Ba^{2+} condition comparing the response to Dex, Triam and Fluo. We identified an effect preventing the molecular changes during MGC swelling of the three GCs, remarkably, we noticed that Fluo (0.012µM) effect was greater than Dex (1780 µM) and Triam (100µM); even if Fluo concentrations was much lower than Dex or Triam (Fig 20).

To better compare the effect of Dex, Triam and Fluo we incubated the retinas with a low (0.012µM) and high (1780 µM) concentrations, of each corticosteroid, to see if both concentration are sufficiently to prevent the MGC swelling observed when the retinas were incubated in hypotonic plus Ba^{2+} solution and if the GCs effect is dose dependent. The concentrations of both GCs Triam and Fluo could prevent the MGC swelling (Fig 21). However, Dex was not able to prevent MGC swelling at the low dose indicating that this GC is less effective that Triam and Fluo and therefore an increase of dose is necessary to prevent the MGC swelling. In this model, we showed a differential effect of 3 GCs usually used in the

treatment of retinal edema. We emphasize that the effect of corticosteroids on MGC is also dose dependent.

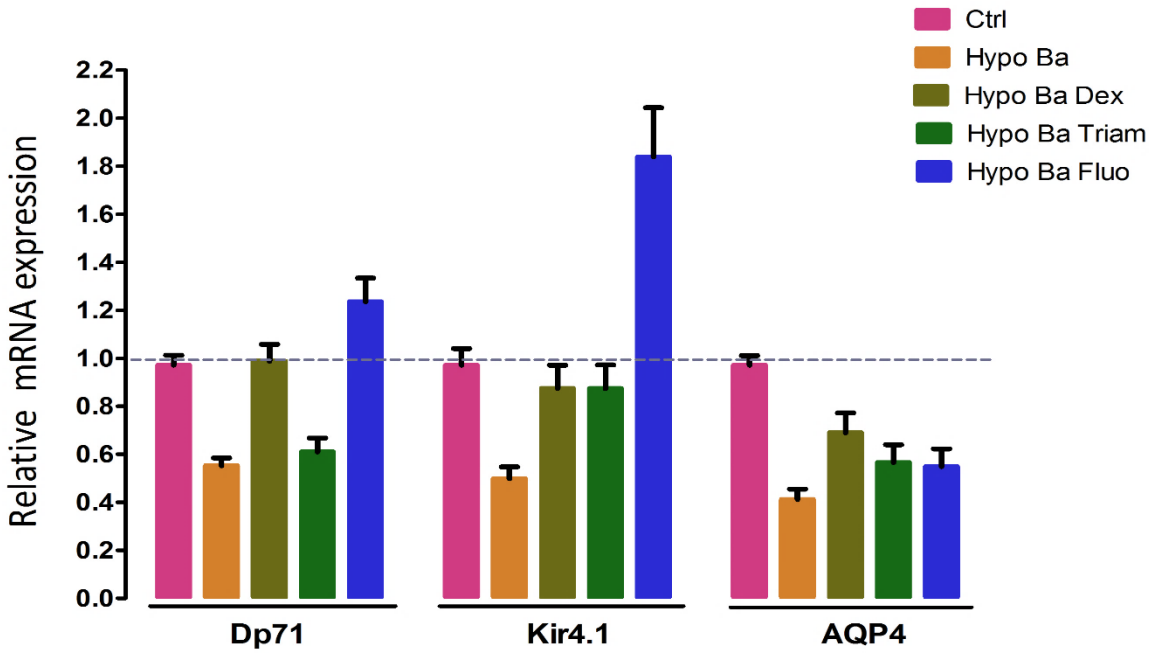


Figure 20.- Effect of tree corticosteroids: Dex, Triam and Fluo con Dp71, Kir4.1 and AQP4 expression.

mRNA quantification by real time PCR of Dp71, Kir4.1 and AQP4 showed that triamcinolone is less effective protecting the retinas from MGC swelling molecular changes; it was not able to prevent Dp71 downregulation. Meanwhile, fluocinolone is more effective than Dex, preventing the molecular changes, an important effect of Fluo is the remarkable increase in Kir4.1 expression. Ba: barium Dex: dexamethasone, Triam: triamcinolone, Fluo: fluocinolone; n=6.

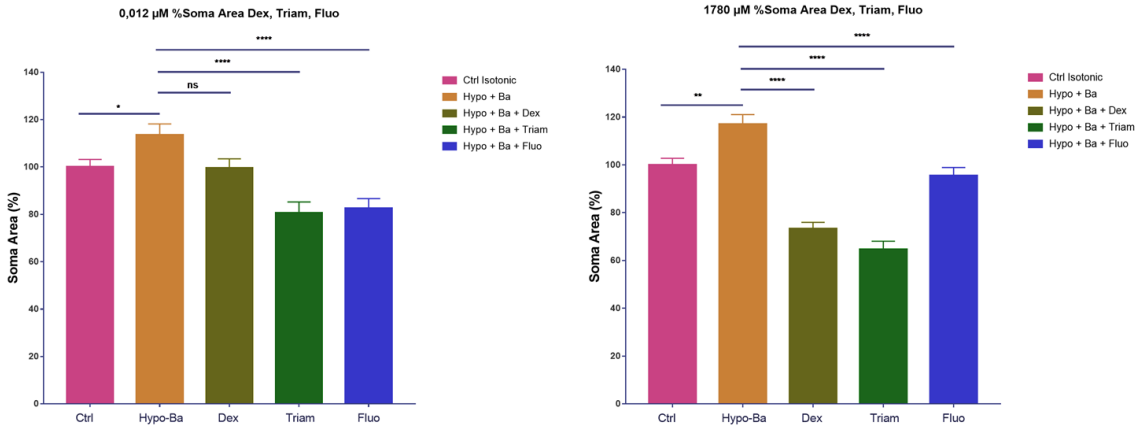


Figure 21.- Effect of a low and high concentrations of the corticosteroids Dex, Triam and Fluo in MGC swelling.

Incubation in hypotonic solution plus Ba^{2+} added with lower (0.012 µM) or higher (1780µM) doses of Triam and Fluo were able to prevent MGC swelling. However, low doses of Dex showed no significant difference in MGC soma area compared with the hypotonic solution added with Ba^{2+} (swelled MGC) at the higher dose Dex was able to prevent MGC swelling. n=20 *P < 0.05; **P<0.005 ****P < 0.0001 considered significant versus control retinas. Ba: barium Dex: dexamethasone, Triam: triamcinolone, Fluo: fluocinolone.

5. Effect of prostaglandins and leukotriene pathway inhibitors on Dp71 and HSF1 expression

With the aim to better identify the mechanism responsible of Dp71, Kir4.1 and AQP4 downregulation during MGC swelling in the retinal explant model; we evaluated the effect of three enzyme inhibitors. Indomethacin (Indo) is a non-steroidal anti-inflammatory drug that work inhibiting the production of prostaglandins by inhibition of the cyclooxygenase activity; 4-Bromofenacil bromide (Bromo) a classic inhibitor of phospholipase A2 (PLA2) and Ferulic acid which is a hydroxycinnamic acid a natural anti-oxidant that reduced the pro-inflammatory cytokines as 5 lipoxygenase activity (5-LOX) inhibitor.

After 8 hours in presence of the different inhibitors, the retinas were processed to quantify the Dp71, Kir4.1 and AQP4 mRNA expression. Indo was not capable to prevent the downregulation of Dp71, Kir4.1 and AQP4, thus discarding the role of prostaglandins. However, both Bromo and Ferulic acid can prevent Dp71, Kir4.1 and AQP4 downregulation. By inhibiting the PLA2 we are inhibiting the leukotrienes pathway since early steps; as Bromo effect is a bigger than Ferulic acid on AQP4 expression, we hypothesize that the molecular mechanism leading to AQP4 downregulation during MGC swelling may be due to more than one mechanism.

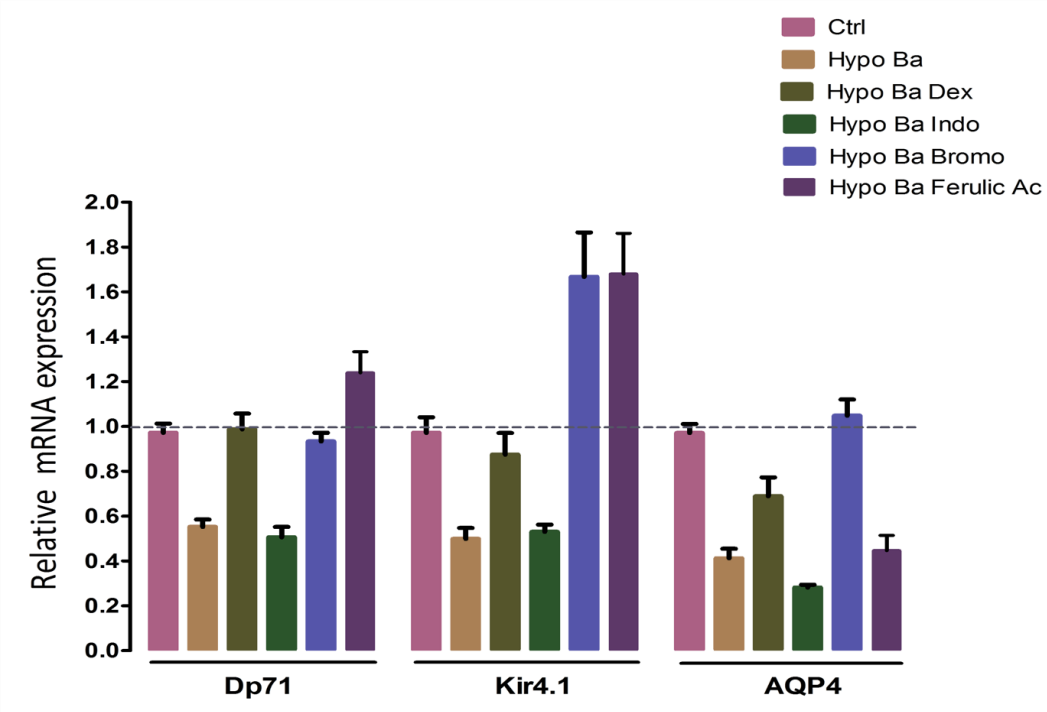


Figure 22.- Effect of prostaglandins and leukotriene pathway inhibitors on Dp71, Kir4.1 and AQP4 expression.

mRNA quantification by real time PCR of Dp71, Kir4.1 and AQP4 after prostaglandins and leukotriene pathway showed that Indo was no able to prevent Dp71, Kir4.1 and AQP4 downregulation during MGC swelling; on the other hand, Ferulic acid, an inhibitor of LOX, was able to prevent the molecular changes observed during MGC swelling. Bromo, the PLA2 inhibitor was also able to prevent the molecular changes. Indo: indomethacin, Bromo: 4-Bromofenacil bromide; n=6.

Discussion and perspectives

By using an experimental mouse model of partial lens surgery, we (1) confirmed the subsequent occurrence of a transient iBRB breakdown; (2) showed that reactive MGC were strongly altered with a downregulation of Dp71 and AQP4 and delocalization of Kir4.1; (3) reversed the impairments of Dp71, AQP4, and Kir4.1 using low-dose dexamethasone both in vivo and ex vivo while no effect was observed on iBRB; and, finally, (4) observed that using dexamethasone led to the overexpression of HSF1, one of the transcription factors for Dp71. In our retinal explant model for MGC swelling we observed that: (1) the PLA2 pathway and leukotrienes pathway is involved in the molecular changes that leads to Dp71, Kir4.1 and AQP4 downregulation during MGC swelling; (2) different GCs have different effect protecting MGC of swelling damage and their effect is dose dependent.

Inner BRB breakdown is one of the factors leading to the formation of macular edema, one of the leading causes of vision loss worldwide in patients with many retinal diseases. In clinical practice, the loss of visual acuity usually correlates poorly with retinal thickness and iBRB breakdown (Diabetic Retinopathy Clinical Research Network et al., 2007). Our results suggest that retinal homeostatic alterations could be independent of iBRB breakdown since injection of a low dose of dexamethasone prevented retinal homeostatic alterations without preventing iBRB breakdown.

An adapted model of iBRB breakdown induced by partial lens surgery and confirmed using the EB method was used in this study (Stahl et al., 1987). Inner BRB breakdown due to partial lens surgery appeared like the Irvine Gass syndrome observed in humans, which is a rare situation in which an iBRB breakdown and a retinal edema appear after cataract surgery. The localization and proper clustering of AQP4/Kir4.1 seem to be crucial to control the osmotic balance of the retina. In healthy retina, the proteins Kir4.1 and AQP4 are strongly expressed in MGC and mainly localized at MGC endfeet or in the processes surrounding the retinal blood vessels

(Dalloz et al., 2003). After partial lens surgery, AQP4 was downregulated and Kir4.1 had lost its polarization.

We also showed that dystrophin Dp71, a protein that plays a crucial role in MGC functions such as retinal water and potassium homeostasis and in iBRB maintenance that is the core of a complex responsible for anchoring and proper clustering of the channels Kir4.1 and AQP4 (Fort et al., 2008; Sene et al., 2009), was also downregulated. Chronologically after lens surgery, the iBRB was restored while the downregulation of Dp71 and AQP4 and delocalization of Kir4.1 were not, suggesting that iBRB breakdown could be an important factor altering Dp71, AQP4, and Kir4.1 expression and localization.

In previous work, we suggested that the constitutional lack of Dp71 in Dp71-null mice could be at the origin of the downregulation of AQP4, changes in Kir4.1 localization, and increase in iBRB permeability. However, conversely here, we showed that the transient iBRB breakdown model induced by partial lens surgery preceded the downregulation of Dp71, which could be responsible for the changes observed in AQP4 and Kir4.1 expression in MGC. We could assume that one of the mechanisms responsible for this phenomenon could be the effect of retinal fluid toxicity on MGC and the resulting MGC gliosis, as previously suggested in a model of retinal detachment, (Sene et al., 2009) or we can also suggest that after breakdown of the iBRB, blood-derived factors may induce alterations in MGC.

We chose to inject dexamethasone in this model because its efficacy as a treatment for retinal edema has been previously shown in humans, and its anti-inflammatory effect is higher than that of other corticosteroids. Previous demonstrated that intravitreal dexamethasone restored an effective iBRB in diabetic rats (Tamura et al., 2005) and inhibited VEGF-induced vascular leakage in rabbits (Edelman et al., 2005). At a high dose (1 µM), in vivo, dexamethasone increased Kir4.1 level in a normal rat retina while a low dose (100 nM) had no effect (Zhao et al., 2011). However, in a pathological model of endotoxin-induced uveitis (EIU), at

low dose (100 nM), dexamethasone was able to regulate the expression of Kir4.1.

To the best of our knowledge, we were the first to use dexamethasone injections in mice to restore iBRB permeability or altered AQP4/Kir4.1 in MGC during iBRB breakdown. We previously adapted the intravitreal dose in rats (50 µg or 115 nM) to the weight of the mice, so 10 µg was injected. Using this low dose of dexamethasone (23 nM), we observed no effect on iBRB permeability, although Dp71 and AQP4 downregulation and Kir4.1 delocalization were prevented. These results are consistent with those reported by Zhao et al., who have demonstrated that dexamethasone could regulate the expression of AQP4/Kir4.1 via its effect on the glucocorticoid receptor (Zhao et al., 2011). Dexamethasone acts also on Dp71, independently of its effect on the iBRB, suggesting that dexamethasone could have a differential effect depending on the dose used. Based on these observations, we hypothesized that at high dose, dexamethasone could help restore iBRB while at a lower dose, it could act on MGC without restoring iBRB; and as a consequence, iBRB permeability, in this model, seemed to be independent of Dp71, Kir4.1, and AQP4 expression. We hypothesized that the observed paradoxical increase of iBRB permeability in comparison to controls observed when surgery was followed by intravitreal injection, was due to the effect of intravitreal injection in a small eye per se even without new lens traumatism.

Noteworthy in the explant model, we also observed that MCG swelling, Dp71, AQP4, and Kir4.1 downregulation after exposure to a hypoosmotic solution containing Ba^{2+} could be prevented using a low dose of dexamethasone. The regulation of Dp71 remains unclear. However, HSF1 has recently been identified as a regulator of Dp71 expression (Tan et al., 2015), acting as a transcription factor. Previous reports have shown that dexamethasone induces and activates HSF1 in mice (Maheshwari et al., 2014; Sun et al., 2000). Here, we observed the upregulation of HSF1 in retinas incubated with dexamethasone. It is conceivable to propose that dexamethasone could prevent downregulation of Dp71, AQP4, and Kir4.1 and MGC swelling via the upregulation of HSF1. Zhao et al. previously

showed that dexamethasone upregulated Kir4.1 expression but not AQP4 in MGC (Zhao et al., 2011). Based on our observations, we could assume that dexamethasone could act on these proteins through the regulation of Dp71 after overexpression of HSF1.

The iBRB-independent regulation of such MGC functions could explain, at least partially, the dissociation between the visual acuity and the edema severity observed in clinical practice (Diabetic Retinopathy Clinical Research Network et al., 2007). These mechanisms need to be understood. Indeed, in clinical practice, the way to eliminate fluid accumulated in the retina is known most of the time; however, how to protect the retina during iBRB breakdown and macular edema remains unknown, and our findings suggest that the use of corticoids but at a very low dose could be useful.

We observed alterations of dystrophin Dp71, AQP4, and Kir4.1 in a mouse model of surgically induced iBRB breakdown. A single injection of low dose of Dex prevented the occurrence of molecular changes without effect on the iBRB. Based on the results of the ex vivo model (retinal explants), we suggest that Dex could upregulate HSF1, one of the transcription factor activating Dp71 expression a stabilizing protein for AQP4/Kir4.1 in MGC. Considering these effects that are independent of its action on the iBRB, low-dose Dex could be a neuroprotective agent with potential utility in clinical practice, probably associated with less complication than when it is used at higher doses.

Furthermore, as Dex is not the only agent used in clinic, we decide to test two more glucocorticoids (GCs) with similar chemical structure: Triamcinolone and Fluocinolone; these 3 GCs have been reported to have an elimination half-life in the vitreous of 2–3 hours in animal models (Edelman, 2010). First, we evaluated the capability of preventing MGC swelling, where all three prevented MGC swelling, but Fluocinolone and Triamcinolone worked at very low concentration (0.012 µM) while, Dex showed no significant effect, even if a decrease in soma cell size tendency is observed. Interestingly, Fluocinolone appears to have better effect protecting from swelling at lowest concentration. According with our

results, one study suggested that low doses of glucocorticoids may have antiedematous effects on the retina with reduced toxicity (Zhao et al., 2011). This is important due to the GCs side effects like diabetes mellitus, peptic ulcer, Cushing's syndrome, osteoporosis, skin atrophy, psychosis, glaucoma, risks of cataract progression, elevation of intraocular pressure, and endophthalmitis, among many others, which limits their use (Edelman, 2010; Schäcke et al., 2004). Therefore, the protective effect of Fluocinolone during MGC edema at this very low concentration (0.012 µM) motivates the continuing investigation of Fluocinolone in the lens surgery model and investigating the possible role of this GC on the Dp71 promoter.

It has been observed for decades that responses to GC vary between patients and different cell types and tissues, and that structurally different GCs can generate different responses in patients, cells or tissues. Remarkably, Ronacher et al. determined that the efficacy of a ligand for both transactivation and transrepression is unrelated to its relative affinity for the receptor (Ronacher et al., 2009). The steroid effects of Dex, Triam and Fluo on gene transcription seems to be cell lineage dependent as well as time and steroid concentration dependent (Edelman, 2010; Nehmé et al., 2009). These facts, increase the importance of studies like this one, comparing different doses of more than one GC, to better understand the effect of GCs in retinal tissue and their role in retinal edema.

The lipid signaling cascades are implicated in inflammatory diseases like diabetes. In this study, we observed that inhibition of PLA2 and LOX enzymes prevent the MGC swelling and the Dp71 and Kir4.1 downregulation; however, COX inhibitor was not able to prevent the molecular changes associates with MGC swelling. This result lead us to propose that the MGC swelling in our retinal explant model respond to a leukotriene pathway activation. However, the *in vivo* response model after lens surgery remains to be investigated. As we observed a doses response effect in the retinal explant model it would be interesting to analyze the effect of different concentration of the 3 GCs tested in the *in vitro* model.

For BRB maintenance, the correct cell to cell interactions is a very important condition and GCs influence the expression of some cell adhesion molecules. Connexin 43 (Cx43), a gap junction protein, was localized in MGC (Ball and McReynolds, 1998) and implicated in neurodegenerative diseases (Orellana et al., 2009); we observed that in Dp71 null mice, Cx43 expression is downregulated (unpublished data). The tight junctions (TJ) are essential to establish the barrier between endothelial cells in the retinal and brain blood vessels and to maintain a proper environment for neuronal function. In diabetes disease, occluding protein expression, specifically claudin-5, expressed in retinal vasculature, is reduced and this is associated with an increase in BRB permeability (Antonetti et al., 1998). No differential changes in Cx43 expression were observed, thus we propose to evaluate claudin or occludin expression in our model is required to clarify the BRB breakdown mechanism and the effect of the different GCs in these adhesion molecules.

Conclusions

In this study, we showed that Dex was able to prevent MGC swelling, suggesting a possible protective role of Dex in MGC edema due to surgery.

As Dex prevent the molecular changes observed during MGC edema, we suggest a neuroprotective effect of Dex and this could be useful in a neuroprotective therapeutic approach.

Dex was able to prevent the edema formation through an overexpression of HSF1 a Dp71 transcriptional factor.

According with our results, the MGC edema observed in the retinal explant model was developed through activation of araquidonic acid pathway, especially the leukotriene pathway.

Dex, Triam and Fluo were able to prevent MGC swelling in the retinal explant model.

The glucocorticoids tested have a dose dependent response to prevent the downregulation of Dp71, AQP4 and Kir4.1.

The possibility of reducing the doses of glucocorticoids in the clinic as a neuroprotective therapeutic approach was proposed.

SECOND PART

"Role of Dp71 and ε-SG in the intercellular junctions of PC12 cells."

Background

Dickens and collaborators in 2002 demonstrated the presence of a homologous domain to cadherin in α and ε-sarcoglycan sequences, these domains are present in adhesion molecules that intervene in a wide range of processes during cell polarization and migration. This leads to the possibility that the ε-sarcoglycan molecule, besides being part of the sarcoglycan complex in DAPC, also participates in cell adhesion (Dickens et al., 2002).

On the other hand, in our study group, we had tested the presence of Dp71 in cell-cell contact sites, Márquez and coworkers using immunofluorescence assays, found that the Dp71f although present in the cellular cytoplasm is not found in the contact sites between cells, while the isoforms belonging to the Dp71d group are strongly localized in cell-cell contact sites (Marquez et al., 2003).

In 2007, Romo and colleagues reported that ε-SG is concentrated at cell-cell contact sites in PC12 cells (Romo-Yáñez et al., 2007). In 2013, it was found that in undifferentiated PC12 cells, the isoforms belonging to the group of Dp71d ($Dp71d_{\Delta 71}$ and $Dp71d_{\Delta 71\text{-}74}$) colocalize with ε-SG in undifferentiated PC12 cells (Fig. 23), being the Pearson correlation coefficients 0.71 and 0.72 respectively (Fig. 24), while the other Dp71 isoforms ($Dp71f_{\Delta 71}$ $Dp71e_{\Delta 71}$ and $Dp71e_{\Delta 71\text{-}74}$) do not colocalize with ε-SG (Fig. 23). Similar results were found in differentiated cells, Dp71d isoforms colocalize with ε-SG, whereas the Dp71 isoforms from groups f and e do not (Fig. 25). An important finding was that the Dp71c isoform is identified as being concentrated at the cell-cell binding sites (Fig. 25) the same colocalization was observed in differentiated PC12 cells (Fig.

25). Interestingly, overexpression of both Dp71d isoforms modified the ε-SG localization and expression (the ε-SG staining was more evident in cells that overexpress Dp71d isoforms). Dp71c isoform presented a strong stained located at the cell to cell contact site suggesting it role in cell to cell adhesion processes (Siqueiros 2014, Master Thesis).

Additionally, mutations in SGCE gene (ε-sarcoglycan) lead to myoclonic dystonia disorder. Myoclonic dystonia is a movement disorder characterized by the presence of rapid and brief contractions of the muscle, called myoclonus, it also presents sustained torsion and repeated movements (dystonia). In addition, patients present symptoms in central nervous system like: obsessive-compulsive disorder, depression, anxiety, personality disorder, alcohol abuse and panic attacks, symptoms develop in childhood or early adolescence (Raymond and Ozelius, 1993). In addition to the importance of the SGCE gene in myoclonic dystonia, Klein and colleagues reported a mutation in the DRD2 gene that codes for the dopamine D2 receptor in neuropsychiatric disorders (Asmus et al., 2002; Klein et al., 2002; Zimprich et al., 2001).

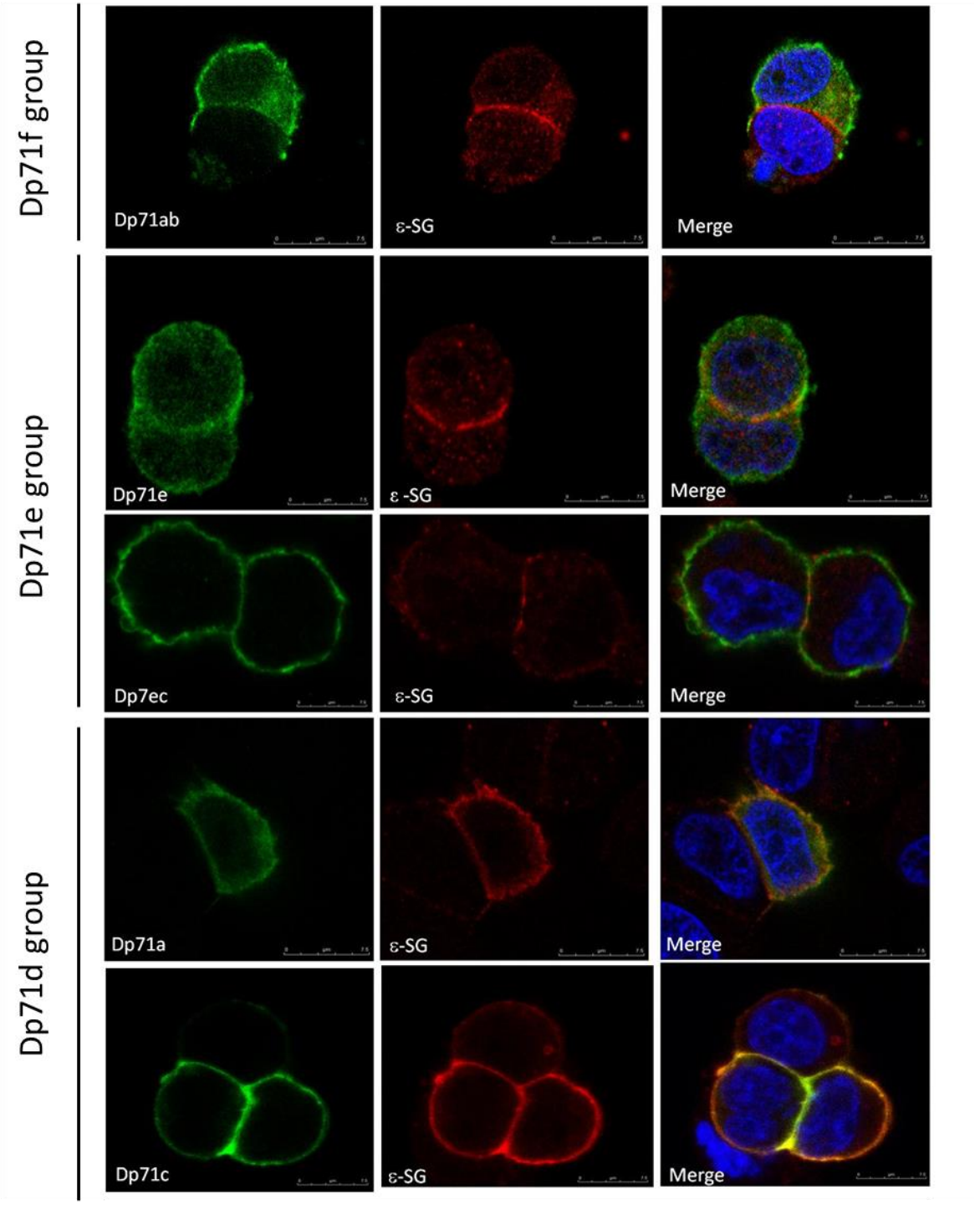
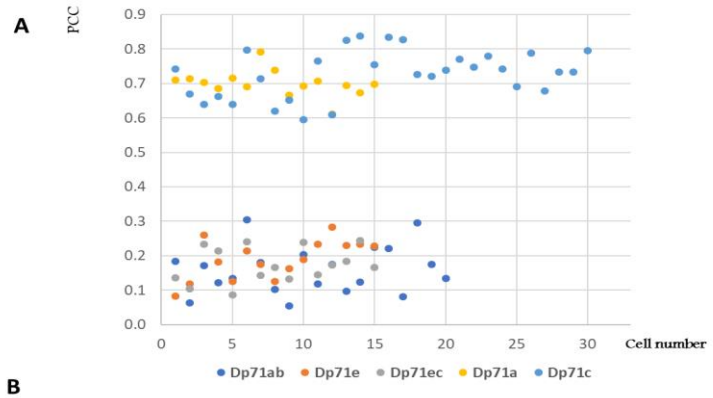


Figure 23.- Colocalization of Dp71 isoforms with ε-SG in PC12/Tet-On cells without differentiation.

Immunofluorescence of PC12/Tet-On cells transfected with the plasmids: pTRE2pur-myc/Dp71ab ($Dp71f_{\Delta 71}$), pTRE2pur-myc/Dp71e ($Dp71e_{\Delta 71}$), pTRE2pur-myc/Dp71ec ($Dp71e_{\Delta 71\text{-}74}$),

pTRE2pur-myc/Dp71a (*Dp71d$_{\Delta 71}$*) and pTRE2pur-myc/Dp71c (*Dp71d$_{\Delta 71\text{-}74}$*) in the inducible Tet-On system. The isoforms are classified by groups: f, e and d. Dp71 isoform (green) and ε-SG (red); the overlap images are observed in left panels. Isoforms Dp71ab (group f), Dp71e and Dp71ec do not colocalize with ε-SG wherefore, the isoforms Dp71a and Dp71c (group d) colocalize with the ε-SG. Images obtained in a confocal microscope of the equatorial zone of the cells; representative result of at least two independent experiments.

A



B

Dp71 Isoform	Pearson correlation coefficient (Average)
Dp71ab (Dp71f$_{\Delta 71}$)	0.16
Dp71e (Dp71e$_{\Delta 71}$)	0.18
Dp71ec (Dp71e$_{\Delta 71\text{-}74}$)	0.14
Dp71a (Dp71d$_{\Delta 71}$)	0.70
Dp71c (Dp71d$_{\Delta 71\text{-}74}$)	0.72

Figure 24.- Pearson correlation coefficient in PC12 expressing Dp71 isoforms.

A. Graphic representation of Person correlation coefficient (PCC) colocalization of Dp71 isoforms and ε-SG in PC12/Tet-On cells transfected with the plasmids: pTRE2pur-myc/Dp71ab (*Dp71f$_{\Delta 71}$*), pTRE2pur-myc/Dp71e (*Dp71e$_{\Delta 71}$*), pTRE2pur-myc/Dp71ec (*Dp71e$_{\Delta 71\text{-}74}$*), pTRE2pur-myc/Dp71a (*Dp71d$_{\Delta 71}$*) and pTRE2pur-myc/Dp71c (*Dp71d$_{\Delta 71\text{-}74}$*). **B.** Mean values of each PCC obtained for each Dp71 isoform.

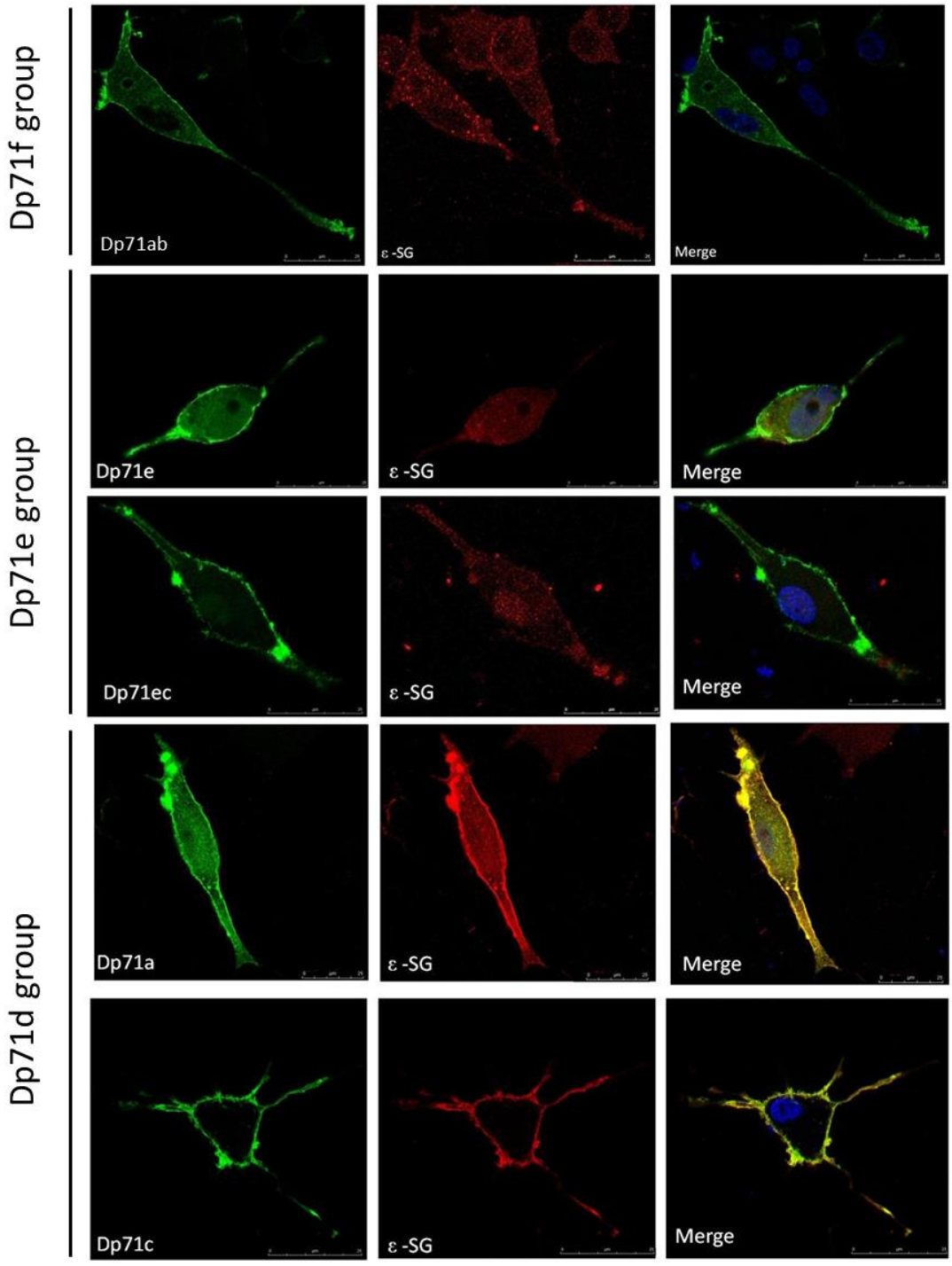


Figure 25.- Colocalization of Dp71 isoforms with ε-SG in differentiated PC12/Tet-On cells.

Immunofluorescence of PC12/Tet-On cells transfected with plasmids: pTRE2pur-myc/Dp71ab (*Dp71f$_{\Delta 71}$*), pTRE2pur-myc/Dp71e (*Dp71e$_{\Delta 71}$*), pTRE2pur-myc/Dp71ec (*Dp71e$_{\Delta 71\text{-}74}$*), pTRE2pur-myc/Dp71a (*Dp71d$_{\Delta 71}$*) and pTRE2pur-myc/Dp71c (*Dp71d$_{\Delta 71\text{-}74}$*). The isoforms are classified by group: f, e and d. Isoform (green), ε-SG (red), the overlap images are observed in right panels. Dp71ab (group f), Dp71e and Dp71ec do not colocalize with ε-SG whereas, Dp71a and Dp71c (group d) colocalize with ε-SG; overexpression of both isoforms modifies the expression level and location of ε-SG. Obtained in a confocal microscope of the equatorial zone of the cells. Representative images of at least two independent experiments.

PC12 cells model

PC12 cells were established from a rat adrenal pheochromocytoma, they are responsive to neuronal growth factor (NGF) differentiating into neurons-like cells. After one week of treatment with NGF PC12 cells stop multiplying and begin to present varicose ramifications, a process similar to the one occurring in sympathetic neurons in primary culture; after several weeks exposed to NGF treatment the neurites reach a length of 500 to 1000 µm. The differentiation process is reversible in PC12 cells and after 72 hours without NGF the cells start duplication. These cells produce and store the neurotransmitters dopamine and norepinephrine, and constitute a useful cellular model for neurobiological and neurochemical studies (Greene and Tischler, 1976).

PC12 cells represent a model for studying the Dp71 isoforms as they express the following isoforms: Dp71d$_{\Delta 71}$ (Dp71a) (GI: 52630317), Dp71f$_{\Delta 71}$ (Dp71ab) (GI: 32966046), Dp71d$_{\Delta 71\text{-}74}$ (Dp71c) (GI: 32966048), Dp71e$_{\Delta 71}$ (Dp71e) (GI: 327422419) and Dp40 (GI: 150036270). It is also known that during the differentiation process of these cells the levels of Dp71f increase (Marquez et al., 2003), the expression of the Dp71 isoforms is fundamental for the development of neurites in differentiated

PC12 cells with both NGF as with cAMP factors (Acosta et al., 2004; Aragón et al., 2011).

In this cell line, dystrophin Dp71 interacts with β-dystroglycan, β1-syntrophin, γ1-syntrophin, β-dystrobrevin, as well as α-, β-, γ- and ε-sarcoglycan (Villarreal-Silva et al., 2010). I has been reported that the Dp71ab associated complex is different in undifferentiated and differentiated PC12 cells (Romo-Yáñez et al., 2007), which lead to think in the relevance of each isoform during the different cellular processes like differentiation.

Results

1. Colocalization of Dp71d isoforms with ε-SG

In order to confirm the colocalization observed in PC12/Tet-On cell transiently transfected with the Dp71 isoforms, we decide to work with PC12/Tet-On stable transfected cells: PC12/Dp71d$_{\Delta 71}$ (clone No. 4) and PC12/Dp71d$_{\Delta 71\text{-}74}$ (clone No. 4). We confirmed the expression of each Dp71 isoform by PCR from genomic DNA using specific primers for the C-terminal of Dp71 isoforms from group d (Table 1); the protein expression was confirmed by Western Blot.

The colocalization between epsilon-sarcoglycan and Dp71 isoforms was evaluated in undifferentiated and differentiated cells, as we expected both isoforms showed a clearly colocalization with ε-SG in (Fig. 26).

We observed that, even if each clone was propagated from a single cell, some cells stained stronger for the Dp71d isoforms (Fig. 26 arrow) and these cells allowed us to observe that the more stained the cell for Dp71d isoforms the more stained for ε-SG; this phenomenon was also observed in transiently transfected cells.

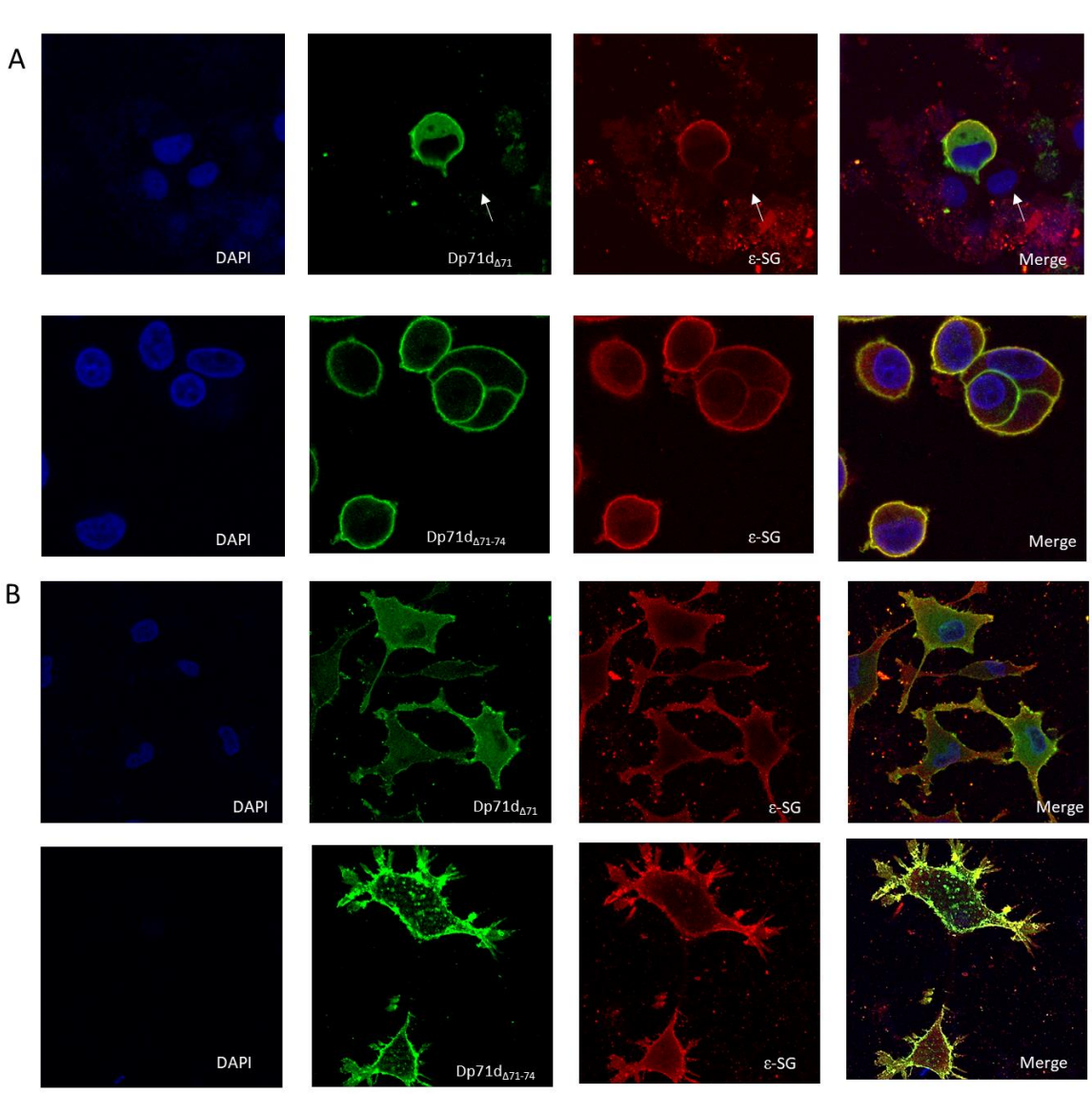


Figure 26.- Colocalization of Dp71 isoforms with ε-SG in PC12 clones expressing Dp71 isoforms.

A. Immunofluorescence of undifferentiated PC12 stable clones: PC12/Dp71d$_{\Delta 71}$ and PC12/Dp71d$_{\Delta 71-74}$ Dp71d isoform (green) was detected by anti-Myc antibody, ε-SG (red) was detected by anti-ε-SG (Lg7) antibody **B.** Immunofluorescence of differentiated cells. Both Dp71d isoforms colocalize with ε-SG in undifferentiated and differentiated cells. The arrow indicates one cell that expresses a low amount of dystrophin Dp71d, which

correlates with a lighter stain for ε-SG compare to the strong stain observed in the cell overexpressing the Dp71d$_{\Delta 71}$ isoform. Images of the equatorial zone of the cells were obtained in a confocal microscope of the equatorial zone of the cells. Representative images of at least two independent experiments.

2. Colocalization of Dp71d isoforms with adhesion molecules

Considering the location of ε-SG and Dp71 in the cell to cell binding sites, it was considered to evaluate the colocalization between proteins involved in adherent unions mediated by cadherins (β-catenin and N-cadherin) and ε-SG. We observed that even if β-catenin and N-cadherin are concentrated in the contact sites as previously reported (Chen, Chen et al., 2005; Lee and Tomarev 2007) they did not show a clear colocalization with Dp71d isoforms in PC12/Dp71d$_{\Delta 71}$ and PC12/Dp71d$_{\Delta 71\text{-}74}$ cells (Fig. 27).

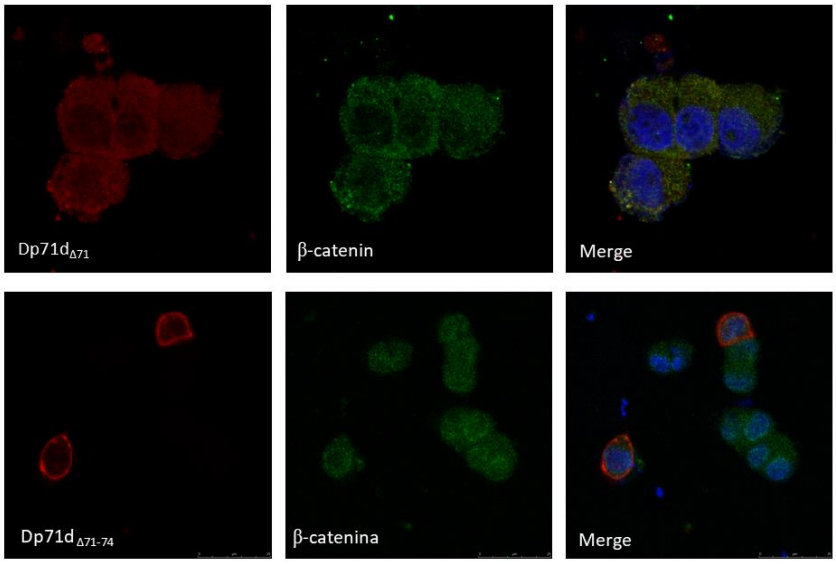


Figure 27.- Colocalization of Dp71 isoforms with beta-catenin in PC12 clones expressing Dp71 isoforms.

Immunofluorescence of undifferentiated PC12 stable clones: PC12/Dp71dΔ71 and PC12/Dp71dΔ71-74 Dp71d isoform (red) was detected by anti-Myc antibody, β-catenin (green) was detected by anti- β-catenin (Abcam) antibody. No clear colocalization was observed. Images of the equatorial zone of the cells were obtained in a confocal microscope of the equatorial zone of the cells. Representative images of at least two independent experiments.

Considering these results, we decide to analyze another adherent mechanism; the gap junctions which involves Connexin 43 (Cx43). We previously observed a decrease in Cx43 expression in hole retina from Dp71 null mice compared with wild-type mice. Moreover, we observed that MGC from Dp71 null mice showed a very weak stain against Cx43 compared with wild-type mice. The immunofluorescences in PC12 clones: PC12/Dp71d$_{\Delta 71}$ and PC12/Dp71d$_{\Delta 71-74}$ showed a differential staining pattern associated with the overexpressed isoform; dystrophin Dp71d$_{\Delta 71}$

(Dp71a) present an evident colocalization with Cx43; both molecules are concentrated in cell to cell binding sites (Fig. 28).

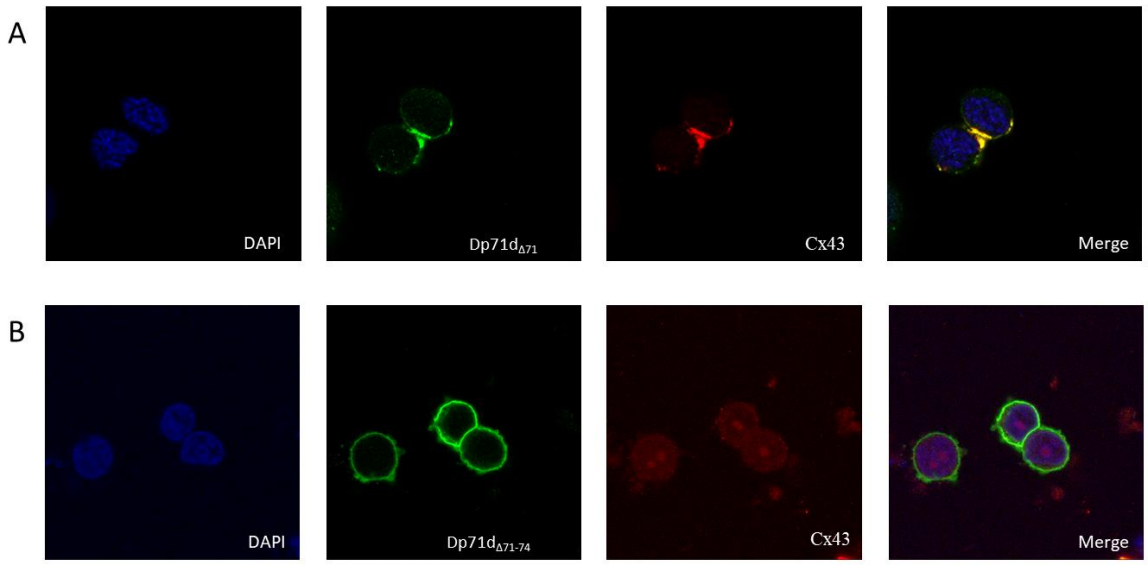


Figure 28.- Colocalization of Dp71 isoforms with Connexin43 in PC12 clones expressing Dp71 isoforms.

Immunofluorescence of PC12/Tet-On clones: A. PC12/Dp71d$_{\Delta 71}$ and B. PC12/Dp71d$_{\Delta 71-74}$. Colocalization between Dp71d isoform (green) using an anti-Myc antibody and connexin 43 (red) using Cx43 Abcam antibody, the overlap images are observed in right panels. Dp71d$_{\Delta 71}$ colocalize clearly with Cx43 at cell to cell binding sites whereas Dp71d$_{\Delta 71-74}$ isoform did not colocalize. Images of the equatorial zone of the cells were obtained in a confocal microscope of the equatorial zone of the cells.

3. Effect of the overexpression of Dp71$_{\Delta 71}$ and Dp71$_{\Delta 71\text{-}74}$ on cell to cell adhesion in PC12 cells

With the aim to study the role of Dp71d group on cell to cell adhesion, we evaluated the PC12/Tet-On clones: PC12/Dp71d$_{\Delta 71}$ and PC12/Dp71d$_{\Delta 71\text{-}74}$. We quantified the ability to form and maintain cell clusters when each Dp71d isoform is overexpressed as well as the number of cells that form these clusters. We observed that both Dp71d isoforms form and maintain more clusters that the control PC12/Tet-On cells transfected with the empty vector. Moreover, the clusters formed for Dp71d overexpressed clones consisted of 3, 4 or more cells being more numerous than the clusters formed in the control cells (Fig. 29).

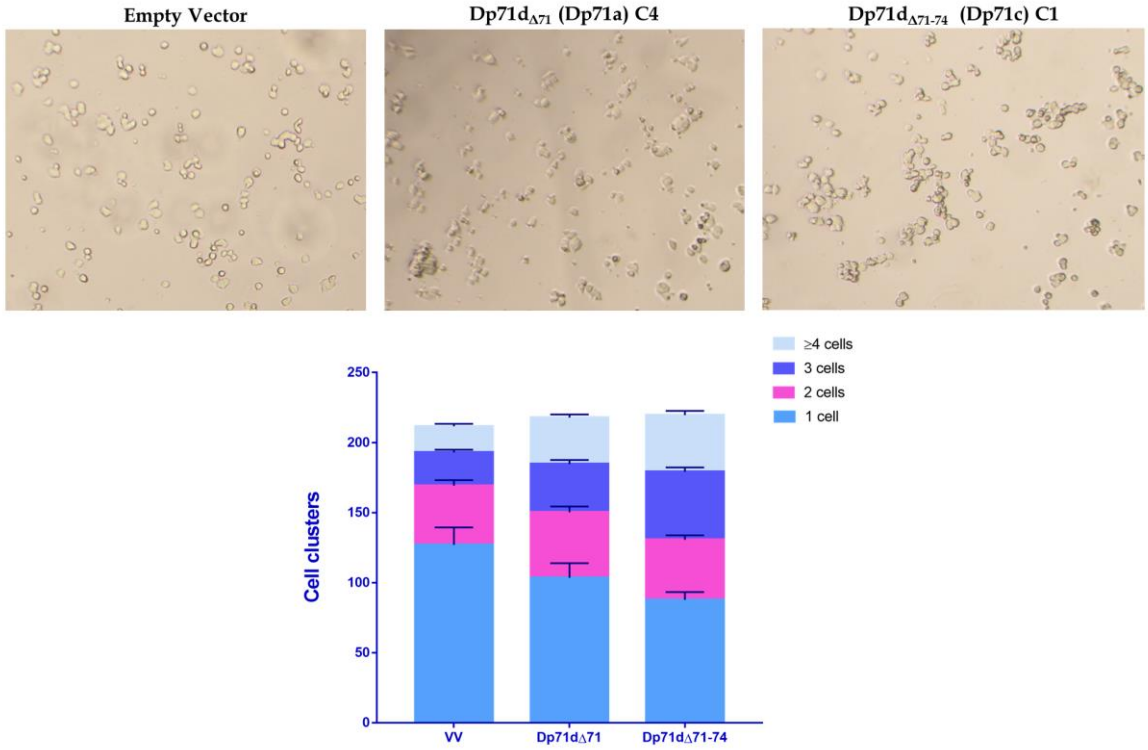


Figure 29.- Cell to cell adhesion quantification.

Quantification of cell cluster as well as the number of cells present in each cluster of clones: PC12/Dp71d$_{\Delta 71}$, PC12/Dp71d$_{\Delta 71\text{-}74}$ and PC12/empty-vector. Upper panel showed representative images of PC12/Tet-On clones; lower panel showed the graphic representation of cell adhesion quantification.

Discussion and perspectives

Dystrophin Dp71 is the main product of the DMD gene in the central nervous system, the importance of Dp71 in this system has been described in several works in addition with the fact that the loss of function of this dystrophin has been associated with an increase in the severity of mental retardation which occurs in patients with DMD (Daoud et al., 2009b; Perronnet and Vaillend, 2010; Waite et al., 2012). The role of Dp71 isoforms in different cell processes as cell adhesion (Cerecedo et al., 2006; Marquez et al., 2003), cell division (Herrera-Salazar et al., 2016; Villarreal-Silva et al., 2011), osmoregulation and vascular permeability (Fort et al., 2008; Sene et al., 2009) as well as in neuronal differentiation (Acosta et al., 2004; Marquez et al., 2003) have been also investigated, however, in most of the cases it is not known which isoform or isoforms are responsible for the different functions, the only data available is the Dp71 isoform group involved in each process.

Recently, the expression of Dp71d and Dp71f in human bronchial epithelium (HBE) have been showed by Tan et al. (Tan et al., 2017); they associated an overexpression of Dp71d and dp71f in HBE with an increase in proliferation rate, invasion and migration capabilities probably due to an over activation of FAK-ERK and with an increased cyclin D expression.

Additionally, it has been reported that the loss of function of the SGCE gene product (ε-SG) causes myoclonic dystonia which affects the function of the CNS (Asmus et al., 2002; Raymond and Ozelius, 1993). Moreover, it has been described that when two cells are in contact, ε-SG is

concentrated in these sites of interaction between cells (Romo-Yáñez et al., 2007). The aim of this study was to assign one specific role to $Dp71d_{\Delta 71}$ (Dp71a) and $Dp71d_{\Delta 71\text{-}74}$ (Dp71c) isoforms in cell to cell adhesion process through their possible interaction with ε-SG as well as their interaction with adhesion proteins involved in cell to cell contacts.

The identification of each isoform of Dp71 in the different processes cannot be performed using antibodies because Dp71 isoform share the epitopes recognized by most of the available antibodies, using antibodies we are able to detect only groups of Dp71 isoforms. For this reason, we decided to work with recombinant proteins, Dp71 isoform fused to Myc epitope, in an inducible system (Tet-On gene expression system).

The immunolocalization assays performed in this work and the cell to cell quantification approach suggest that Dp71d isoforms have a role in cell to cell adhesion processes. Nevertheless, only $Dp71_{\Delta 71}$ colocalize with Cx43 at cell to cell binding sites which associates $Dp71_{\Delta 71}$ with gap junctions but no $Dp71_{\Delta 71\text{-}74}$. This is important because so far there are no specific function related to specific Dp71 isoforms. It is possible to think that the presence of the exon 78 as well as the presence of exons 72-74 allow the formation of a $Dp71d_{\Delta 71}$ complex in which gap junction proteins such as Cx43 interact.

On the other hand, as we observed an important increase of cell clusters in the cells that overexpress both isoforms; we think that $Dp71d_{\Delta 71\text{-}74}$ has also a role in cell to cell adhesion. Complex associated to this isoform may interact with additional adhesion molecules like cadherins, integrins, etc.

We observed that both Dp71 isoform tested: $Dp71d_{\Delta 71}$ (Dp71a) and $Dp71d_{\Delta 71\text{-}74}$ (Dp71c) colocalize with ε-SG and it has been suggested that ε-SG has a role in maintaining cell adhesion (Maréchal et al., 2003). Dystrophins Dp71f have been related with FAK (focal adhesion kinase) (Tan et al., 2017) and has been reported as a structural component of β1-integrin adhesion complex, however, as far as we know, Dp71d has not been directly implicated in adhesion processes.

Our results suggest that at least these two Dp71d isoforms have a role in cell adhesion throughout at least wo different mechanisms. $Dp71d_{\Delta 71}$ seems to form gap junctions with Cx43 in PC12 cells and this interaction seems to regulate ε-SG localization and expression due to the fact that when more Dp71 staining was observed, more ε-SG was detected. It is important to emphasize that these results need to be confirmed by other methods, to confirm the interactions suggested.

Dystrophin Dp71d has been reported as the more abundant isoforms group expressed in brain (Aragón et al., 2017), persist in the study of these Dp71 isoforms could allow us to better understand the functioning of the central nervous system as well as the alterations observed in patients with mental retardation.

The fact that Cx43 is expressed in retina, Dp71 null mice has a strong Cx43 downregulation, Dp71 null mice shows an increase in BRB permeability and Dp71 has a role during formation and resolution of MGC edema makes important to study the role of Dp71d-associated complex in retina and brain.

It is also interesting to evaluate the function of the Dp71 groups f and e in cell adhesion; the Dp71 f group is the most abundant in the retina as mentioned in the first part of this work. Increasing knowledge about the role of Dp71 in cell adhesion will contribute to find new therapeutic targets to control and/or prevent edema and its complications.

Conclusions

In this work, it is suggested, for the first time, the participation of the Dp71d$_{\Delta 71}$ and Dp71d$_{\Delta 71\text{-}74}$ isoforms in the intercellular adhesion process.

The participation of Dp71d$_{\Delta 71}$, this process is apparently mediated by gap-type junctions.

Dp71d$_{\Delta 71\text{-}74}$ isoform also has a role in adhesion process, but this role seemingly is not mediated by Cx43.

The overexpression of Dp71d$_{\Delta 71}$ and Dp71d$_{\Delta 71\text{-}74}$ isoforms improve the PC12 ability to form cell clusters.

References

Acosta, R., Montañez, C., Fuentes-Mera, L., Gonzalez, E., Gómez, P., Quintero-Mora, L., Mornet, D., Alvarez-Salas, L.M., and Cisneros, B. (2004). Dystrophin Dp71 is required for neurite outgrowth in PC12 cells. Exp. Cell Res. 296, 265–275.

Antonetti, D.A., Barber, A.J., Khin, S., Lieth, E., Tarbell, J.M., and Gardner, T.W. (1998). Vascular permeability in experimental diabetes is associated with reduced endothelial occludin content: vascular endothelial growth factor decreases occludin in retinal endothelial cells. Penn State Retina Research Group. Diabetes 47, 1953–1959.

Antonetti, D.A., Wolpert, E.B., DeMaio, L., Harhaj, N.S., and Scaduto, R.C. (2002). Hydrocortisone decreases retinal endothelial cell water and solute flux coincident with increased content and decreased phosphorylation of occludin. J. Neurochem. 80, 667–677.

Aragón, J., Romo-Yáñez, J., Martínez-Herrera, A., Ceja, V., Rendon, A., and Montañez, C. (2011). Characterization of Dp71Δ(78-79), a novel dystrophin mutant that stimulates PC12 cell differentiation. J. Neurochem. 119, 697–707.

Aragón, J., González-Reyes, M., Romo-Yáñez, J., Vacca, O., Aguilar-González, G., Rendón, A., Vaillend, C., and Montañez, C. (2017). Dystrophin Dp71 Isoforms Are Differentially Expressed in the Mouse Brain and Retina: Report of New Alternative Splicing and a Novel Nomenclature for Dp71 Isoforms. Mol. Neurobiol.

Ashwell, J.D., Lu, F.W., and Vacchio, M.S. (2000). Glucocorticoids in T cell development and function. Annu. Rev. Immunol. 18, 309–345.*

Asmus, F., Zimprich, A., Tezenas Du Montcel, S., Kabus, C., Deuschl, G., Kupsch, A., Ziemann, U., Castro, M., Kühn, A.A., Strom, T.M., et al. (2002). Myoclonus-dystonia syndrome: ε-sarcoglycan mutations and phenotype. Ann. Neurol. 52, 489-492.

Austin, R.C., Morris, G.E., Howard, P.L., Klamut, H.J., and Ray, P.N. (2000). Expression and synthesis of alternatively spliced variants of Dp71 in adult human brain. Neuromuscul. Disord. NMD 10, 187-193.

Ball, A.K., and McReynolds, J.S. (1998). Localization of gap junctions and tracer coupling in retinal Müller cells. J. Comp. Neurol. 393, 48-57.

Bar, S., Barnea, E., Levy, Z., Neuman, S., Yaffe, D., and Nudel, U. (1990). A novel product of the Duchenne muscular dystrophy gene which greatly differs from the known isoforms in its structure and tissue distribution. Biochem. J. 272, 557-560.

Barnes, P.J. (2006). How corticosteroids control inflammation: Quintiles Prize Lecture 2005. Br. J. Pharmacol. 148, 245-254.

Barnes, P.J. (2011). Glucocorticosteroids: current and future directions. Br. J. Pharmacol. 163, 29-43.

Benabdesselam, R., Sene, A., Raison, D., Benmessaoud-Mesbah, O., Ayad, G., Mornet, D., Yaffe, D., Rendon, A., Hardin-Pouzet, H., and Dorbani-Mamine, L. (2010). A deficit of brain dystrophin 71 impairs hypothalamic osmostat. J. Neurosci. Res. 88, 324-334.

Beutler, B., and Cerami, A. (1986). Cachectin/tumor necrosis factor: an endogenous mediator of shock and inflammation. Immunol. Res. 5, 281-293.

Blake, D.J., Hawkes, R., Benson, M.A., and Beesley, P.W. (1999). Different dystrophin-like complexes are expressed in neurons and glia. J. Cell Biol. 147, 645-658.

Blake, D.J., Weir, A., Newey, S.E., and Davies, K.E. (2002). Function and Genetics of Dystrophin and Dystrophin-Related Proteins in Muscle. Physiol. Rev. 82, 291-329.

Brem, H., Gresser, I., Grosfeld, J., and Folkman, J. (1993). The combination of antiangiogenic agents to inhibit primary tumor growth and metastasis. J. Pediatr. Surg. 28, 1253-1257.

Bringmann, A., Pannicke, T., Grosche, J., Francke, M., Wiedemann, P., Skatchkov, S.N., Osborne, N.N., and Reichenbach, A. (2006).

Müller cells in the healthy and diseased retina. Prog. Retin. Eye Res. 25, 397–424.

Burgermeister, E., Endl, J., and Scheuer, W.V. (2003). Activation of cytosolic phospholipase A2 in human T-lymphocytes involves inhibitor-κB and mitogen-activated protein kinases. Eur. J. Pharmacol. 466, 169–180.

Burridge, K., and Chrzanowska-Wodnicka, M. (1996). Focal adhesions, contractility, and signaling. Annu. Rev. Cell Dev. Biol. 12, 463–518.

Byers, T.J., Lidov, H.G., and Kunkel, L.M. (1993). An alternative dystrophin transcript specific to peripheral nerve. Nat. Genet. 4, 77–81.

Ceccarini, M., Rizzo, G., Rosa, G., Chelucci, C., Macioce, P., and Petrucci, T.C. (1997). A splice variant of Dp71 lacking the syntrophin binding site is expressed in early stages of human neural development. Brain Res. Dev. Brain Res. 103, 77–82.

Cerecedo, D., Mondragón, R., Cisneros, B., Martínez-Pérez, F., Martínez-Rojas, D., and Rendón, A. (2006). Role of dystrophins and utrophins in platelet adhesion process. Br. J. Haematol. 134, 83–91.

Cerna, J., Cerecedo, D., Ortega, A., García-Sierra, F., Centeno, F., Garrido, E., Mornet, D., and Cisneros, B. (2006). Dystrophin Dp71f associates with the beta1-integrin adhesion complex to modulate PC12 cell adhesion. J. Mol. Biol. 362, 954–965.

Claudepierre, T., Rodius, F., Frasson, M., Fontaine, V., Picaud, S., Dreyfus, H., Mornet, D., and Rendon, A. (1999). Differential distribution of dystrophins in rat retina. Invest. Ophthalmol. Vis. Sci. 40, 1520–1529.

Claudepierre, T., Mornet, D., Pannicke, T., Forster, V., Dalloz, C., Bolaños, F., Sahel, J., Reichenbach, A., and Rendon, A. (2000). Expression of Dp71 in Müller glial cells: a comparison with utrophin- and dystrophin-associated proteins. Invest. Ophthalmol. Vis. Sci. 41, 294–304.

Cotton, S., Voudouris, N.J., and Greenwood, K.M. (2001). Intelligence and Duchenne muscular dystrophy: full-scale, verbal, and performance intelligence quotients. Dev. Med. Child Neurol. 43, 497–501.

Coutinho, A.E., and Chapman, K.E. (2011). The anti-inflammatory and immunosuppressive effects of glucocorticoids, recent developments and mechanistic insights. Mol. Cell. Endocrinol. 335, 2–13.

Cox, G.A., Sunada, Y., Campbell, K.P., and Chamberlain, J.S. (1994). Dp71 can restore the dystrophin-associated glycoprotein complex in muscle but fails to prevent dystrophy. Nat. Genet. 8, 333–339.

Cronstein, B.N., Kimmel, S.C., Levin, R.I., Martiniuk, F., and Weissmann, G. (1992). A mechanism for the antiinflammatory effects of corticosteroids: the glucocorticoid receptor regulates leukocyte adhesion to endothelial cells and expression of endothelial-leukocyte adhesion molecule 1 and intercellular adhesion molecule 1. Proc. Natl. Acad. Sci. U. S. A. 89, 9991–9995.

Cunha-Vaz, J. (2017). The Blood-Retinal Barrier in the Management of Retinal Disease: EURETINA Award Lecture. Ophthalmologica 237, 1–10.

Dalloz, C., Sarig, R., Fort, P., Yaffe, D., Bordais, A., Pannicke, T., Grosche, J., Mornet, D., Reichenbach, A., Sahel, J., et al. (2003). Targeted inactivation of dystrophin gene product Dp71: phenotypic impact in mouse retina. Hum. Mol. Genet. 12, 1543–1554.

Daoud, F., Angeard, N., Demerre, B., Martie, I., Benyaou, R., Leturcq, F., Cossée, M., Deburgrave, N., Saillour, Y., Tuffery, S., et al. (2009a). Analysis of Dp71 contribution in the severity of mental retardation through comparison of Duchenne and Becker patients differing by mutation consequences on Dp71 expression. Hum. Mol. Genet. 18, 3779–3794.

Daoud, F., Candelario-Martínez, A., Billard, J.-M., Avital, A., Khelfaoui, M., Rozenvald, Y., Guegan, M., Mornet, D., Jaillard, D., Nudel, U., et al. (2009b). Role of Mental Retardation-Associated Dystrophin-Gene Product Dp71 in Excitatory Synapse Organization, Synaptic Plasticity and Behavioral Functions. PLoS ONE 4.

Deconinck, A.E., Rafael, J.A., Skinner, J.A., Brown, S.C., Potter, A.C., Metzinger, L., Watt, D.J., Dickson, J.G., Tinsley, J.M., and Davies, K.E. (1997). Utrophin-dystrophin-deficient mice as a model for Duchenne muscular dystrophy. Cell 90, 717–727.

Derynck, R. (1990). Transforming growth factor-α. Mol. Reprod. Dev. 27, 3–9.

Diabetic Retinopathy Clinical Research Network, Browning, D.J., Glassman, A.R., Aiello, L.P., Beck, R.W., Brown, D.M., Fong, D.S., Bressler, N.M., Danis, R.P., Kinyoun, J.L., et al. (2007). Relationship between optical coherence tomography-measured central retinal thickness and visual acuity in diabetic macular edema. Ophthalmology 114, 525–536.

Dickens, N.J., Beatson, S., and Ponting, C.P. (2002). Cadherin-like domains in alpha-dystroglycan, alpha/epsilon-sarcoglycan and yeast and bacterial proteins. Curr. Biol. CB 12, R197-199.

D'Souza, V.N., Nguyen, T.M., Morris, G.E., Karges, W., Pillers, D.A., and Ray, P.N. (1995). A novel dystrophin isoform is required for normal retinal electrophysiology. Hum. Mol. Genet. 4, 837–842.

Dyer, M.A., and Cepko, C.L. (2001). Regulating proliferation during retinal development. Nat. Rev. Neurosci. 2, 333–342.

Edelman, J.L. (2010). Differentiating intraocular glucocorticoids. Ophthalmol. J. Int. Ophtalmol. Int. J. Ophthalmol. Z. Augenheilkd. 224 Suppl 1, 25–30.

Edelman, J.L., Lutz, D., and Castro, M.R. (2005). Corticosteroids inhibit VEGF-induced vascular leakage in a rabbit model of blood-retinal and blood-aqueous barrier breakdown. Exp. Eye Res. 80, 249–258.

El Mathari, B., Sene, A., Charles-Messance, H., Vacca, O., Guillonneau, X., Grepin, C., Sennlaub, F., Sahel, J.-A., Rendon, A., and Tadayoni, R. (2015). Dystrophin Dp71 gene deletion induces retinal vascular inflammation and capillary degeneration. Hum. Mol. Genet. 24, 3939–3947.

Feener, C.A., Koenig, M., and Kunkel, L.M. (1989). Alternative splicing of human dystrophin mRNA generates isoforms at the carboxy terminus. Nature 338, 509–511.

Felinski, E.A., Cox, A.E., Phillips, B.E., and Antonetti, D.A. (2008). GLUCOCORTICOIDS INDUCE TRANSACTIVATION OF TIGHT JUNCTION GENES OCCLUDIN AND CLAUDIN-5 IN RETINAL ENDOTHELIAL CELLS VIA A NOVEL CIS-ELEMENT. Exp. Eye Res. 86, 867–878.

Ferrara, N., Houck, K., Jakeman, L., and Leung, D.W. (1992). Molecular and biological properties of the vascular endothelial growth factor family of proteins. Endocr. Rev. 13, 18–32.

Fett, J.W., Strydom, D.J., Lobb, R.R., Alderman, E.M., Bethune, J.L., Riordan, J.F., and Vallee, B.L. (1985). Isolation and characterization of angiogenin, an angiogenic protein from human carcinoma cells. Biochemistry (Mosc.) 24, 5480–5486.

Folkman, J., and Shing, Y. (1992). Angiogenesis. J. Biol. Chem. 267, 10931–10934.

Fort, P.E., Sene, A., Pannicke, T., Roux, M.J., Forster, V., Mornet, D., Nudel, U., Yaffe, D., Reichenbach, A., Sahel, J.A., et al. (2008). Kir4.1 and AQP4 associate with Dp71- and utrophin-DAPs complexes in specific and defined microdomains of Müller retinal glial cell membrane. Glia 56, 597–610.

Giocanti-Auregan, A., Vacca, O., Bénard, R., Cao, S., Siqueiros, L., Montañez, C., Paques, M., Sahel, J.-A., Sennlaub, F., Guillonneau, X., et al. (2016). Altered astrocyte morphology and vascular development in dystrophin-Dp71-null mice. Glia 64, 716–729.

Goldman, D. (2014). Müller glia cell reprogramming and retina regeneration. Nat. Rev. Neurosci. 15, 431–442.

González-Ramírez, R., Morales-Lázaro, S.L., Tapia-Ramírez, V., Mornet, D., and Cisneros, B. (2008). Nuclear and nuclear envelope localization of dystrophin Dp71 and dystrophin-associated proteins (DAPs) in the C2C12 muscle cells: DAPs nuclear localization is modulated during myogenesis. J. Cell. Biochem. 105, 735–745.

Górecki, D.C., and Barnard, E.A. (1995). Specific expression of G-dystrophin (Dp71) in the brain. Neuroreport 6, 893–896.

Górecki, D.C., Lukasiuk, K., Szklarczyk, A., and Kaczmarek, L. (1998). Kainate-evoked changes in dystrophin messenger RNA levels in the rat hippocampus. Neuroscience 84, 467–477.

Grady, R.M., Teng, H., Nichol, M.C., Cunningham, J.C., Wilkinson, R.S., and Sanes, J.R. (1997). Skeletal and cardiac myopathies in mice lacking utrophin and dystrophin: a model for Duchenne muscular dystrophy. Cell 90, 729–738.

Greene, L.A., and Tischler, A.S. (1976). Establishment of a noradrenergic clonal line of rat adrenal pheochromocytoma cells which respond to nerve growth factor. Proc. Natl. Acad. Sci. U. S. A. 73, 2424–2428.

Haenggi, T., and Fritschy, J.-M. (2006). Role of dystrophin and utrophin for assembly and function of the dystrophin glycoprotein complex in non-muscle tissue. Cell. Mol. Life Sci. CMLS 63, 1614–1631.

Harizi, H., Corcuff, J.-B., and Gualde, N. (2008). Arachidonic-acid-derived eicosanoids: roles in biology and immunopathology. Trends Mol. Med. 14, 461–469.

Herrera-Salazar, A., García-Villegas, R., Aragón, J., Sánchez-Trujillo, A., Ceja, V., Martínez-Herrera, A., Merino-Jiménez, C., and

Montañez, C. (2016). Overexpression of mutant dystrophin Dp71[INCREMENT]$_{78-79}$ stimulates cell proliferation. Neuroreport 27, 6–11.

Howard, P.L., Dally, G.Y., Wong, M.H., Ho, A., Weleber, R.G., Pillers, D.-A.M., and Ray, P.N. (1998). Localization of Dystrophin Isoform Dp71 to the Inner Limiting Membrane of the Retina Suggests a Unique Functional Contribution of Dp71 in the Retina. Hum. Mol. Genet. 7, 1385–1391.

Hugnot, J.P., Gilgenkrantz, H., Vincent, N., Chafey, P., Morris, G.E., Monaco, A.P., Berwald-Netter, Y., Koulakoff, A., Kaplan, J.C., and Kahn, A. (1992). Distal transcript of the dystrophin gene initiated from an alternative first exon and encoding a 75-kDa protein widely distributed in nonmuscle tissues. Proc. Natl. Acad. Sci. U. S. A. 89, 7506–7510.

Hynes, R.O. (1999). Cell adhesion: old and new questions. Trends Cell Biol. 9, M33-37.

Keil, J.M., Liu, X., and Antonetti, D.A. (2013). Glucocorticoid induction of occludin expression and endothelial barrier requires transcription factor p54 NONO. Invest. Ophthalmol. Vis. Sci. 54, 4007–4015.

Klaassen, I., Van Noorden, C.J.F., and Schlingemann, R.O. (2013). Molecular basis of the inner blood-retinal barrier and its breakdown in diabetic macular edema and other pathological conditions. Prog. Retin. Eye Res. 34, 19–48.

Klein, C., Liu, L., Doheny, D., Kock, N., Müller, B., De Carvalho Aguiar, P., Leung, J., De Leon, D., Bressman, S.B., Silverman, J., et al. (2002). ε-sarcoglycan mutations found in combination with other dystonia gene mutations. Ann. Neurol. 52, 675–679.

Koenig, M., Hoffman, E.P., Bertelson, C.J., Monaco, A.P., Feener, C., and Kunkel, L.M. (1987). Complete cloning of the Duchenne muscular dystrophy (DMD) cDNA and preliminary genomic organization of the DMD gene in normal and affected individuals. Cell 50, 509–517.

Koeppen Bruce M, and Stanton Bruce A (2008). Berne & Levy Physiology (Elsevier).

Kofuji, P., and Connors, N.C. (2003). Molecular substrates of potassium spatial buffering in glial cells. Mol. Neurobiol. 28, 195–208.

Lederfein, D., Levy, Z., Augier, N., Mornet, D., Morris, G., Fuchs, O., Yaffe, D., and Nudel, U. (1992). A 71-kilodalton protein is a

major product of the Duchenne muscular dystrophy gene in brain and other nonmuscle tissues. Proc. Natl. Acad. Sci. U. S. A. 89, 5346–5350.

Lidov, H.G., and Kunkel, L.M. (1997). Dp140: alternatively spliced isoforms in brain and kidney. Genomics 45, 132–139.

London, A., Benhar, I., and Schwartz, M. (2012). The retina as a window to the brain—from eye research to CNS disorders. Nat. Rev. Neurol. 9, nrneurol.2012.227.

Lumeng, C.N., Hauser, M., Brown, V., and Chamberlain, J.S. (1999). Expression of the 71 kDa dystrophin isoform (Dp71) evaluated by gene targeting. Brain Res. 830, 174–178.

Ma, S., Kwon, H.J., and Huang, Z. (2012). A Functional Requirement for Astroglia in Promoting Blood Vessel Development in the Early Postnatal Brain. PLOS ONE 7, e48001.

Maheshwari, M., Bhutani, S., Das, A., Mukherjee, R., Sharma, A., Kino, Y., Nukina, N., and Jana, N.R. (2014). Dexamethasone induces heat shock response and slows down disease progression in mouse and fly models of Huntington's disease. Hum. Mol. Genet. 23, 2737–2751.

Maréchal, L., Raux, G., Dumanchin, C., Lefebvre, G., Deslandre, E., Girard, C., Campion, D., Parain, D., Frebourg, T., and Hannequin, D. (2003). Severe myoclonus-dystonia syndrome awsocictud with a novel epsilon-sarcoglycan gene truncating mutation. Am. J. Med. Genet. B Neuropsychiatr. Genet. 119B, 114–117.

Marquez, F.G., Cisneros, B., Garcia, F., Ceja, V., Velázquez, F., Depardón, F., Cervantes, L., Rendón, A., Mornet, D., Rosas-vargas, H., et al. (2003). Differential expression and subcellular distribution of dystrophin Dp71 isoforms during differentiation process. Neuroscience 118, 957–966.

Moizard, M.P., Billard, C., Toutain, A., Berret, F., Marmin, N., and Moraine, C. (1998). Are Dp71 and Dp140 brain dystrophin isoforms related to cognitive impairment in Duchenne muscular dystrophy? Am. J. Med. Genet. 80, 32–41.

Monaco, A.P., Neve, R.L., Colletti-Feener, C., Bertelson, C.J., Kurnit, D.M., and Kunkel, L.M. (1986). Isolation of candidate cDNAs for portions of the Duchenne muscular dystrophy gene. Nature 323, 646–650.

Muntoni, F., Torelli, S., and Ferlini, A. (2003). Dystrophin and mutations: one gene, several proteins, multiple phenotypes. Lancet Neurol. 2, 731–740.

Murakami, T., Frey, T., Lin, C., and Antonetti, D.A. (2012). Protein Kinase Cβ Phosphorylates Occludin Regulating Tight Junction Trafficking in Vascular Endothelial Growth Factor–Induced Permeability In Vivo. Diabetes 61, 1573–1583.

Nehmé, A., Lobenhofer, E.K., Stamer, W.D., and Edelman, J.L. (2009). Glucocorticoids with different chemical structures but similar glucocorticoid receptor potency regulate subsets of common and unique genes in human trabecular meshwork cells. BMC Med. Genomics 2, 58.

Newman, E.A. (1987). Distribution of potassium conductance in mammalian Muller (glial) cells: a comparative study. J. Neurosci. 7, 2423–2432.

Newman, E.A. (2004). Glial Modulation of Synaptic Transmission in the Retina. Glia 47, 268–274.

Newman, E.A., Frambach, D.A., and Odette, L.L. (1984). Control of extracellular potassium levels by retinal glial cell K+ siphoning. Science 225, 1174–1175.

Orellana, J.A., Sáez, P.J., Shoji, K.F., Schalper, K.A., Palacios-Prado, N., Velarde, V., Giaume, C., Bennett, M.V.L., and Sáez, J.C. (2009). Modulation of brain hemichannels and gap junction channels by pro-inflammatory agents and their possible role in neurodegeneration. Antioxid. Redox Signal. 11, 369–399.

Pannicke, T., Iandiev, I., Wurm, A., Uckermann, O., vom Hagen, F., Reichenbach, A., Wiedemann, P., Hammes, H.-P., and Bringmann, A. (2006). Diabetes alters osmotic swelling characteristics and membrane conductance of glial cells in rat retina. Diabetes 55, 633–639.

Perretti, M., and Ahluwalia, A. (2000). The microcirculation and inflammation: site of action for glucocorticoids. Microcirc. N. Y. N 1994 7, 147–161.

Perronnet, C., and Vaillend, C. (2010). Dystrophins, utrophins, and associated scaffolding complexes: role in mammalian brain and implications for therapeutic strategies. J. Biomed. Biotechnol. 2010, 849426.

Purves, Dale, Augustine, G.J., Fitzpatrick, D., Katz, L.C., LaMantia, A.-S., McNamara, J.O., and Williams, S.M. (2001). Neuroscience.

Raymond, D., and Ozelius, L. (1993). Myoclonus-Dystonia. In GeneReviews(®), M.P. Adam, H.H. Ardinger, R.A. Pagon, S.E. Wallace, L.J. Bean, H.C. Mefford, K. Stephens, A. Amemiya, and N. Ledbetter, eds. (Seattle (WA): University of Washington, Seattle), p.

Reichenbach, A., and Bringmann, A. (2013). New functions of Müller cells. Glia 61, 651–678.

Rivier, F., Robert, A., Hugon, G., Bonet-Kerrache, A., Nigro, V., Fehrentz, J.-A., Martinez, J., and Mornet, D. (1999). Dystrophin and Utrophin Complexed with Different Associated Proteins in Cardiac Purkinje Fibres. Histochem. J. 31, 425–432.

Roberts, R.G., Coffey, A.J., Bobrow, M., and Bentley, D.R. (1993). Exon structure of the human dystrophin gene. Genomics 16, 536–538.

Romo-Yáñez, J., Ceja, V., Ilarraza-Lomelí, R., Coral-Vázquez, R., Velázquez, F., Mornet, D., Rendón, A., and Montañez, C. (2007). Dp71ab/DAPs complex composition changes during the differentiation process in PC12 cells. J. Cell. Biochem. 102, 82–97.

Ronacher, K., Hadley, K., Avenant, C., Stubsrud, E., Simons, S.S., Louw, A., and Hapgood, J.P. (2009). Ligand-selective transactivation and transrepression via the glucocorticoid receptor: role of cofactor interaction. Mol. Cell. Endocrinol. 299, 219–231.

Rotsos, T.G., and Moschos, M.M. (2008). Cystoid macular edema. Clin. Ophthalmol. Auckl. NZ 2, 919–930.

Runkle, E.A., and Antonetti, D.A. (2011). The blood-retinal barrier: structure and functional significance. Methods Mol. Biol. Clifton NJ 686, 133–148.

Saint Martín, A., Aragón, J., Depardon-Benítez, F., Sánchez-Trujillo, A., Mendoza-Hernández, G., Ceja, V., and Montañez, C. (2012). Identification of Dp71e, a new dystrophin with a novel carboxy-terminal end. FEBS J. 279, 66–77.

Sarig, R., Mezger-Lallemand, V., Gitelman, I., Davis, C., Fuchs, O., Yaffe, D., and Nudel, U. (1999). Targeted inactivation of Dp71, the major non-muscle product of the DMD gene: differential activity of the Dp71 promoter during development. Hum. Mol. Genet. 8, 1–10.

Sawamiphak, S., Ritter, M., and Acker-Palmer, A. (2010). Preparation of retinal explant cultures to study ex vivo tip endothelial cell responses. Nat. Protoc. 5, 1659–1665.

Schäcke, H., Schottelius, A., Döcke, W.-D., Strehlke, P., Jaroch, S., Schmees, N., Rehwinkel, H., Hennekes, H., and Asadullah, K. (2004). Dissociation of transactivation from transrepression by a selective glucocorticoid receptor agonist leads to separation of therapeutic effects from side effects. Proc. Natl. Acad. Sci. U. S. A. 101, 227–232.

Sene, A., Tadayoni, R., Pannicke, T., Wurm, A., El Mathari, B., Benard, R., Roux, M.J., Yaffe, D., Mornet, D., Reichenbach, A., et al. (2009). Functional implication of Dp71 in osmoregulation and vascular permeability of the retina. PloS One 4, e7329.

Siqueiros-Marquez, L., Bénard, R., Vacca, O., Charles-Messance, H., Bolaños-Jimenez, R., Guilloneau, X., Sennlaub, F., Montañez, C., Sahel, J.A., Rendon, A., et al. (2017). Protection of Glial Müller Cells by Dexamethasone in a Mouse Model of Surgically Induced Blood-Retinal Barrier Breakdown. Invest. Ophthalmol. Vis. Sci. 58, 876–886.

Spence, H.J., Chen, Y.-J., and Winder, S.J. (2002). Muscular dystrophies, the cytoskeleton and cell adhesion. BioEssays News Rev. Mol. Cell. Dev. Biol. 24, 542–552.

Stahl, J.H., Miller, D.B., Conway, B.P., and Campochiaro, P.A. (1987). Dexamethasone and indomethacin attenuate cryopexy. Graefes Arch. Clin. Exp. Ophthalmol. 225, 418–420.

Standring, Susan, Borley Neil R, Collins Patricia, Crossman Alan R, Gatzoulis Michael A, Healy Jeremiah C, Johnson David, Mahadevan Vishy, Newell Richard LM, and Wigley Caroline (2008). Gray's anatomy : the anatomical basis of clinical practice - NLM Catalog - NCBI (New York: Elsevier Limited,).

Sun, L., Chang, J., Kirchhoff, S.R., and Knowlton, A.A. (2000). Activation of HSF and selective increase in heat-shock proteins by acute dexamethasone treatment. Am. J. Physiol. Heart Circ. Physiol. 278, H1091-1097.

Suzuki, A., Yoshida, M., Yamamoto, H., and Ozawa, E. (1992). Glycoprotein-binding site of dystrophin is confined to the cysteine-rich domain and the first half of the carboxy-terminal domain. FEBS Lett. 308, 154–160.

Suzuki, A., Yoshida, M., Hayashi, K., Mizuno, Y., Hagiwara, Y., and Ozawa, E. (1994). Molecular organization at the glycoprotein-complex-binding site of dystrophin. Three dystrophin-associated proteins bind directly to the carboxy-terminal portion of dystrophin. Eur. J. Biochem. 220, 283–292.

Szabó, A., Jancsik, V., Mornet, D., and Kálmán, M. (2004). Immunofluorescence mapping of dystrophin in the rat brain: astrocytes contain the splice variant Dp71f, but this is confined to subpopulations. Anat. Embryol. (Berl.) 208, 463–477.

Tadayoni, R., Rendon, A., Soria-Jasso, L.E., and Cisneros, B. (2012). Dystrophin Dp71: the smallest but multifunctional product of the Duchenne muscular dystrophy gene. Mol. Neurobiol. 45, 43–60.

Tamura, H., Miyamoto, K., Kiryu, J., Miyahara, S., Katsuta, H., Hirose, F., Musashi, K., and Yoshimura, N. (2005). Intravitreal injection of corticosteroid attenuates leukostasis and vascular leakage in experimental diabetic retina. Invest. Ophthalmol. Vis. Sci. 46, 1440–1444.

Tan, J., Tan, S., Zheng, H., Liu, M., Chen, G., Zhang, H., Wang, K., Tan, S., Zhou, J., and Xiao, X. (2015). HSF1 functions as a transcription regulator for Dp71 expression. Cell Stress Chaperones 20, 371–379.

Tan, S., Zhao, S., Chen, Z., Ma, Q., Wang, W., Cheng, S., Wen, Q., Tan, S., and Xie, J. (2017). Altered Biological Properties in Dp71 Over-Expressing HBE Cells. Cell. Physiol. Biochem. 43, 2022–2036.

Tinsley, J.M., Blake, D.J., and Davies, K.E. (1993). Apo-dystrophin-3: a 2.2kb transcript from the DMD locus encoding the dystrophin glycoprotein binding site. Hum. Mol. Genet. 2, 521–524.

Trattler William, Kaiser Peter K, and Friedman Neil J (2012). Review of Ophthalmology (Elsevier Saunders).

Vecino, E., Rodriguez, F.D., Ruzafa, N., Pereiro, X., and Sharma, S.C. (2016). Glia–neuron interactions in the mammalian retina. Prog. Retin. Eye Res. 51, 1–40.

Villarreal-Silva, M., Suárez-Sánchez, R., Rodríguez-Muñoz, R., Mornet, D., and Cisneros, B. (2010). Dystrophin Dp71 is critical for stability of the DAPs in the nucleus of PC12 cells. Neurochem. Res. 35, 366–373.

Villarreal-Silva, M., Centeno-Cruz, F., Suárez-Sánchez, R., Garrido, E., and Cisneros, B. (2011). Knockdown of dystrophin Dp71 impairs PC12 cells cycle: localization in the spindle and cytokinesis structures implies a role for Dp71 in cell division. PloS One 6, e23504.

Waite, A., Brown, S.C., and Blake, D.J. (2012). The dystrophin–glycoprotein complex in brain development and disease. Trends Neurosci. 35, 487–496.

Wymann, M.P., and Schneiter, R. (2008). Lipid signalling in disease. Nat. Rev. Mol. Cell Biol. 9, 162–176.

Yang, Y., Bailey, C., Loewenstein, A., and Massin, P. (2015). INTRAVITREAL CORTICOSTEROIDS IN DIABETIC MACULAR EDEMA. Retina Phila. Pa 35, 2440–2449.

Yarla, N.S., Bishayee, A., Vadlakonda, L., Chintala, R., Duddukuri, G.R., Reddanna, P., and Dowluru, K.S.V.G.K. (2016). Phospholipase A2 Isoforms as Novel Targets for Prevention and Treatment of Inflammatory and Oncologic Diseases. Curr. Drug Targets 17, 1940–1962.

Zhao, M., Bousquet, E., Valamanesh, F., Farman, N., Jeanny, J.-C., Jaisser, F., and Behar-Cohen, F.F. (2011). Differential regulations of AQP4 and Kir4.1 by triamcinolone acetonide and dexamethasone in the healthy and inflamed retina. Invest. Ophthalmol. Vis. Sci. 52, 6340–6347.

Zimprich, A., Grabowski, M., Asmus, F., Naumann, M., Berg, D., Bertram, M., Scheidtmann, K., Kern, P., Winkelmann, J., Müller-Myhsok, B., et al. (2001). Mutations in the gene encoding epsilon-sarcoglycan cause myoclonus-dystonia syndrome. Nat. Genet. 29, 66–69.

Annexes

The work that I developed at CINVESTAV in Mexico and at The Vision Institute in France allowed me to be author of four articles already published and two articles that are in preparation.

The main part of my thesis work was published in the Investigative Ophthalmology and Visual Science (IOVS) journal in which I appear as the first author.

During the training at the Vision Institute; I studied on the formation and resolution of edema in mouse retina, allowed myself to publish a first author paper, also allowed me to participate in the study of astrocyte morphological alterations observed in Dp71 null mice as well as the vascular alterations observed in these mice. Additionally, the work in the Vision Institute using retinal explants as a model to study retinal disorders, allowed me to collaborate with the study on the role of subretinal accumulation of mononuclear phagocytes in the induction of loss of the conic segment through IL-1β.

During the training at CINVESTAV, I studied the participation of Dp71 and ε-SG in the cellular interactions of PC12 cells, this article is in preparation, once we complete the last experiments in order to probe the $Dp71d_{\Delta 71}$ and $Dp71d_{\Delta 71\text{-}74}$ participation in the intercellular PC12 unions. As part of my master's thesis, I carried out the construction of the

expression plasmid: pTRE2pur-myc/Dp71e; using this plasmid, I participated in the obtaining of PC12 cells line that overexpress the Dp71e$_{\Delta 71}$ which have been used as a study subject for a PhD student at CINVESTAV studying the neuronal differentiation and neurite growth in PC12 cells; this study is in preparation to publish.

List of figures

Figure 1.-Cellular organization in the retina. ---------- 10 -
Figure 2.- Blood Retina Barrier ---------- 13 -
Figure 3.- Astrocytes morphology of WT and Dp71-null mice retina. --- 16 -
Figure 4.- Eicosanoid biosynthesis from arachidonic acid---------- 20 -
Figure 5.- Schematic representation of DMD gene and dystrophin protein. ---------- 25 -
Figure 6.- Schematic representation of Dp71 isoforms. ---------- 29 -
Figure 7.- Model of Dp71 complex binding Kir4.1 and AQP4 in retina- 33 -
Figure 8.- Lens surgery.---------- 39 -
Figure 9.- Partial lens surgery induces iBRB breakdown for 48 hours.-- 48 -
Figure 10.- Downregulation of dystrophin Dp71, Kir4.1 and AQP4 after partial lens surgery.---------- 50 -
Figure 11.- Downregulation of Kir4.1 and AQP4 protein expression after partial lens surgery.---------- 52 -
Figure 12.- Astrocytes morphology in control and 24 and 48 hours post-surgery retinas. ---------- 53 -

Figure 13.- Inflammation in WT retinas 24 and 48 hours post-surgery. - 55 -
Figure 14.- Dp71 expression after 6 and 12 hours in an inflammation environment. ---------- 56 -
Figure 15.- Dexamethasone prevented Dp71 downregulation, but did not restore permeability after partial lens surgery. ---------- 58 -
Figure 16.- Dexamethasone prevented Dp71, Kir4.1, and AQPA alterations.---------- 60 -
Figure 17.- MGC swelling after hypotonic solution plus Ba^{2+} and hypotonic solution plus Ba^{2+} and Dex incubation. ---------- 62 -
Figure 18.- DAPs mRNA expression in complete retinas incubated in hypotonic solution plus Ba^{2+} or in hypotonic solution plus Ba^{2+} and Dex.---------- 63 -
Figure 19.- Utrophin and HSF1 mRNA expression in complete retinas incubated in hypotonic solution plus Ba^{2+} or in hypotonic solution plus Ba^{2+} and Dex. ---------- 64 -
Figure 20.- Effect of tree corticosteroids: Dex, Triam and Fluo con Dp71, Kir4.1 and AQP4 expression.---------- 66 -
Figure 21.- Effect of a low and high concentrations of the corticosteroids Dex, Triam and Fluo in MGC swelling. ---------- 67 -
Figure 22.- Effect of prostaglandins and leukotriene pathway inhibitors on Dp71, Kir4.1 and AQP4 expression. ---------- 69 -
Figure 23.- Colocalization of Dp71 isoforms with ε-SG in PC12/Tet-On cells without differentiation. ---------- 79 -
Figure 24.- Pearson correlation coefficient in PC12 expressing Dp71 isoforms. ---------- 80 -
Figure 25.- Colocalization of Dp71 isoforms with ε-SG in differentiated PC12/Tet-On cells. ---------- 81 -
Figure 26.- Colocalization of Dp71 isoforms with ε-SG in PC12 clones expressing Dp71 isoforms. ---------- 85 -

Figure 27.- Colocalization of Dp71 isoforms with beta-catenin in PC12 clones expressing Dp71 isoforms. ---------- 87 -
Figure 28.- Colocalization of Dp71 isoforms with Connexin43 in PC12 clones expressing Dp71 isoforms. ---------- 88 -
Figure 29.- Cell to cell adhesion quantification. ---------- 89 -

Résumé

PREMIÈRE PARTIE : *Altérations moléculaires dans les cellules gliales de Müller de souris au cours de l'œdème cellulaire et analyse du mécanisme de traitement*

La rupture de la barrière hémato-rétinienne interne (iBRB) se produit dans de nombreux troubles de la rétine et peut provoquer un œdème rétinien souvent responsable de la perte de vision. La dexamethasone est utilisé en clinique pour restaurer l'iBRB. Le but de cette étude était de caractériser l'impact d'une rupture de l'iBRB induite chirurgicalement sur les changements homéostatiques rétiniens de la dystrophine Dp71, de l'aquaporine-4 (AQP4) et du canal potassique Kir4.1provoqués par les altérations de cellules gliales de Müller. L'effet protecteur à de doses différentes de la dexamethasone, de la triamcinolone et de la fluocinolone a été également étudié dans ce modèle. Par ailleurs, les explants rétiniens ont été utilisé pour étudier la formation et la résolution de l'œdème de cellules gliales de Müller sans l'influence de l'inflammation du cristallin ainsi que l'effet de différentes doses de glucocorticoïdes (dexamethasone, triamcinolone et fluocinolone) et des inhibiteurs de la voie de l'acide arachidonique. L'efficacité de la triamcinolone et la fluocinolone a été testée et comparée à l'effet de la dexamethasone.

Nous avons observé que la chirurgie partielle du cristallin induit une rupture de l'iBRB et des changements moléculaires dans le MGC, y compris une diminution de l'expression de la Dp71 et d'AQP4 et la délocalisation de Kir4.1. La dexamethasone semble protéger la rétine de ces modifications au niveau moléculaires par l'augmentation de l'expression du HSF1. Nous avons également observé que même si les trois glucocorticoides étudié ont des effets différents sur l'expression de la Dp71, AQP4 et Kir4 .1 ont un effet différent sur l'expression de Dp71, AQP4 et Kir4.1 les trois sont capables de prévenir la formation de

l'œdème de cellules de Müller. Nos résultats suggèrent également que la formations d'œdème semblent être régulée par la voie des leucotriènes.

SECONDE PARTIE : *Rôle de la Dp71 et de l'ε-SG dans les jonctions intercellulaires de cellules PC12*

En parallèle aux travaux présentés dans la première partie, nous avons étudié le rôle des isoformes du groupe de la dystrophine Dp71d dans les processus d'adhésion intercellulaire des cellules PC12 en culture. Nos résultats suggèrent l'existence d'au moins deux mécanismes différents seraient impliqués dans l'adhésion intercellulaire associée à la Dp71, l'une impliquant $Dp71d_{\Delta 71}$ et les jonctions lacunaires (Cx43).

Abstract

FIRST PART: *Molecular alterations in the mouse Müller glial cells (MGC) during cellular edema and the analysis of the action mechanism of the treatment.*

The internal blood-retinal barrier (iBRB) breakdown occurs in many retinal diseases and can lead to retinal edema, which is often responsible for vision loss. Dexamethasone is used in clinics to restore the iBRB. The purpose of this study was to characterize the impact of a surgically induced iBRB breakdown, on the changes in retinal homeostasis caused by alterations in the expression and localization of dystrophin Dp71, aquaporin-4 (AQP4) and the potassium channel Kir4.1 in MGC. We also investigated the use of dexamethasone as treatment in this model. In addition, retinal explants were used to study the formation and resolution of MGC edema without the influence of lens inflammation, in this model, we analyzed the protective effect of different doses of glucocorticoids (dexamethasone, triamcinolone and fluocinolone) as well as the effect of arachidonic acid pathway inhibitors on the edema formation. The efficacy of triamcinolone and fluocinolone was tested and compared with dexamethasone effect.

The results show that partial lens surgery induces a iBRB breakdown and molecular changes in CGM, including a decrease in Dp71 and AQP4 expression, as well as the delocalization of Kir4.1. Dexamethasone appears to protect the retina from such molecular changes by increasing HSF1 expression. Also, we observed that, although the three glucocorticoids have different effects on Dp71, AQP4 and Kir4.1 expression, all three are able to prevent the formation of MGC edema. Our

results also suggest that edema formation seems to be mediated by the leukotriene pathway.

SECOND PART: *Role of Dp71 and ε-SG in the intercellular junctions of PC12 cells*

Parallel to the work presented in the first part, we studied the role of the Dp71 isoforms belonging to the Dp71d group in the intercellular adhesion processes of PC12 cells in culture. Our results suggest the existence of at least two different mechanisms involved in the intercellular adhesion associated with Dp71, one of which involves the formation of a $Dp71d_{\Delta 71}$ associated protein complex that includes a gap junction protein (Cx43).

Resumen

PRIMERA PARTE: *Alteraciones moleculares en células gliales de Müller (CGM) de ratón durante el edema celular y análisis del mecanismo de acción del tratamiento*

La ruptura de la barrera hemato-retiniana interna (iBHR) ocurre en muchos padecimientos de la retina y puede causar edema retiniano, este es a menudo responsable de la pérdida de la visión. La dexametasona es usado como tratamiento para estos padecimientos. El propósito de este estudio fue caracterizar el impacto de la ruptura de la iBHR, inducida quirúrgicamente, en los cambios en la homeostasis retiniana provocados por alteraciones en la expresión y localización de la distrofina Dp71, aquaporina-4 (AQP4) y el canal de potasio Kir4.1 en CGM. También investigamos el uso de dexametasona como tratamiento en este modelo. Además, se utilizaron explantes de retina para estudiar la formación y resolución del edema de CGM sin la influencia de la inflamación del cristalino; se estudió el efecto protector de diferentes dosis de glucocorticoides (dexametasona, triamcinolona y fluocinolona) así como inhibidores de la vía del ácido araquidónico en la formación del edema. Finalmente, la eficacia de triamcinolona y fluocinolona se probó y se comparó con el efecto de la dexametasona.

Los resultados muestran que la cirugía parcial de cristalino induce la ruptura de la iBHR y los cambios moleculares en CGM, incluyendo una disminución en la expresión de Dp71 y AQP4, así como la deslocalización de Kir4.1. La dexametasona parece proteger la retina de dichos cambios moleculares al aumentar la expresión de HSF1. También, observamos que, aunque los tres glucocorticoides estudiados tienen diferentes efectos sobre la expresión de Dp71, AQP4 y Kir4.1, los tres son capaces de prevenir la formación del edema de CGM. Nuestros resultados también sugieren que la formación del edema parece estar mediada por la vía de leucotrienos.

SEGUNDA PARTE: *Papel de Dp71 y ε-SG en las uniones intercelulares de células PC12*

Paralelamente al trabajo presentado en la primera parte, estudiamos el papel de las isoformas de la distrofina Dp71 del grupo Dp71d, en los procesos de adhesión intercelular de las células PC12 en cultivo. Nuestros resultados sugieren la existencia de al menos dos mecanismos diferentes implicados en la adhesión intercelular asociada con Dp71, uno de los cuales implica la formación de un complejo de proteínas asociadas a $Dp71d_{\Delta 71}$ y proteínas de las uniones tipo gap (Cx43).